SYNTHESIS AND CHARACTERISATION OF CHITOSAN FROM SHRIMP SHELLS

JUDSON HWANG WONG SHYH LONG

UNIVERSITI TUNKU ABDUL RAHMAN

SYNTHESIS AND CHARACTERISATION OF CHITOSAN FROM SHRIMP SHELLS

JUDSON HWANG WONG SHYH LONG

A project report submitted in partial fulfilment of the requirements for the award of Bachelor of Engineering (Hons.) Materials and Manufacturing Engineering

Faculty of Engineering and Science
Universiti Tunku Abdul Rahman

April 2013

DECLARATION

I hereby declare that this project report is based on my original work except for citations and quotations which have been duly acknowledged. I also declare that it has not been previously and concurrently submitted for any other degree or award at UTAR or other institutions.

Signature : _____

Name : Judson Hwang Wong Shyh Long

ID No. : 09UEB01185

Date : 3/5/2013

APPROVAL FOR SUBMISSION

I certify that this project report entitled **"SYNTHESIS AND CHARACTERISATION OF CHITOSAN FORM SHRIMP SHELLS"** was prepared by **JUDSON HWANG WONG SHYH LONG** has met the required standard for submission in partial fulfilment of the requirements for the award of Bachelor of Engineering (Hons.) Materials and Manufacturing Engineering at Universiti Tunku Abdul Rahman.

Approved by,

Signature : _____

Supervisor : Ms. Chew Chee Sean

Date : _____

ACKNOWLEDGEMENTS

I would like to thank everyone who had contributed to the successful completion of this project. I would like to express my gratitude to my research supervisor, Ms Chew Chee Sean for her valuable advice, guidance and her enormous patience throughout the development of this research. She has spent lots of time learning together with me, helping me when I was in need, guiding me when I was lost and never giving up on me. She is a great tutor who leaded me to my success.

Next, I would also like to express my gratitude to my loving parent who had helped and provided me encouragement and financial support so that I could concentrate and focus on this study.

Then, I would also like to thank my friends and lab assistants who assist and guide me through some apparatus, equipment and some inquiries on my study.

Last but not least, I am grateful to have a girlfriend as my partner who assists and regulate my documentation for the study. Thank you.

SYNTHESIS AND CHARACTERISATION OF CHITOSAN FROM SHRIMP SHELLS

ABSTRACT

Chitin and chitosan are the second most available biopolymer after cellulose. Chitosan as a result of N-deactylation from chitin and has linear chain of β-(1, 4)-linked 2-acetamino-2-deoxy-β-D-glucopyranose and 2-amino-2-deoxy-β-D-glucopyranose. Chitosan extraction consists of four common steps such as demineralisation, deproteinisation, decolourisation and N-deacetylation. In this study, chitosan was extracted using four methods which were named as Method 1(M1), Method 2(M2), Method 3(M3) and Method 4(M4). M3 is the most efficient method. Meanwhile, M2 and M4 used the longest treatment time of 120 hours. The final products produced from each method were named as M1_CHS, M2_CHS, M3_CHS and M4_CHS, respectively. All the products were then characterised using preliminary solubility test, X-ray Diffractometry (XRD), Fourier Transform Infrared Spectroscopy (FT-IR), Scanning Electron Microscopy (SEM) and Electron Dispersive Spectroscopy (EDS). M1_CHS is found as chitin with high CrI_{020} of 93.37% and degree of deacetylation (DDA) of 10.51%. Then, FT-IR spectra and XRD have proven that M2_CHS, M3_CHS and M4_CHS as chitosan with above 50% DDA and below 70% of crystallinity index at 020 phase (CrI_{020}). The solubility test shows that M2_CHS and M3_CHS are soluble in acetic acid while M4_CHS exhibits solubility behaviour only after 72 hours. The condition of M4_CHS is suggested to be caused bycalcified protein on the outer layer. In addition, composite of dried dissolved chitosan with iron oxide nanoparticle exhibits chemical relationship relatively.

TABLE OF CONTENTS

LIST OF TABLES

LIST OF FIGURES

LIST OF SYMBOLS / ABBREVIATIONS

°	Angular degree
Å	Angstrom
M	Concentration, molarity
N	Concentration, normality
mA	Current, miliampere
DDA	Degree of deacetylation
θ	Degree, Theta
s^{-1}	Frequency, hertz
MHz	Frequency, megahertz
λ	Lambda
mg	Mass, miligram
g	Mass, grams
%	Percentage
%T	Percentage of Transmission
%wt	Weight percentage
ppm	*parts per million*
w/v	Ratio, weight over volume
s	Time, seconds
min	Time, minutes
h	Time, hours

°C	Temperature, degree celsius
kV	Voltage, kilovolt
ml	Volume, milliliter
cm^{-1}	Wavenumber
CrI	Crystallinity index
CrI_{020}	Crystallinity index at 020 reflection
CrI_{110}	Crystallinity index at 110 reflection
Cu Kα	*Copper-potassium* α
CO_2	Carbon dioxide
$CaCO_3$	Calcium carbonate
DCl in D_2O	Deuterium chloride solution
EDS	Electron Dispense Spectroscopy
etc.	Et cetera
FT-IR	Fourier Transform Infrared Spectroscopy
HCl	Hydrochloric acid
Ni	Nikel
KOH	Potassium hydroxide
KBr	Potassium bromide
$KMnO_4$	Potassium permanganate
^1H NMR	Proton Nuclear Magnetic Resonance Spectroscopy
RT	Room Temperature, 25~30 °C
SEM	Scanning Electron Microscopy
NaOH	Sodium hydroxide
XRD	X-ray Diffraction

LIST OF APPENDICES

CHAPTER 1

INTRODUCTION

1.1 Background Study

Biopolymers are abundantly available from its natural sources of extraction. These natural sources are said to be renewable with its ability to be replenished through plantations or growth of animals. Typically, it is categorised by its biological compositions into a few major groups, including polysaccharides, proteins, lipids, polyphenols and others (Kaplan, 1998, Mohanty, Misra and Drzal, 2005). Among them, polysaccharides like cellulose, chitin and chitosan are commonly applied. Chitin and chitosan are the second most available biopolymer after cellulose. They are sourced mainly from exoskeleton of crustaceans such as shrimp, but are also available from other sources such as fungi and some insect's wing (Al Sagheer, Al-Sughayer, Muslim and Elsabee, 2009). In some studies, chitosan was reported to be developed from squilla (mantis shrimp), crab (Yen, Yang and Mau, 2009, Bolat et al., 2010) and silkworm chrysalides (Paulino, Simionato, Garcia and Nozaki, 2006) , etc.

Chitosan as a result of N-deactylation from chitin and has a chemical structure of linear chain consisting β-(1, 4)-linked 2-acetamino-2-deoxy-β-D-glucopyranose with 2-amino-2-deoxy-β-D-glucopyranose. It is well known for having common properties of polysaccharides such as biocompatibility, biodegradability, non-toxicity while possessing some unique properties like film forming ability, chelation and absorption properties as well as antimicrobial characteristic. In near decade, chitosan has been involved practically in dietary supplements, water treatment, food preservation, agriculture, cosmetics, pulp, paper, and medical applications (Al

Sagheer, Al-Sughayer, Muslim and Elsabee, 2009, Mohammed, Williams and Tverezovskaya, 2013, Teli and Sheikh, 2012, Islam et al., 2011).

Shrimp compiled a major portion of the processed seafood industry that its exoskeleton (shells) and cephathoraxes consist of about 30 - 40% of raw shrimp weight and is discarded as waste. Shrimp shells are insoluble in nature and take up a big portion of physical space as well as creating pollution However, the potential for shrimp shells to chemically be modified into chitosan has become more and more popular in recent years (Al Sagheer, Al-Sughayer, Muslim and Elsabee, 2009, Mohammed, Williams and Tverezovskaya, 2013, Teli and Sheikh, 2012, Islam et al., 2011).

For chitosan to be extracted from shrimp shells, it is necessary to first be converted to chitin. Generally, extraction of chitin from raw shrimp shells consists of three steps including demineralisation for removal of calcium carbonate/phosphate, deproteinisation for removal of protein and last step is decolourisation for removal of pigments. Then, chitin can be converted into chitosan by N-deacetylation which partially removal of acetyl group from the polymers chain composition (Islam et al., 2011, Mohammed, Williams and Tverezovskaya, 2013).

Chitosan was extracted with variation in processing parameters found in different studies such as nitrogen purging (Mirzadeh et al., 2002) , reflux condition (Mirzadeh et al., 2002, Mohammed, Williams and Tverezovskaya, 2013), high temperature (Mohammed, Williams and Tverezovskaya, 2013), long treatment time and concentration (Islam et al., 2011). The produced chitosan was tested with Proton Nuclear Magnetic Resonance (^{1}H NMR) and Fourier Transform Infrared Spectroscopy (FT-IR) to identify its degree of deacetylation (DDA); X-ray Diffractometry (XRD) for its lattice parameters, Scanning Electron Microscopy (SEM) for its morphology (Zhang et al., 2005, Islam et al., 2011, Alvarenga, 2011, Teli and Sheikh, 2012, Mohammed, Williams and Tverezovskaya, 2013).

1.2 Rationale of the Research

Synthetic polymers have all along been the major materials involving in our daily life. They are seen in a wide range of applications from dietary to mechanical support. However, they have also created problems in disposal as they are considered not biodegradable and take up millions years to degrade back to the nature. In other words, they consume a large space and become a major issue as environmental pollution increasing the demands for biopolymers which exhibit the characteristic of biocompatibility, biodegradable and non-toxicity. Chitosan being as a biopolymer extracted from shrimp shells can be developed to act as a solution for environmental issue. In addition, chitosan also gains its fame in wastewater treatment field and medical field due to its metal absorption and antibacterial properties respectively.

These demands then create the need for mass production of chitosan. Therefore, understanding the effectiveness and efficiency of chitosan extraction method will improve the quality of product and will definitely give many benefits. Nevertheless, chitosan composite with iron oxide nanoparticles with paramagnetic properties is expected to show better characteristic in the absorption of heavy metal in wastewater treatment process.

1.3 Aim and Objectives

The aim of this study is to investigate the least contaminate and effective way of chitosan production from shrimp shells.

The objectives incorporated in this study are

i. To produce chitosan from different synthesizing methods.

   Chitosan was produced using four different methods with variation in parameters

ii. To analyze and compare the characteristic of synthesized chitosan by solubility test, SEM, EDX, XRD and FT-IR.

   The products from each method were tested with different test to identify its dissolution, degree of deactylation (DDA), surface morphology, element distribution and crystallinity index.

iii. To tailor and characterise the composite of chitosan and iron oxide nanoparticles.

   The synthesized chitosan dissolved in acetic acid together with iron oxide nanoparticles and it was tested by FT-IR

1.4 Scope of Study

The scope of study is identified as follows:-

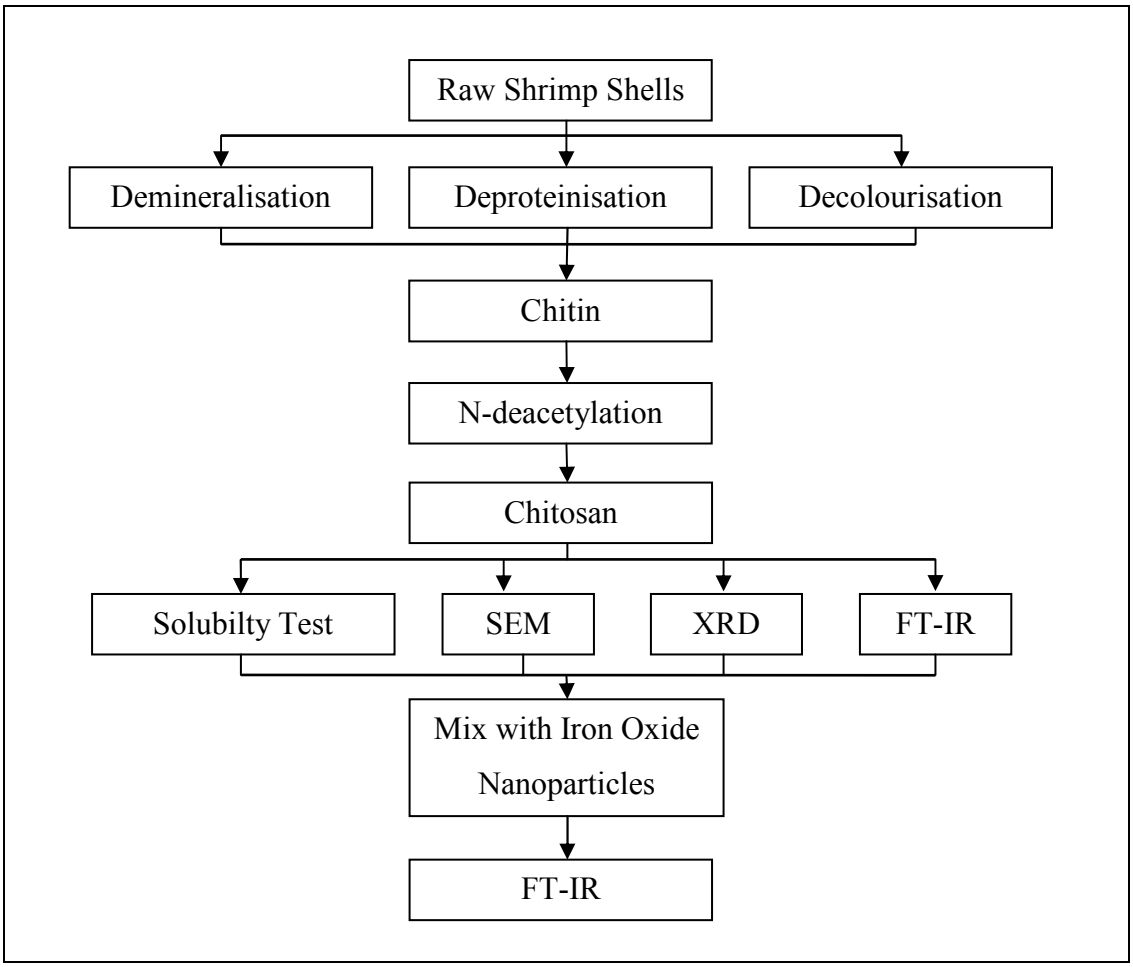

Figure 1.1: Scope of Study

Figure 1.1 shows the scope of study of the study. In this study, the shrimp shells were withdrawn from freshly bought shrimps by separating the shells from the fleshes. The shells were then processed to powder form through blending and grinding. Next, the shrimp shells powder underwent demineralisation, deproteinisation, decolourisation and N-deacetylation and the product from these processes were characterised using solubility test, scanning electron microscopy (SEM), X-ray diffractometry (XRD), fourier tranform infrared spectroscopy (FT-IR). Lastly, one of the characterised chitosan was then mixed with iron oxide nanoparticles to create a composite material and tested by using FT-IR.

1.5 Limitations

Although having many advantages, chitosan does show some limitation especially on its biodegradability. As biopolymer, it can biologically degraded under many possible environmental conditions. This then create a situation where the uses of synthesized chitosan are restricted under controlled factors such as moisture, nutrient, microorganisms, temperature and so on. Therefore, chitosan may experience undesired degradation where it is termed as premature. However, this is beneficial when comparing chitosan to other synthetic polymers. As unwanted junk of synthetic polymer will take up thousands and millions of years just to degrade back to mother nature (Kaplan, 1998, Mohanty, Misra and Drzal, 2005).

Furthermore, chitosan like any other biopolymer can be extracted from wide varieties of sources. The chitosan extracted from different sources such as crustacean, algae and so on were reported with differences in physiochemical properties such as molecular weight, polymer structure, stereochemistry, primary sequence and chemical reactivity, etc. The properties were found varying among species caused the conclusion on properties to be limited to species and the needs to control the genetic manipulation of extraction sources (Alvarenga, 2011).

CHAPTER 2

LITERATURE REVIEW

2.1 Biopolymers

Biopolymers are natural polymers that are abundantly available and extractable from natural sources. These sources can normally be replenished through plantations or growth of animal providing renewability compare to synthetic polymers (Kaplan, 1998, Mohanty, Misra and Drzal, 2005).

These biologically synthesized biopolymers have numerous advantages; one of the many is its environmental compatibility which in turn reduces the environmental burden as they are totally inherent to ecosystem. Next, most of the biopolymers are extracted from renewable sources and providing an incentive compared to non renewable petrochemical supplies. In addition, they are biodegradable creating minimum waste in comparison to petroleum synthesized polymer that requires special disposals facilities (Kaplan, 1998, Mohanty, Misra and Drzal, 2005).

The types of biopolymers are categorised as shown in Table 2.1. These biopolymers are derived from a wide range of biological compositions, including polysaccharides, protein, lipids, polyphenols and some biomaterials produced by bacteria, fungi, plants and animals. Some of them such as cellulose, starch and chitosan possess high potential that can be biologically and chemically synthesized into wide range of material applications (Kaplan, 1998, Mohanty, Misra and Drzal, 2005).

Table 2.1: List of Biopolymers and Its Categories [Adapted from Mohanty, Misra and Drzal (2005) and Kaplan (1998)]

Categories	Biopolymers
Polysaccharide	Starch(amylase, amylopectin), cellulose, pectin, konjac, alginate, carageenan, gums, hyaluronic acid, pullulan, elsinan, scleroglucan, chitin, chitosan, levan, xanthan, polygalactosamine, curdlan, gellan
Protein	Soy, zein, gluten, casein, serum albumin, silks, adhesives, elastin, resilin, polyamino acids, polyarginyl-polyaspartic acid, collagen/gelatin, polylsine, poly(γ-glutamic acid
Polyesters	polyhydroxyalkanoates, polylactic acid, polymalic acid
Lipids/Surfactants	Acetoglycerides, waxes, surfactants
Speciality Polymers	Lignin, shellac, natural rubber

2.2 Polysaccharide

2.2.1 Definition, Structure and Properties

Polysaccharide has high availability from a wide range of source. Cellulose, chitin and chitosan are polysaccharide and being as the most plentiful renewable resource in the world (Lapasin and Pricl, 1999).

Polysaccharide is a carbohydrate polymer which consists of ten to thousands monosaccharide units, which is normally glucose. The monosaccharide is the building unit of the biopolymer which is usually a six membered heterocyclic structure with oxygen and carbon atoms (Lapasin and Pricl, 1999, Mohanty, Misra and Drzal, 2005). The common structure of polysaccharides is shown in Figure 2.1.

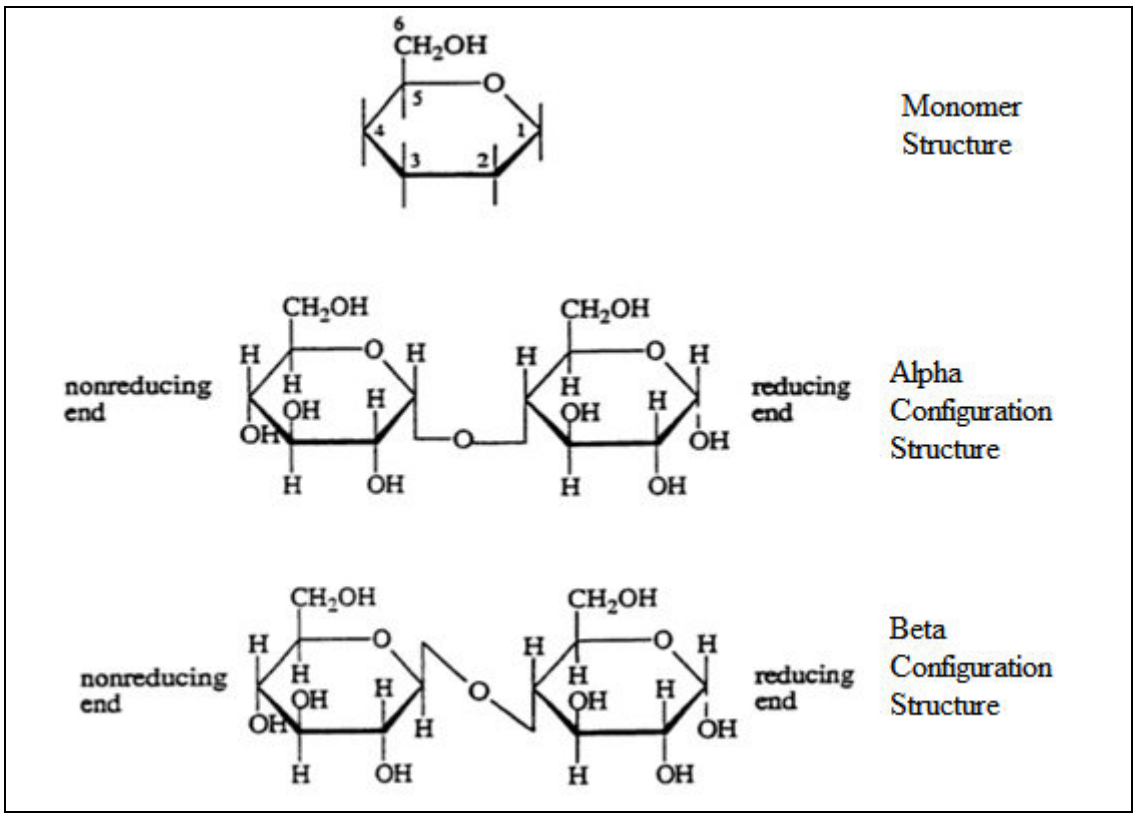

Figure 2.1: Nomenclature of Polysaccharides; Top-Monomer Structure (Saccharide); Middle-Alpha Configuration Structure; Bottom- Beta Configuration Structure [Adapted from Kaplan (1998), Mohanty, Misra and Drzal (2005)]

Figure 2.1 shows the chemical structure of a monosaccharide unit, and polysaccharide with alpha and beta configuration. The structure of polysaccharides diverted into primary, secondary, tertiary and quaternary structure which is similar to other polymers or biopolymers. The primary structure is the covalent sequence of monomeric unit along the chain. These linkages between adjacent saccharide are not completely flexible but limit the monomers to a narrow range of relative orientation which allow only certain shape to be adopted by an isolated polysaccharide. Secondary structure depends on their primary arrangement and with high degree of organization favourable interaction between shaped chains may result into tertiary structure. The further interaction of these structures obtains higher level of organisation and is called as quaternary structures (Lapasin and Pricl, 1999, Mohanty, Misra and Drzal, 2005).

2.2.2 Applications

In nature, polysaccharide is a multifunctional substance. It is used to stored energy in the form of starch, glycogen, etc. They also provide the structural integrity and mechanical strength of organisms by forming a hydrated crosslinked three-dimensional network, like pectin in land plants, and carrageenans in marine species. Polysaccharide such as cellulose and chitin act as the main support of an organism by formation of solid structure or tough fibers with close pack of chains. Furthermore, it is also the fundamental parts that influencing the structure build up of intracellular matrix and some physiological fluids. For some organisms, polysaccharide is the substance of protection purpose. It acts as an antigenic and immunogenic exocellular microbial polysaccharide or by exudation of gums from plants which provide preventive function by sealing off injured part (Lapasin and Pricl, 1999, Mohanty, Misra and Drzal, 2005).

Beside from polysaccharides, there are also others source of biopolymers. Proteins can be derived from either animal or plant sources. Proteins have been used to form film with particular emphasis on edible coatings. These materials are good oxygen barriers although hydrophilic behaviours make them to have poor moisture

barriers properties. For instance, soy protein can be used in food industry as coatings (Kaplan, 1998, Mohanty, Misra and Drzal, 2005).

The concept of biodegradable introduces the production of packaging materials and garbage bags. The first generation of the product made of oil derived resin was withdrawn from the market without significant effect of degradable consists of low starch content. Various studies show that starch content must exceed 60 percent before any sign of degradation. This phenomenon creates uncertainties for polysaccharide to be used as biodegradable bags (US Congress, 1993).

Polymeric material plays a vital role in medical application. United State of America reported that the usages of polymeric materials in medical product were more than 2 billion annually. Therefore, it is important to practise the uses of biocompatible materials. Biocompatibility defined the ability of the material of not creating any side effect or disastrous chemical reaction on the users. Polysaccharides as the most abundant biopolymers are found to be broadly used as any medical appliances with its recognised biocompatibility (Kasapis, Norton and Ubbink, 2009, US Congress, 1993).

Nowadays, companies have developed the concept of biopolymers into functions such as gold teeth, loose-fill packaging, compost bag, cutlery, pharmaceutical capsule and agricultural mulch film. EcoChem, a corporate joint venture by Cargill and DuPont-ConAgra focus their development in polylactic acid (PLA) materials. Being produced by lactic acid monomers from potato skins and corn, these materials are said to have similar mechanical and physical properties as compared to petroleum based polymers but it degrades rapidly under certain environmental conditions. Then, suture made from chitin and modified cellulose are able to form natural bonds with surrounding tissue and speed up the healing process. Nevertheless, bioadhesives made of protein polymer serve as a suture enhancement and is suggested to be used for attaching prostheses or dental application. In the near future, biopolymer will enhance to be use in facilitating tissue growth and organ regeneration or serve as a vascular support meshes for blood vessel regeneration (Kasapis, Norton and Ubbink, 2009, US Congress, 1993).

2.3 Chitin and Chitosan

Chitin and chitosan are bipolymers that have excellent properties in biodegradablility, biocompability, non-toxicity and absorption. Chitin and chitosan consist of 6.9 %wt nitrogen in its structure which acts as a chelating agent (Hudson and Smith, 1998).

Chelating agent is the term for organic compound with the ability to perform chelation. Meanwhile, chelation is described as the ability of the ion or molecule to bind with metal ion. The process involved the formation of two or more separate condinate bond between a polydentate ligand with a central atom. This chelate effect described the enhanced affinity of the chelating ligand on metal ions. With possession of these ligands, chitin and chitosan are both excellent chelating agents. The other chemical and physical definition for these two substances comes in the next context as followed (McNaught and Wilkinson, 2006).

2.3.1 Chitin – Definition, Structure and Properties

After cellulose, chitin is considered as the second most abundant polysaccharide on the planet with a production of approximately 10^{10}-10^{12} Tons (Robert, 1992). Chitin is a homopolymer of 2-acetamido-2deoxy-D-glucose (N-acetyglucosamine) residue linked by β-(1-4) bonds (Wang et al., 2006). This structure is also known as N-acetylglucosamine (Pradip, Joydeep and Tripathi, 2004) as shown in Figure 2.2. This structure is compact and disallows chitin to be soluble in most solvent. Therefore, it brings the demand for chitin to be transformed into chitosan (Peter, 1995).

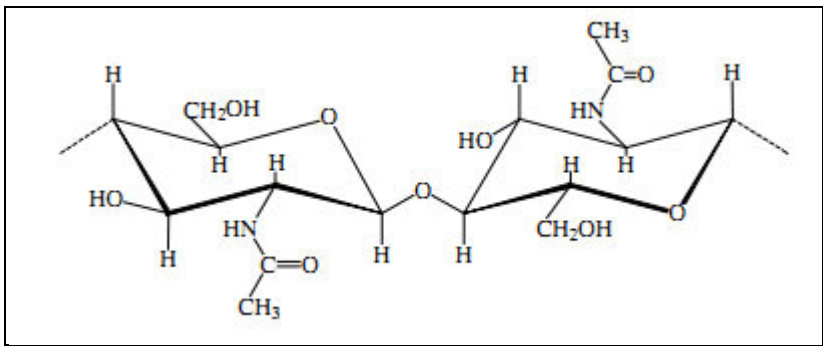

Figure 2.2 : Structure of Chitin [Adapted from Pradip, Joydeep and Tripathi (2004)]

In referred to the chemical structure, chitin is often considered as a derivative of a cellulose where both having polysaccharide as the functional group but it has acetamide groups (-$NHCOCH_3$) at the C-2 position (Pradip, Joydeep and Tripathi, 2004). Physically, chitin is a white, hard, inelastic, nitrogenous polysaccharide (Pradip, Joydeep and Tripathi, 2004).

Naturally, there are three type of chitin that is different in structures, which are α-chitin, β-chitin and γ-chitin. α-chitin being the most abundant has a tightly compacted orthorhombic cell formed by alternated sheets of antiparallel chains (Minke and Blackwell, 1978); β-chitin having a monoclinic unit cell with polysaccharide chains attaching in a parallel manner (Gardner and Blackwell, 1975); γ-chitin is said to be the combination of α and β structure rather than a third polymorph (Robert, 1992).

2.3.2 Chitosan - Definition, Structure and Properties

Chitosan is one of the derivatives of chitin. Differed from chitin, chitosan are soluble in most solvent especially acidic aqueous which enable it to behave as a cationic polyelectrolyte. In recent years, chitosan has turned to be more preferable than chitin as it is more tractable in solution process. Chitosan contains properties as common biopolymers such biocompatibility, biodegradability, non-toxicity while it is unique because of some properties such as film forming ability, chelation and absorption properties, and antimicrobial activity (Kumar, 2000). In addition, its great formability enable it to be converted into fibers, films, coating, beads, powders and solution which allow it to diverse its usefulness(Kumar, 2000, Al Sagheer, Al-Sughayer, Muslim and Elsabee, 2009).

Generally, chitosan is a cationic polysaccharide in a result of deacetylation of chitin with a linear chain structure consisting β-(1,4)-linked 2-acetamino-2-deoxy-β-D-glucopyranose with 2-amino-2-deoxy-β-D-glucopyranose (Marthur and Narang, 1990), consequently a homopolymer of N-acetylgucisamine and glucosamine that shown in Figure 2.3.

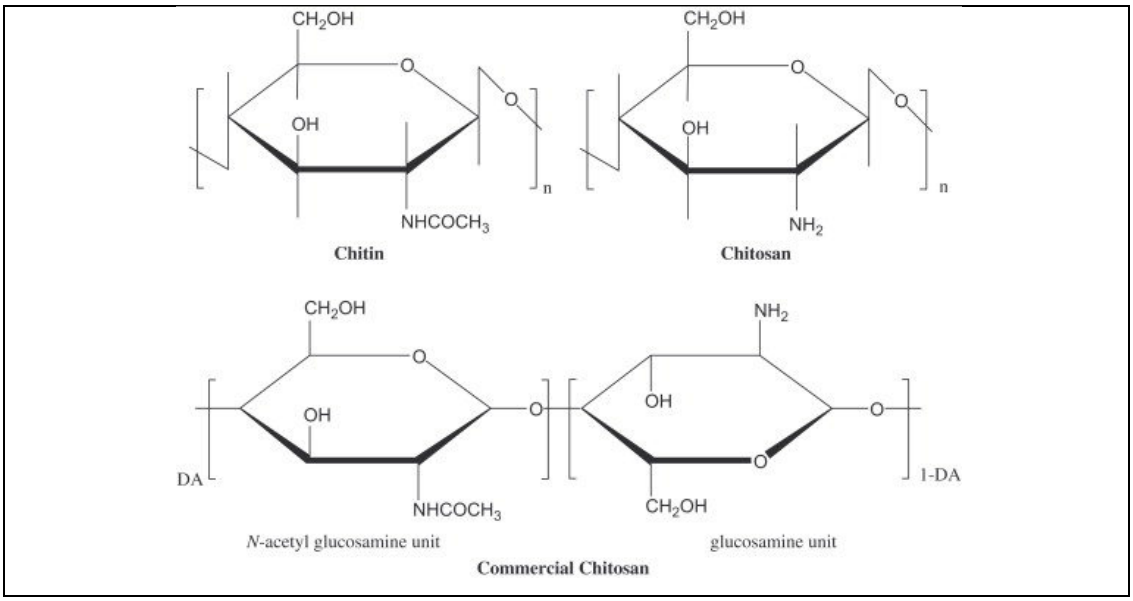

Figure 2.3 : Nomenclature of Chitin and Deacetylated Chitin (Up) and Partially Deacetylated Chitin, Chitosan (Down) [Adapted from Crini and Badot (2008)]

2.3.3 Source of Materials

Chitin and chitosan are carbohydrate derived natural polymers found in the exoskeleton of crustaceans, such as shrimp, and marine zooplankton species (Shahidi and Abuzaytoun, 2005). Insect's wing and fungi's cell wall are also reported to contain chitin (Tharanathan and Kittur, 2003). Shrimp consists about 45 % of raw material used for processed seafood industry and among them about 30 - 40 % by weight of raw shrimp is discarded as waste which composed of the its exoskeleton (shells) and cephathoraxes (Ibrahim, Salama and El-Banna, 1991). Without proper disposals, these have become a big problem for the environment. However, these wastes have the potential to be derived into further materials (Al Sagheer, Al-Sughayer, Muslim and Elsabee, 2009). Beside chitin and chitosan, shrimp shells also contains a considerable content of astaxanthin, a carotenoid used in fish food additive industry (Pradip, Joydeep and Tripathi, 2004).

2.3.4 Applications

Chitin, chitosan and other derivatives have more than 200 applications currently and they are still expanding (Al Sagheer, Al-Sughayer, Muslim and Elsabee, 2009). The functionability of chitosan depends greatly on it molecular weight which in turn influence its viscosity (No and Lee, 1995). Its polycationic behaviour allows chitosan to be used as flocculating agent and heavy metal trapper in the application for waste water treatment industry (Pradip, Joydeep and Tripathi, 2004).

Chitosan with amine group in C-2 position provides some unique properties which have been reported in the application of dietary supplements, waste water treatment, food preservation, agriculture, cosmetics, pulp and paper, and medical applications (Pradip, Joydeep and Tripathi, 2004). With its antibacterial activity, chitosan is applied in medical application such as wound dressing and suturing thread (Harish Prashanth and Thanathan, 2007). In some studies, chitosan has been involved in the treatment of surface for non woven fabric and polypropylene film to improve antibacterial properties (Abdou, Elkholy, Elsabee and Mohamed, 2008).

2.4 Preparation Methods

There are two major steps in developing chitosan from raw materials which are isolation of chitin and N-deacetylation of chitin into chitosan (Al Sagheer, Al-Sughayer, Muslim and Elsabee, 2009, Islam et al., 2011).

There are several methods reported in extraction of chitin from raw shrimp shells. However, the two major steps which commonly used are demineralisation and deproteinisation , while some studies involved in Decolourisation (Pradip, Joydeep and Tripathi, 2004).

In the extraction of chitin of some studies, raw materials are necessary to prepared where the shells are scraped free from the shells, washed, dried, and grounded to pass through 250 micron sieve before being further processed (Al Sagheer, Al-Sughayer, Muslim and Elsabee, 2009).

2.4.1 Demineralisation, Deproteinisation and Decolourisation of Shrimp Shells to Chitin

In demineralisation, organic matter specifically calcium carbonate ($CaCO_3$) are eliminated in diluted acidic medium, this is known as demineralisation which usually involved hydrochloric acid (HCl). Meanwhile, protein content of the shells is withdrawn from the main chemical structure during deproteinisation. Conventionally, this process is done by treating the shells in alkaline aqueous solution composed of sodium hydroxide (NaOH) or potassium hydroxide (KOH) (Al Sagheer, Al-Sughayer, Muslim and Elsabee, 2009). In several studies, deproteinisation comes after demineralisation (Islam et al., 2011).

Decolourisation is to remove natural pigment existed in chitin (Mirzadeh et al., 2002). In the study of Mirzadeh et al. (2002) acetone was added to chitin residue under reflux condition for 2 hours.

In a study by Islam et al. (2011), the raw shrimp shells was demineralised under suspension of HCl with concentration of 4 % at room temperature with a solid to solvent ratio of 1 g : 14 ml (w/v) for 36 hours. The resulting was squashy remains of shells and calcium chloride in the form of solution. Then, it is deproteinised by treating the demineralised shells in 5 % concentration of NaOH at 90 °C for duration of 24 hours at the solid to solvent ratio of 1 g : 12 ml (w/v). The remaining was dried and the product was chitin.

Al Sagheer, Al-Sughayer, Muslim and Elsabee (2009) used 0.25 M of HCl solution at room temperature with a solid to solvent ratio of 1 g : 40 ml for duration of 15-180 min. Then, it was neutralized by washing with distilled water. Carbon dioxide (CO_2) emission are observed and differed among species. The author and colleagues carried out deproteinisation with 1.0 M of NaOH with solid to solvent ratio of 10 g : 20 ml at 70 °C and the process was repeated several times until absence of colour in the medium which represents the absence of protein. It was then washed to neutral and boiled with acetone to remove pigment and later dried into chitin.

In a study of Teli and Sheikh (2012), after the raw shrimp shells was washed, dried and grinded, it was soaked in 1 M of NaOH for 24 hours, washed and dried. It was then demineralised with 1 M of HCl, deprotenised with 5 % NaOH, discoloured with $KMnO_4$ and oxalic acid to obtain chitin powder.

2.4.2 N-deacetylation (from Chitin to Chitosan)

N-deacetylation is a step to convert chitin to chitosan. In more specific term, it is a process that involves partial removal of acetyl groups from a chitin structure (Islam et al., 2011). In industrial, this step is normally involved with an alkaline bath (Pradip, Joydeep and Tripathi, 2004).

Islam et al. (2011) achieved this step by treating chitin with 70 % concentration of NaOH solution with a solid to solvent ratio of 1 g : 14 ml (w/v) at room temperature for 72 hours. The resulting chitosan was washed to neutrality and dried under the sun (Islam et al., 2011). Chitin was deacetylated by Teli and Sheikh (2012) with 50 % NaOH and higher degree of deacetylation was observed with repetitive measurements.

Al Sagheer et al. (2009) used two methods in its deacetylation of chitin to chitosan. A conventional method that involved treating chitin with 45 % concentration of NaOH in 1 g : 15 ml solid to solvent ratio at 110 °C. It was also steeped with strong hydroxide at room temperature before treatment for one day. Chitosan formed was purified in 2% concentration of acetic acid and re-precipitate with 20% concentration of NaOH solution. The chitosan was freeze dried with methanol and further lyophilized under -70 °C. Another method was microwave method which involved mixture of chitin in 45 % concentration of NaOH in conical flask covered tightly with cotton under microwave radiation. It was then cooled with cold water, washed to neutrality and freeze dried. Microwave method was investigated to reduce time of deacetylation for ~8 hours to ~15 minutes and produced higher molecular weight and crystallinity (Al Sagheer, Al-Sughayer, Muslim and Elsabee, 2009).

In a study, Tan, Khor, Tan and Wong (1996) were able to manipulate the degree of deacetylation (DDA) of chitosan at 75%, 87%, and 96% with modification of parameters like temperature, time and times of deacetylation as shown in Table 2.2.

Table 2.2: Parameters Required to Obtain Degree of Deacetylation. [Adapted from Tan, Khor, Tan and Wong (1996) and Trung et al. (2006)]

DDA of Chitosan	% NaOH	Temperature (°C)	Time (h)	Time(s) of Deacetylation
75	50	40	24	1
87	50	65	20	1
96	50	65	20	2

2.4.3 Degree of Deacetylation (DDA) and Its Effect

Properties of chitosan to a varying extent are strongly dependant on degree of N-deacetylation of chitin. It is an essential factor to study the structure-property relationship. Degree of deacetylation was determined by using FT-IR spectroscopy while the spectrum was obtained with a Brucker IFS-48 spectrometer (Mirzadeh et al., 2002). Table 2.3 shows the physical characteristics of chitosan as processed to different degree of deactylation (DDA).

Table 2.3: Physical Characteristic of Different Degree of Deacetylation.
[Adapted from Trung et al. (2006)]

Characteristic[1]	Chitosans; degree of deacetylation[2]		
	75 %DDA	87 %DDA	96 %DDA
Bulk density (g/ml)	0.59±0.02	0.54±0.02	0.53±0.01
Color	White	White	White
Crystallinity (%)	28.1±2.1	34.1±1.6	37.9±1.9
Swelling index (%)	682±43	453±31	466±24
Viscosity (cPs)	78.3±8.5	73.3±7.1	77.3±7.6
Turbidity (NTU)	22.7±2.1	28.3±2.5	26.3±2.1
Fat binding capacity (%)	95±7	226±13	219±12
Crystal violet (cationic)	122.7±3.8	30.6±2.1	28.6±3.0
Orange II (anioic)	37.1±3.5	47.1±2.5	53.2±3.2

[1] Mean ± standard deviation of triplicate determinations.
[2] The chitosans were ground to small particle size (<150μm) prior to analysis.

It was reported that chitin with a degree of deacetylation of above 50 % can be considered as chitosan which it was soluble under 1% of acetic acid (Peter, 1995).

Relationship between degree of deacetylation (DDA) on chitin and chitosan determined by FT-IR and ^{1}H NMR and crystallinity index of 020 (CrI_{020}) and 110 phase (CrI_{110}) from XRD was compiled by Zhang et al. (2005) as shown in Table 2.4.

Table 2.4: Degree of Deacetylation (DDA) of Chitin and Chitosan by FT-IR and ^{1}H NMR and Crystallinity by XRD on CrI_{110} and CrI_{020}. [Adapted by Zhang et al. (2005)]

DDA (%)		Crystallinity (CrI,%)	
FT-IR	**^{1}H NMR**	**CrI_{110}**	**CrI_{020}**
16.9	-	90.7	91.3
49.4	49.8	63.5	66.1
63.5	50.2	62.9	64.2
58.7	57.4	62.8	61.6
71,4	66.8	58.7	55.7
87.0	86.4	59.9	40.7
28.7	94.0	58.6	30.9

Zhang et al. (2005) discovered that there are a linear proportional relationship between CrI_{020} and DDA. The linear relationship was proposed by the author as a possibility to determine DDA through XRD via the calculation of CrI_{020}. Equation 2.1 shows the possible linear equation proposed for the relationship between DDA and CrI_{020}.

$$y = -0.7529x + 103.97, R^2 = 0.9924 \quad (2.1)$$

where,

y = Degree of deacetylation (DDA)

x = Crystalinity index at 020 phase (CrI_{020})

As stated by Zhang et al. (2005), the estimation allows overall impurities of less than 3 %wt. With this allowance and linear relationship, CrI_{020} could act to enhance the precision of estimating DDA. After chitosan was produced, it is characterised to be confirmed as chitosan and understand its properties.

2.5 Characterisation Methods

The major physical characteristics that determine the functional properties of the polymer are the molecular weight and the crystallinity (Trung et al., 2006). Chitosan is known to be dissolvable under common organic acid such as acetic acid while chitin shows contrast. This characteristic is commonly used to preliminary identify the product produced is chitosan or chitin (Islam et al., 2011, Al Sagheer, Al-Sughayer, Muslim and Elsabee, 2009, Trung et al., 2006, Mirzadeh et al., 2002).

2.5.1 Fourier Transform Infrared Spectroscopy (FT-IR)

Infrared spectroscopy is one of the most common characterisation method for chitin and chitosan due its simplicity, relative instrument availability and independence of sample solubility (Ng, Hein and Stevens, 2006).

Teli and Sheikh (2012) investigated the FT-IR spectra of chitin and chitosan extracted from shrimp shells as well as shrimp shells itself. In the studies, chitin has characteristic absorption bands at 1550.7 cm^{-1}, 1674.1 cm^{-1} and stretching vibration of C=O and NH from ($NHCOCH_3$) was displayed at the area of 3085.9 cm^{-1} and 3265.3 cm^{-1} correspondingly. As for chitosan, absorption band featuring bending vibration of NH from R-NH_2 was observed at 1620.1 cm^{-1} indicating increase degree of deacetylation while C-H was displayed with stretching vibration of 2916.1 cm^{-1} , 2858.3 cm^{-1} and bending vibration of 1415.7 cm^{-1}, 1375.2 cm^{-1}. The result was compared with commercial chitosan and a significant degree of similarities was observed. The FT-IR investigation were recorded using FT-IR spectrophotometer (Shimadzu 8400s, Japan) using attenuated total

reflectance (ATR) sampling technique by recording 45 scan in %T mode in the range of 4000 - 600 cm^{-1}. The spectra of shrimp shells, chitin and chitosan extracted from shrimp shells are shown in Figure 2.4.

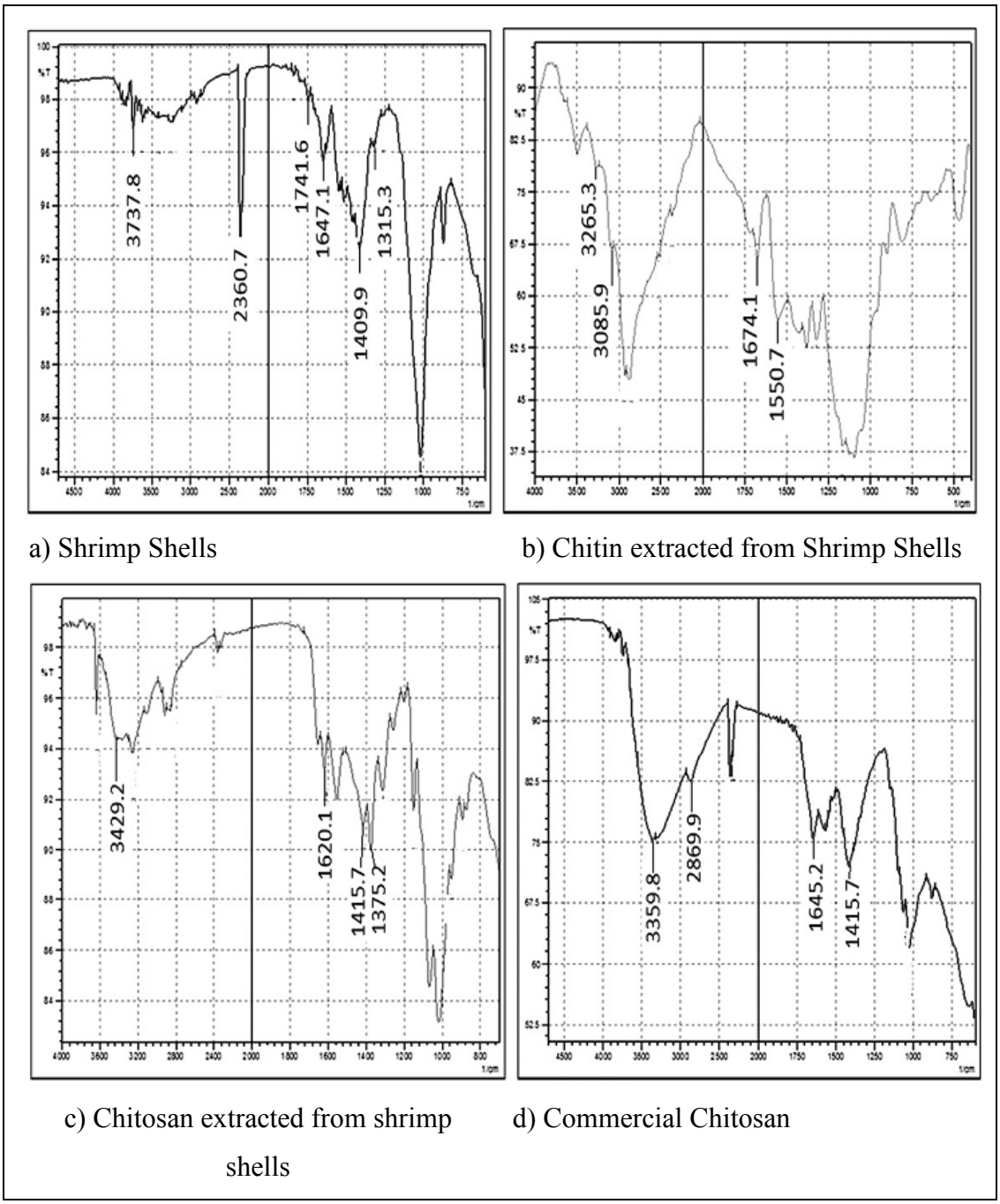

a) Shrimp Shells

b) Chitin extracted from Shrimp Shells

c) Chitosan extracted from shrimp shells

d) Commercial Chitosan

Figure 2.4 : FT-IR Spectra of Shrimp Shells (A), Chitin Extracted from Shrimp Shells (B), Chitosan Extracted from Shrimp Shells (C), Commerical Chitosan
[Adapted from Teli and Sheikh (2012)]

In a study to extract chitin and chitosan from shrimp shells, Mohammed, Williams and Tverezovskaya (2013) presented that FT-IR spectrum of chitin has absorbance bands around 3450, 3262, 3114, 2960, 2930, 2888, 1658, 1628, 1560, 1418, 1382, 1318, 1260, 1204, 1158, 1118, 1074, 1026, 952 and 896 cm^{-1}. This was also supported by works of Acosta, Jimenez, Borau and Heras (1993) classified as α-chitin. Meanwhile, extra bands in the region of 1605 - 1566 cm^{-1} was reported due to amine group where 3450, 3262, 3114 and 1658 cm^{-1} were missing due to amide group withdrew during deacetylation. As for dried shrimp shells powder, bands around 1798, 1420 - 1430, 876 cm^{-1} for minerals ($CaCO_3$) and 1540 cm^{-1} for protein were absence after transformed to chitin. Figure 2.5 shows the comparison of FT-IR spectrum recorded by Mohammed, Williams and Tverezovskaya (2013) using Perkin Elmer FT-IR Spectrometer over the range of 4000 - 625 cm^{-1} at a resolution of 4 cm^{-1}.

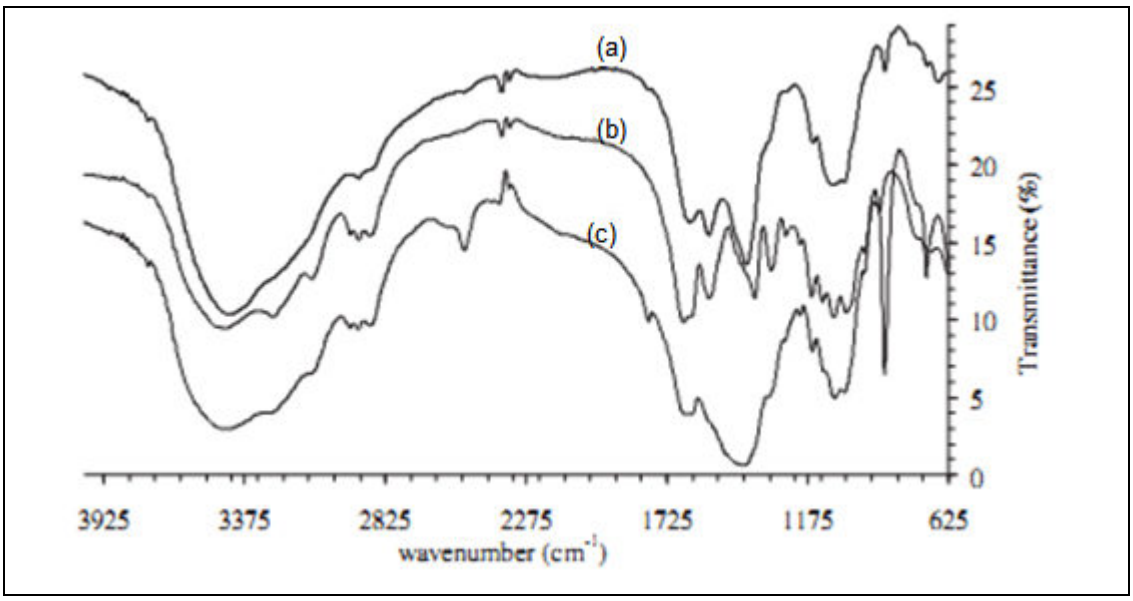

Figure 2.5 : Comparison of FT-IR Spectrum between (A) Prawn Shells, (B) Extracted Chitin and (C) Chitosan [Adapted from Mohammed, Williams and Tverezovskaya (2013)]

Figure 2.6 shows the FTIR spectra of chitin and chitosan. It is observed that the chitin has high absorbance as compare to chitosan. Chitin is transform to chitosan through n-deacetylation which reduce the amide content. This is observed as the reductions of band at1655 cm^{-1} as it transformed from chitin to chitosan.

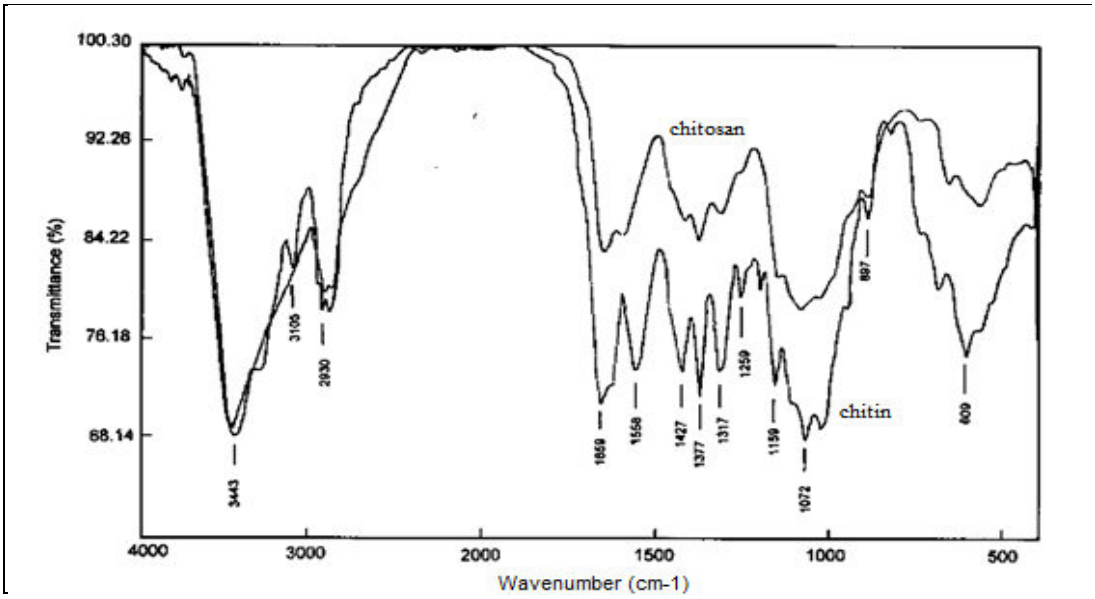

Figure 2.6 : FT-IR Spectra of Chitin and Chitosan [Adapted from Yaghobi and Hormozi (2010)]

With the spectrum obtained, accurate DDA is investigated with FT-IR spectra using Baxter, Dillon, Anthony Taylor and Roberts (1992)'s formula as shown in Equation 2.2 :

$$\% \text{ DDA} = 100 - \left({}^{A_{1655}}/_{A_{3450}} \times 115 \right) \tag{2.2}$$

where,

A_{1655} =Absorption of band at 1655 cm^{-1}

A_{3450} = Absorption of band at 3450 cm^{-1}

However, Kasaai (2008) reviewed that there are a few reference bands that can be used to determine the degree of deacetylation for chitosan. Table 2.5 shows the reference bands, corresponding wave number, advantages and disadvantages of referring to the bands.

Table 2.5 : Reference Bands, Waves Number and Their Advantages and Disadvantages. [Adapted from Kasaai (2008)]

Absorption Band	Wave number (cm^{-1})	Advantages	Disadvantages
O-H stretching	3450	OH has highly intense absorption band	(1) O-H of water molecule appears in this region; (2) O-H groups involve with intra- and intermolecular hydrogen bonds and result in a broad peak; (3) N-H stretching band appear around 3300 cm^{-1} and creates an interference peak and its intensity changes with the DA
C-H stretching	2870	The intensity of peak is significant; the band does not involve in hydrogen bonds; and water does not create any interference peak	The position of C-H stretching corresponsing to N-acetyl groups changes with the DA
CH_2 bending	1420		Shape and intensity of the peak change with changing the crystallinity of chitosan samples through rearrangement of hydrogen bonds at position of primary OH-groups
C-O stretching C-O stretching C-O stretching of glycoside linkage Glycoside linkage/ C-O-C bridge (asymmetric CO-stretching)	1030 1070 897 1160		Several absorption bands appear in this region; and the peak is not clearly separated, and its intensity is weak

2.5.2 Scanning Electron Microscopy (SEM)

The dried samples need to be ground and coated with gold in vacuum using sputter coater. Then, high magnification of surface morphology was observed using JEOL JSM - 630 J operating at 20 kV where chitin have uniform morphology with lamellar organization and specifically more crystalline appeared for α-chitin (Al Sagheer, Al-Sughayer, Muslim and Elsabee, 2009). The SEM micrograph of chitin is shown in Figure 2.7.

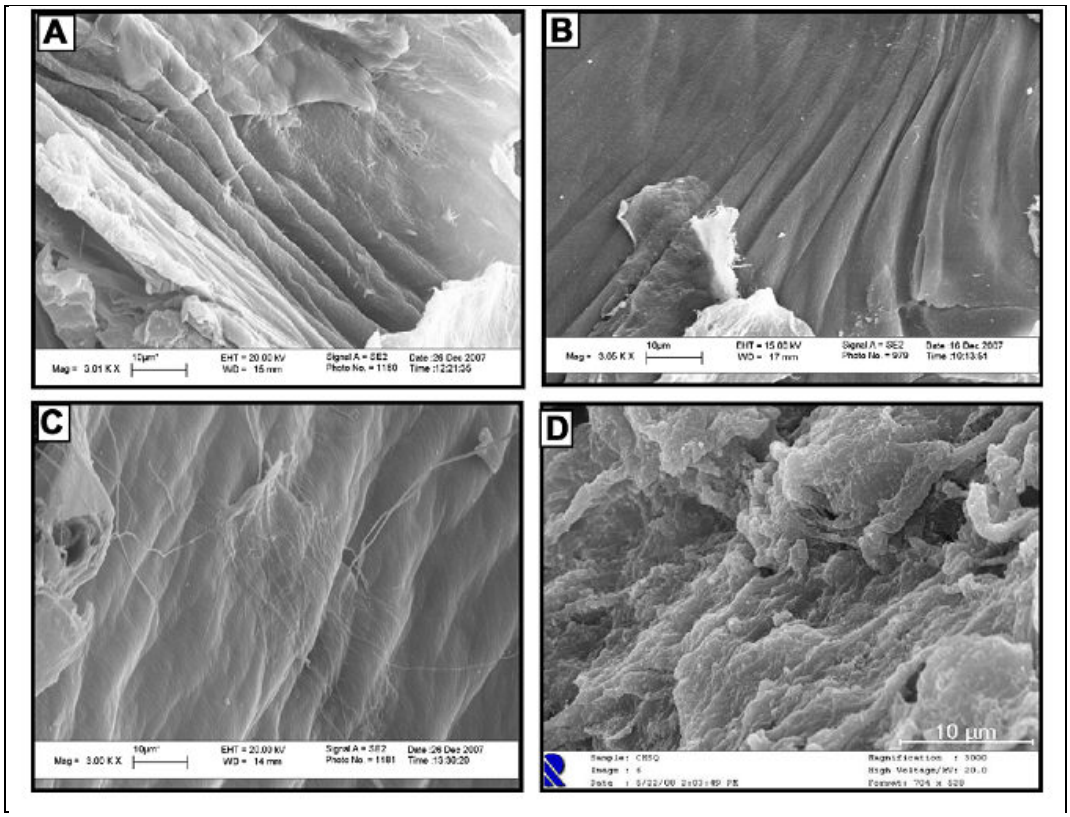

Figure 2.7 : SEM Micrograph for α-chitin Extracted from (A) Jinga Prawn, (B) Blue Swimming Crab – Female (C) Scyllarid Lobster and (d) β-Chitin from Cuttlefish [Adapted from Al Sagheer, Al-Sughayer, Muslim and Elsabee (2009)]

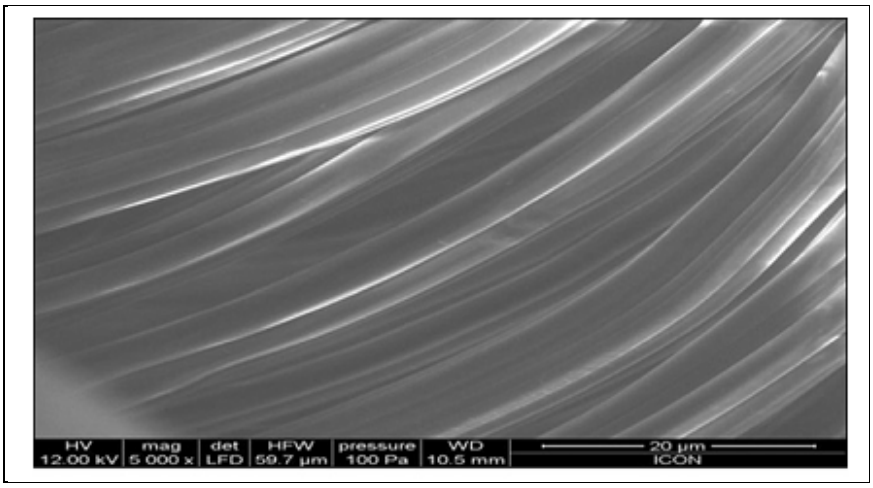

Figure 2.8 : SEM Micrograph of Chitosan from Shrimp Shells [Adapted from Teli and Sheikh (2012)]

The SEM Mircograph of chitosan shown in Figure 2.8 was a result from Teli and Sheikh (2012) by using SEM of Philips XL30, Netherlands stating that chitosan has smooth surface morphology with minimum residues.

2.5.3 X-ray Diffractometry (XRD)

In the study of Al Sagheer, Al-Sughayer, Muslim and Elsabee (2009) the XRD measurement on powder samples were done at 5°-40° and room temperature with a D500 Siemens diffractometer equipped with Ni-filtered Cu Kα radiation ($\lambda = 1.5406$ Å). It was operated with 1° diverging and receiving slit at 50 kV and 40 mA and continuous scan was carried out with step size of 0.015° and step time of 0.2 s. The crystallinity of chitin was shown to be reduced after being transformed to chitosan and strong reflection was observed at 9-10° due to the incorporation of bound water molecule into crystal lattice. Figure 2.9 is the comparison of XRD pattern between α-chitin of tiger prawn, chitosan prepared under microwave heating and chitosan prepared under traditional heating.

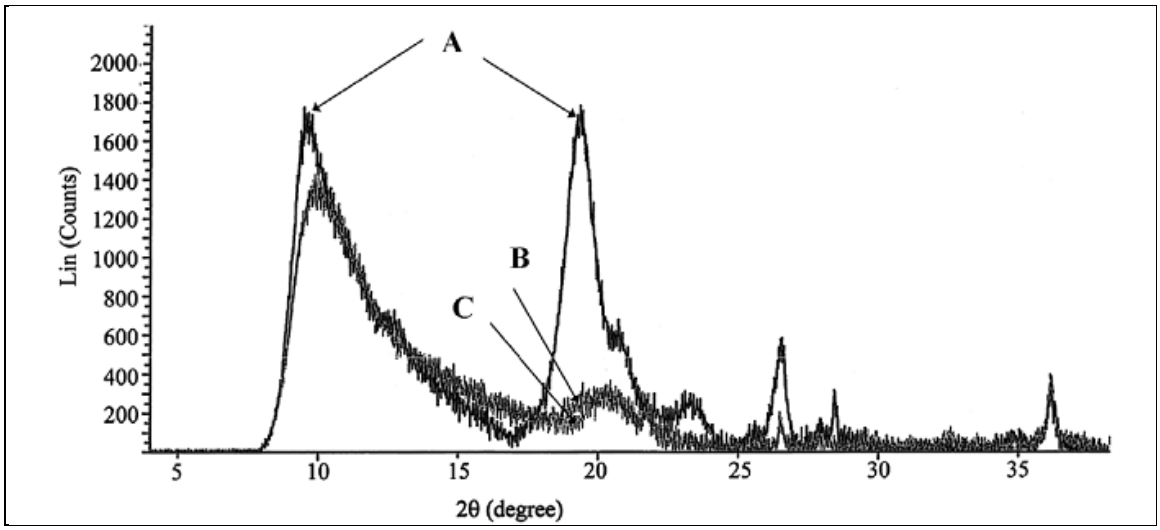

Figure 2.9 : XRD Pattern of (A) α-chitin of Tiger Prawn, (B) Corresponding Chitosan Prepared under Microwave Heating, (C) Chitosan Prepared under Traditional Heating [Adapted from Al Sagheer, Al-Sughayer, Muslim and Elsabee (2009)]

The crystalline index (CrI) of chitosan can be calculated from 110 phase judged based on polysaccharide diffraction studies after mathematical modification of the peaks with Lorentzian function (Focher, Beltrame, Naggi and Torri, 1990). The intensities of the peaks at 110 lattices (I_{110}, before 20° corresponding to maximum intensity) and at 16° (amorphous diffraction) were used to determine CrI_{110} is calculated based on Klug and Alexander's (1974) Equation as shown in Equation 2.3 (Al Sagheer, Al-Sughayer, Muslim and Elsabee, 2009, Klug and Alexander, 1974).

$$CrI_{110} = ({}^{I_{110} - I_{am}}/_{I_{110}}) \times 100 \qquad (2.3)$$

where,

CrI_{110} = Crystallinity index at 110 phase

I_{110} = Maximum intensity at around 20°

I_{am} = Amorphous diffraction at 16°

In a study of Zhang et al. (2005), 10° as was indexed as 020 phase and 20° as 110 phase. In his study, he proposed that crystallinity index at 020 phases shows

relative significance with degree of deacetylation (DDA). The crystallinity index of CrI_{020} is calculated based on Equation 2.4 (Focher, Beltrame, Naggi and Torri, 1990, Zhang et al., 2006).

$$CrI_{020} = (I_{020} - I_{am}) \times {}^{100}/_{I_{020}} \quad (2.4)$$

where,

CrI_{020} = Crystallinity index at 020 phase

I_{020} = maximum intensity below 13°

I_{am} = intensity of amorphous diffraction at 16°

XRD pattern was also investigated by Islam et al. (2011), which showed broad diffraction peaks at 2 θ = 10° and 21° that symbolised semi-crystalline chitosan. This was supported by Yen, Yang and Mau (2009) as the two characteristic crystalline peaks of chitosans at 9 - 10° and 19 - 20° with comparable crystallinity. The patterns were recorded with Philips PWO_4 XPert pro x-ray diffractometer sourced from Cu Kα with a voltage of 40 kV and a current of 30 mA at a range of 5 - 70° with scanning speed of 50 s^{-1}. Figure 2.10 shows the XRD pattern of chitosan from shrimp shells.

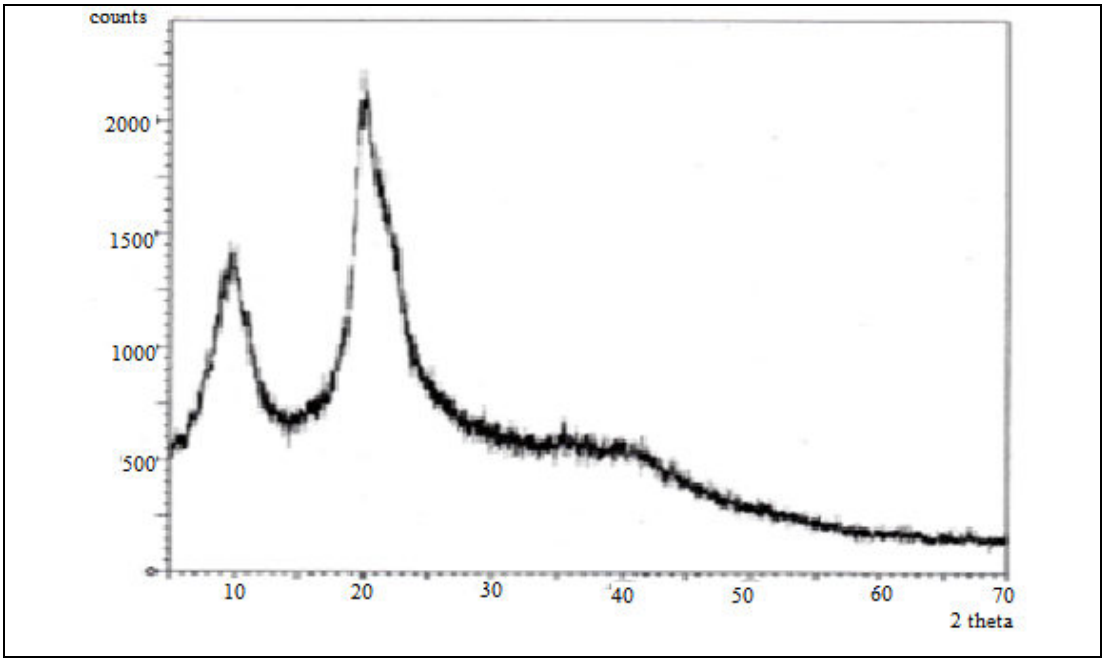

Figure 2.10 : XRD Pattern of Chitosan Extracted From Shrimp Shells [Adapted from Islam et al. (2011)]

At an effort of Trung et al. (2006) to produce chitosan from shrimp shells, two identical peaks approximately at 10° and 20° on a few different sample at different degree of deacetylation (DDA). In addition, higher crystallinity was observed from chitosan with lower DDA. Figure 2.11 shows the XRD pattern of chitosan with different DDA.

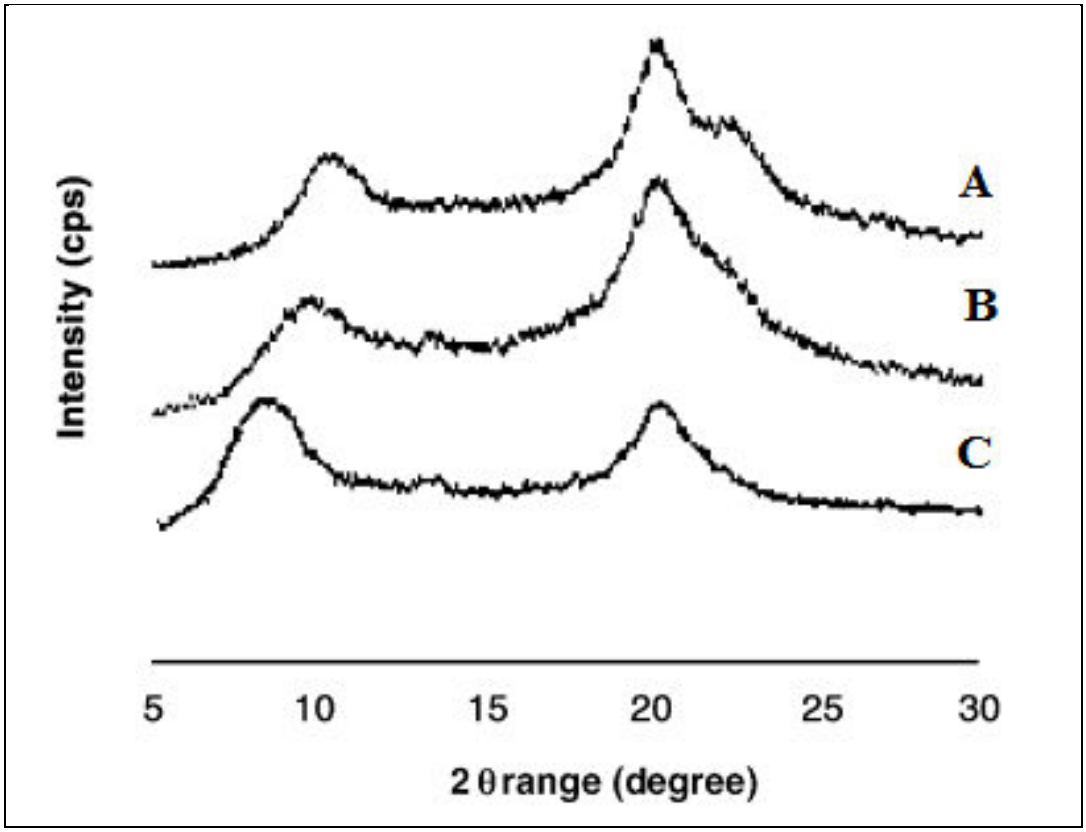

Figure 2.11 : XRD Pattern of Chitosan with (A) 96 % DDA, (B) 87 % DDA and (C) 75 % DDA [Adapted from Trung et al. (2006)]

2.5.4 Proton Nuclear Magnetic Resonance Spectroscopy (^{1}H NMR)

The degree of deacetylation (DDA) can also be determined by Proton Nuclear Magnetic Resonance Spectroscopy (^{1}H NMR) by integrals of the peak of the proton of the CH group connected to nitrogen moiety at 3.11 ppm of the deacetylated monomer unit (H1-D) and of the peak of the three protons of the acetyl group (H-Ac) at 1.99 ppm of the acetylated monomer unit as shown in the Equation 2.5.

$$\mathrm{DDA\%} = \left[\frac{\text{Area of } 3 \times \mathrm{H1-D}}{\text{Area of } 3 \times \mathrm{H1-D} + \text{Area of } \mathrm{H-Ac}}\right] \times 100 \qquad (2.5)$$

where,

H1-D = Intergrals of peak for deacetylated monomer unit

H-Ac = Intergrals of peak for three protons of acetyl group

Equation 2.5 was used by Mohammed, Williams and Tverezovskaya (2013) to determine the DDA% of its chitosan produced from shrimp shells. The ^{1}H NMR spectra was recorded by Bruker Avance DRX-500 (500 MHz) Spectrometer while the sample was prepared by dissolving 7 – 10 mg of chitosan in Deuterium chloride solution (1-10% DCl in D_2O) before the test. Figure 2.12 shows the ^{1}H NMR spectra of chitosan extracted from shrimp shells.

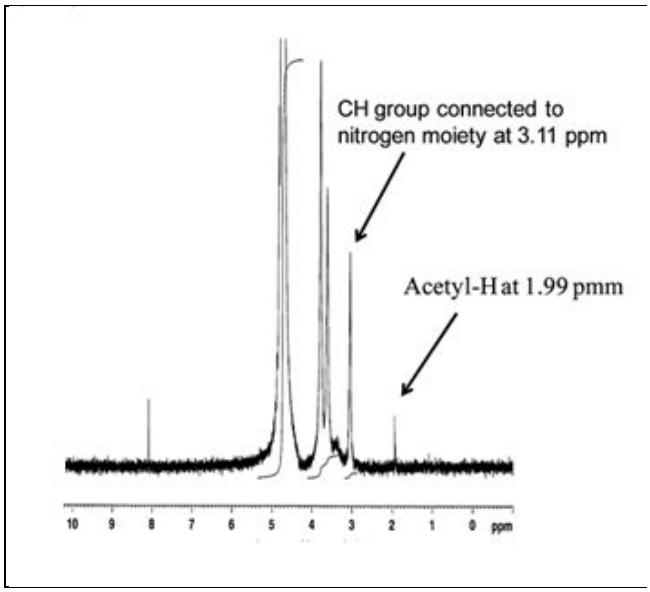

Figure 2.12 : ^{1}H NMR Spectrum of Chitosan Extracted from Shrimp Shells

[Adapted from Mohammed, Williams and Tverezovskaya (2013)]

CHAPTER 3

METHODOLOGY

3.1 Raw Materials and Chemicals Preparation

Raw shrimps stated as XL size were purchased from the local hypermarket, TESCO. In the study, two forms of sodium hydroxide were used. The liquid sodium hydroxide (NaOH) was obtained from R&M with purity of 48 – 50 % while the solid NaOH used in the study was purchased from CHEMSOLN with 99 % purity. Hydrochloride acid (HCl) having purity of 37 % and acetic acid used (AA) with purity of 99.8 % were bought from SYSTHERM. They were then diluted to the concentration required for the steps with distilled water. All chemicals were used without further purification.

3.2 Experimental procedures

The shells of these shrimps were scraped free of loose tissue, washed and dried. The product was then blended with electric blender and crushed with mortar to create shrimp shells powder.

After the shrimp shells powder was obtained, the effort to extract chitosan from shrimp shells was attempted with four methods naming as Method 1 (M1), Method 2 (M2), Method 3 (M3) and Method 4 (M4). The sequence of process, chemical concentration and treatment times were varied among the four methods.

The time, sequence, concentration of chemical used was compiled into Table 3.1. The details of the four methods will be described in the following topics.

Table 3.1 : Sample Name, Chemical, Time and Parameters for the Stages of Each Method

Method	M1	M2	M3	M4
Stage 1	**Deproteinisation** 2 N NaOH 1g:12ml 65°C 4 hrs	**Demineralisation** 1.3 N HCl 1g:14ml RT 24 hrs	**Deproteinisation** 1.25 N NaOH 1g:8ml 60°C (reflux) 2 hrs	**Precursor + Demineralisation** 1N NaOH + 1N HCl 1g:10ml + 1g:10ml 24hrs + 24 hrs
Stage 2	**Demineralisation** 3.25 N NaOH 1 g : 14 ml RT 4 hrs	**Deproteinisation** 1.25 N NaOH 1 g : 12 ml 90 °C 24 hrs	**Decolourisation** Acetone No ratio RT 24 hrs	**Deproteinisation** 1 N NaOH 1 g : 10 ml RT 24 hrs
Stage 3	Step Omitted	Step Omitted	**Demineralisation** 0.32N HCl 1g:10ml RT 24hrs	**Decolourisation** Acetone No ratio RT 24 hrs
De-acetylation	8.75N NaOH 1g:14 ml RT 72 hrs	17.5N NaOH 1g:14ml RT 72 hrs	12.5N NaOH 1g:5ml 100°C 10 hrs	12.5N NaOH 1g:10ml RT 24 hrs
Total Time at treatment (drying and preparation time neglected)	80 hrs	120 hrs	60 hrs	120 hrs

3.2.1 Method 1 (M1) for Chitosan Preparation

First, prepared shrimp shells powder was weighed with analytical balance to specific mass. Then, deproteinisation was carried out in using 2N NaOH with ratio of 12ml : 1 g (w/v) at 65 °C. The treatment was carried out for duration of 4 hours. The solution was then washed to neutrality under running tap water. The residue was then collected with 300 µm sieve and washed with distilled water. The immediate residue was brought to demineralisation process. The residue was then dried under the fume hood to a constant weight as it remained the same weight after three hours.

The residue from deproteinisation was weighed with analytical balance. Demineralisation was carried out with diluted HCl solution. The sample was treated with 10 % HCl (3.25 N) with ratio of 14ml : 1g (w/v) at room temperature. The treatment lasted for duration of 4 hours. The residue was then collected with 300 µm sieve and washed with distilled water. The residue was then dried under the fume hood to a constant weight and labelled as M1_CHT.

The product from demineralisation was measured with analytical balance. Then, it underwent deacetylation with 35 % NaOH (8.75 N) with ratio of 14 ml : 1g (w/v) at room temperature. The treatment lasted for duration of 72 hours. The solution was stirred with glass rod after some time. The residue was then collected with 300 µm sieve and washed with distilled water. The residue was then dried under the fume hood to a constant weight and then labelled as M1_CHS. M1_CHS was the final product of M1.

3.2.2 Method 2 (M2) for Chitosan Preparation

First, prepared shrimp shells were weighed with analytical balance to specific mass. Then, demineralisation was done with 4 % HCl (1.3 N) with ratio of 14ml : 1g (w/v) at room temperature. The treatment was carried out for duration of 24 hours. The solution was then washed to neutrality under running tap water. The residue was then collected with 300 µm sieve and washed with distilled water. The residue was dried under the fume hood to a constant weight before proceeding to deproteinisation.

The residue from demineralisation was weighed with analytical balance. Followed by, deproteinisation was carried out using 5 % NaOH (1.25 N) with ratio of 12ml : 1g (w/v) at 90 °C. The treatment lasted for duration of 24 hours. The residue was then collected with 300 µm sieve and washed with distilled water. The residue was dried under the fume hood to a constant weight and labelled as M2_CHT before proceeding to N-deacetylation.

From demineralisation, the product was weighed with analytical balance. Then, it was treated with 70 % NaOH (17.5 N) with ratio of 14ml: 1g (w/v) at room temperature. The treatment lasted for duration of 72 hours. The solution was stirred with glass rod after some time. The residue was then collected with 300 µm sieve and washed with distilled water. The residue was then dried under the fume hood to a constant weight and labelled as M2_CHS.

3.2.3 Method 3 (M3) for Chitosan Preparation

First, the prepared shrimp shells were weighed with an analytical balance to specific mass. The deproteinisation process was proceded using 5 % NaOH (1.25 N) with a weight to volume ratio of 1 g : 8 ml (w/v). The solution with shrimp shells was then set under reflux condition with a condition of 60 °C for 2 hours. The product was then collected with 300 µm sieve and washed until clear solution. It was then dried under the fume hood to constant weight.

The product from deproteinisation was then decolourised with pure acetone for 24 hours. The product was then collected with a 300 µm sieve and washed to neutrality. It was then dried under the fume hood to constant weight.

The products from decolourisation was demineralised using 1% HCl (0.32 N) with a weight to volume ratio of 1 g : 10 ml for 24 hours at room temperature. The product was then collected with a 300 µm sieve and washed to light brown powder which name as M3_CHT.

From demineralisation, the product was weighed with analytical balance. The sample was N-deacetylated using 50 % NaOH (12.5 N) with weight to volume ratio of 1 g : 5 ml at 100 °C for 10 hours. The product labelled as M3_CHS was washed with distilled water and dried under the fume hood to constant weight.

3.2.4 Method 4 (M4) for Chitosan Preparation

First, the prepared shrimp shells was weighed with analytical balance to a specific mass. It was then soaked into 1 N NaOH (4 %) with weight to volume ratio of 1 g: 10 ml for 24 hours at room temperature as a precursor treatment. It was washed and dried in vacuum to constant weight.

The residues from the precursor alkaline treatment were then treated using 1N HCl (3%) with weight to volume ratio of 1 g: 10 ml for 24 hours at room temperature for demineralisation. It was washed and dried in vacuum to constant weight.

The product from demineralisation was treated using 1 M NaOH (4 %) with weight to volume ratio of 1 g: 10 ml for 24 hours at room temperature. It was washed and dried in vacuum to constant weight.

The product from deproteinisation was decolourised using pure acetone with for 24 hours at room temperature. It was washed and dried in vacuum to a constant weight and the product is named as M4_CHT.

From decolourisation, the product was then deacetylated using 50 % NaOH with weight to volume ratio of 1 g: 10 ml for 24 hours at room temperature. The product labelled as M2_CHS was then washed and dried in vacuum to a constant weight.

The products from the four methods were required to be characterised into chitosan. First, solubility of the product in acetic acid acts as a preliminary test. Then, scanning electron microscopy (SEM) and electron dispense spectroscopy (EDS) were done to observe the surface morphology of the product in microscopic range. X-ray

diffractometry (XRD) to analyse the crystallinity of the product. Lastly, a Fourier Transform Infrared Spectroscopy (FT-IR) to identify the functional group within the product and to characterise the product as chitosan.

3.2.5 Dissolved Chitosan and Mixture with Iron Oxide Nanoparticles (S2_IO)

For dissolved chitosan, the specimens were diluted in 10% acetic acid with weight to volume ratio of 1 g: 100 ml. Only M2_CHS was diluted in acetic acid and dissolved sample is named as M2_CHS_AA.

The diluted chitosan extracted from M2 was also mixed with same weight portion of iron oxide nanoparticles labelled as S2_IO the mixture was then diluted in 10% acetic acid with weight to volume ratio of 1 g: 50 ml. The mixture is named as M2_S2_AA.

A drop of the dissolved chitosan solution and the mixture solution with iron oxide nanoparticles were dried on pieces of aluminium foil 2 cm x 2 cm and allowed to be dried under the fume fume hood for 2 hours to create a thin layer of film on the aluminium foil. After dried, the samples were named as D_M2_CHS_AA and D_M2_S2_AA respectively.

3.3 Characterisation

3.3.1 Solubility Test

According to Alvarenga (2011) chitosan is soluble after stirring in acids such as acetic, nitric, hydrochloric, perchloric and phosphoric but still insoluble in water, organic solvents and aqueous bases.

The final product from the four methods (M1_CHS, M2_CHS, M3_CHS & M4_CHS) were tested with solubility test to preliminary identify the product as chitosan. In the solubility test, acetic acid was diluted to concentration of 10%. Then, the acetic acid was poured to the chitosan at ratio of 1g: 100mL. It was then left at room temperature to dissolve for 24 hrs.

3.3.2 Scanning Electron Microscopy (SEM) and Energy-dispersive Spectroscopy (EDS/EDAX)

Scanning Electron Microscopy (SEM) analysis is a non-destructive testing where x-ray generated by electron interactions do not lead to volume loss of the sample, so it is possible to analyze the same sample repeatedly. The SEM projects visualization at the surface of solid specimens from the signal derived from the focused beam of high-energy electrons emitted, which is called as surface morphology. With help of certain functional device, the signals also recovered information on distribution of chemical composition with EDS, crystalline structure and orientation of the compiling compounds with electron backscatter diffraction (EBSD) (Swapp, 2012, Goldstein, 2003, Egerton, 2005).

The SEM has the choice to analyze at selected point locations on the sample and useful in qualitatively analysis at distributions of chemical compositions with EDS function. Data were collected over a selected area of surface of the sample, where a 2 dimensional image is generated. Normally ranging from approximately 1 cm to 5 microns in width, the area of observation can be imaged in a scanning mode

with SEM in magnification ranging from 20X to approximately 30,000X and spatial resolution of 50 to 100 nm (Swapp, 2012, Goldstein, 2003, Egerton, 2005).

When the focused electron beam with high kinetic energy reached the solid sample, it will decelerate and produce a variety of signal such as secondary electrons (generates 2d SEM images), backscattered electrons (BSE), diffracted backscattered electrons (used by EBSD to determine crystal structures and orientations of minerals), photons (used for elemental analysis and continuum x-ray), cathodoluminescence (CL), and heat. In common application of SEM, Secondary electrons and backscattered electrons are commonly involved. Secondary electron shows morphology and topography on samples while backscattered electrons provide illustrating contrasts in composition in multiphase samples (Swapp, 2012, Goldstein, 2003, Egerton, 2005).

During the scanning, an inelastic collision between incident electrons with the electrons in discrete shells of atoms and excite the electron. As the excited electrons return to its normal states, they generate x-ray that with fixed wavelength for certain element depending on its oritials. Thus, the x-ray generated acts as characteristic trait for elements. The EDS function collects data on the magnitude of this x-ray and analyze on the chemical composition (Swapp, 2012, Goldstein, 2003, Egerton, 2005).

The surface morphology of the entire specimen was observed using Scanning Electron Microscopy. The samples powder were completely dried and then coated with gold in vacuum using sputter coater. The micrograph was captured using HITACHI S-3400N scanning electron microscope operated at 20kV.

The HITACHI S-3400N having EDAX function was also used to perform electron dispersive spectrometry (EDS) to analyse the distribution of element on the material surface. The sample used during SEM was also investigated using EDS function.

3.3.3 X-ray Difratometry (XRD) Analysis

X-ray diffraction (XRD) also known as x-ray crystallography is defined as an analytical technique used to indentify phase of a material and provided information on and unit cell dimensions. A key component of all diffraction is the angle between the incident and diffracted rays. Powder and single crystal diffraction vary in instrumentation beyond this. Generally, XRD is based on diffracted ray of monochromatic x-ray and a crystalline sample where crystalline structure will act as three-dimensional diffraction gratings for the x-ray wavelengths. This is similar to the spacing of planes in a crystal lattice (Dutrow and Clark, 2012, Cullity, 1978, Bish, 1989).

X-ray diffraction is now a common technique for the study of crystal structures and atomic spacing. Its application are 1) characterisation of crystalline materials, 2) identification of fine-grained minerals that are difficult to determine optically, 3) determination of unit cell dimensions and 4) measurement of sample purity. The analyzed materials were usually finely ground and homogenized before being tested (Dutrow and Clark, 2012, Cullity, 1978, Bish, 1989).

All diffraction method involves the use of x-ray where the x-ray were generated from a cathode ray tube. The x-ray produced is then filtered to generate monochromatic radiation which is directed towards the sample. According Bragg's Law ($n\lambda=2d \sin \theta$), The interaction of the incident rays with the sample produces diffracted ray which relates the wavelength of electromagnetic radiation to diffraction angle and the lattice spacing in a crystalline sample. The diffracted x-ray is then detected, processed and counted. By scanning the sample through a range of 2θangles, all possible diffraction directions of the lattice should be attained due to the random orientation of the powdered material. The diffraction peaks were then converted to d-spacings allows identification of the mineral where each mineral has a set of unique d-spacing (Dutrow and Clark, 2012, Cullity, 1978, Bish, 1989).

The entire specimen to be tested was weighed to a constant weight of 0.2g. The 1 cm diameter specimen holder was filled with Faster PVP stick glue and the 0.2g of specimen was poured to the surface and covered the filled glue. The surface

of the specimen holder must be made sure to be fully filled with sample and then it was compressed using a piece of flat, clean glass. The prepared specimen holder was then put in the allocated holder near the x-ray dispenser.

XRD measurement on powder samples were carried out (at 5-40° and RT) using SHIMAZU XRD-6000 x-ray diffractometer equipped with Ni-filtered Cu Kα radiation (λ=1.5406Å). The diffractometer was operated with 2° diverging and receiving slits at 50kV and 40mA and a continous scan was carried out with a step size of 0.02° and a step time of 0.2s.

The crystalinity index of 020 phases (CrI_{020}) was then found out using Equation 2.4 based on the date obtained from the diffractograms.

3.3.4 Fourier Transform Infrared (FT-IR) Spectroscopy

Fourier Transform Infrared Spectroscopy having the acronym of FT-IR is one of commonly used method of infrared spectroscopy. Infrared spectroscopy has been an effective technique for materials analysis in the laboratory for over few decades. In infrared Spectroscopy, IR radiation in different wavelength is released on to the sample where certain degree of radiation will be absorbed by the sample while the remains will transmit through. An infrared spectrum represents a fingerprint of a sample with absorption peaks. This will then form a spectrum showing the absorption and transmission of the sample molecule which correspond to the frequencies of vibrations between the bonds of the atoms which compile the material. The spectrum is unique for the material as it has the unique combination of atoms and no other compound can produce the same spectrum. Therefore infrared spectroscopy can result in a positive qualitative analysis of every different kind of material. In addition, the size of the peaks in the spectrum directly indicates the density of material present (Griffiths and de Hasseth, 2007, ThermoNicolet, 2001, Nishikida, Nishio and Hannah, 1995).

The test can be applied in several type of analysis such as identifying unknown materials, determine the quality or consistency of a sample, it can

determine the amount of components in a mixture. Some of advantages of FT-IR are non-destructive analysis where it gives precise measurement which need for external calibration; comparably better speed, sensitivity and user friendly. Together with modern software algorithms, infrared is an excellent tool for quantitative analysis (Griffiths and de Hasseth, 2007, ThermoNicolet, 2001, Nishikida, Nishio and Hannah, 1995).

Attenuated total reflection (ATR) is one of the common sampling techniques in FT-IR spectroscopy. FT-IR spectrometer nowadays comes with lots of accessory for simplicity of testing. For Instance, diamond ATR device suitable for hard and solid sample and germanium accessory is common with absorbing sample. However, these simplicities does present some challenge. ATR accessory generate different infrared spectrum of a sample as compared to the spectrum obtained by transmission. This is ATR technique generated difference in band intensity and frequency of the spectroscopy. The shift in intensity was slight while the major shift in frequency can result to displacement of peak maximum by several wavenumbers. This is important as most of the common available spectral library refers to transmission spectra, and the differences may create difficulties in interpretation of spectrum and ambiguous matching. Nevertheless, these relative shifts were understood and able to be corrected using a technique called advanced ATR correction (Nunn and Nishikida).

All the Infrared spectra were plotted on all specimen over the frequency range 4000-400cm^{-1} at resolution of 4cm^{-1} using Thermo Nicolet*IS*10 FT-IR Spectrometer with Thermo Scientific Smart Orbit accessory. The accessory is a diamond ATR device that has an indenter to indent solid onto the diamond reflector.

All the dried samples were ground to powder using mortar, placed sufficiently and indented onto the diamond reflector. As for the dissolved chitosan and the composite solution of chitosan/ iron oxide nanoparticles, the spectra were recorded after a drop of the both solution was placed on the diamond reflector.

The solution of dissolve chitosan and composite was dried a piece of aluminium foil. A random piece with size of 2 mm × 2 mm was cut out and indented

on the diamond reflector for FT-IR investigation. After all the obtained spectra obtained underwent advance attenuated total reflectance (ATR) correction.

Degree of deacetylation (DDA) of chitosan was estimated with the produced spectra of sample. The DDA of the chitosan sample was the calculated from absorbance at 1655 and 3450 cm^{-1} according to the following Equation 2.2 (Baxter, Dillon, Anthony Taylor and Roberts, 1992, Alvarenga, 2011):

.

CHAPTER 4

RESULTS AND DISCUSSION

4.1 Chitosan Yields & Efficiency of Methods

The yielding proportions of various products obtained at various stages of extraction by using four different methods are tabulated in Table 4.1.

Table 4.1 : Experimental Yield of Each Stage For Extraction of Chitosan from Shrimp Shells

Method	M1		M2		M3		M4	
	g	%	g	%	g	%	g	%
Shrimp Shells Powder	10.00		10.00		10.00		10.00	
Stage 1 %wt of Product Remained	5.42	54	3.12 ± 0.41	31	4.70	47	4.52	45
Stage 2 %wt of Product Remained	3.81	70	1.34 ± 0.07	43	4.04	86	2.05	45
Stage 3 %wt of Product Remained (CHT)	Step Omitted		Step Omitted		2.58	64	1.55	76
Deacetylation %wt of Product Remained (CHS)	1.65	43	0.82 ± 0.07	61	1.93	75	2.83	182
%wt of Final Product (CHS) Based On Dried Shells	17 %		8 %		19 %		28 %	

Fresh shrimp of 2005.00 g was purchased from TESCO. After shrimp shells were dried and grounded, 201.89 g shrimp shells powder was obtained. All the four

methods were purposed to extract chitosan from shrimp shells and they were suggested to be chitin before going through N-deactylation.

4.1.1 Method 1 (M1)

In this modified method, the treatment time used to produce expected chitin was shorten without compensate with any additional heating process, pressure, or higher concentration of chemical. Having a similar structure of treatment process with the study of Islam et al. (2011), it has withdrawn the decolourisation process which only discharges carotene pigment from the chitin (Bolat et al., 2010).

Method 1 (M1) that begins with deproteinisation, removed ~55 %wt from the shrimp shells powder. Followed by demineralisation which take away ~30 %wt of product left from deproteinisation. Skipped of decolourisation, N-deacetylation of M1 produced 1.65 g from 38.1 g left from stage 2 which generates a yield of ~43 %wt.

Compiling M1, the total treatment time used was 80 hours neglecting the drying time and specimen preparation time. In regards to the overall yield, M1 yield 17% of product from the dried shrimp shells.

This method was a combination of chitosan extraction method from different study. It was developed prior as to improve simplicity and efficiency. For deproteinisation and demineralisation, it was derived from a study by Mirzadeh et al. (2002) to synthesize chitosan from shrimp shells of Persian gulf. Meanwhile, N-deacetylations was referred to the effort of Islam et al. (2011) to create chitosan from shrimp shells. For M1, decolourisation was removed from the four steps procedure of shrimp shells chitosan extraction.

Rout (2001) reported that chitosan produced without decolourisation process had better fat binding capacity where other properties such as solubility were retained. However, withdrawing deproteinisation stage as attempted by No, Park, Lee and Meyers (2002) may result to product with drawback on solubility, higher

molecular weight, lower fat and water binding capacity. These results did not represent the characteristics of chitosan.

Extraction of chitosan from stage 1 to stage 2 took a day and only deacetylation used longer treatment time as it was the only process without complicated requirements such as autoclave condition (Bolat et al., 2010), nitrogen purging and high temperature reflux (Mirzadeh et al., 2002) at the time of reference. The effectiveness of the modification to produce chitosan will be discussed in later context.

4.1.2 Method 2 (M2)

Started with demineralisation, M2 left average of ~31 %wt in 3 attempts of synthesis in stage 1. Then, average of ~43 %wt of stage 1 product was left after deproteinisation. Similar to M1 which skipped decolourisation step, deacetylation of M2 yielded average of ~61 %wt of product with 3 attempts from the previous process.

Method 2 (M2) added up to a treatment time of 120 hours which did not include drying time and specimen preparation time. M2 has a general yield of ~8 %wt based on the shrimp shells powder used.

This method was slightly modified from the chitosan synthesizing method from shrimp shells used by Islam et al. (2011). Having accurate statement on ratio of chemical used with residue, treatment time and temperature implied, the method was said to be lengthy and less efficiency.

4.1.3 Method 3 (M3)

The product after deproteinisation is ~47 %wt from dried shrimp shells powder. Then, ~14 %wt of deproteinisation product was withdrawn in decolourisation step.

About 64 %wt of product from decolourisation remained after going through demineralisation of M3. Lastly, deacetylation of M3 gives a yield of 75 %wt from the product of its previous stage.

M3 was a modified chitosan extraction method from a study by Mohammed, Williams and Tverezovskaya (2013). As referred to their study, deproteinisation gave ~45 %wt of product as the first stage. Then, decolourisation took off 0.7 - 1.4 %wt from the remained of deproteinisation.

M3 used a total of 60 hours treatment time to produce the final product and has a general yield of 19 %wt based on dried shrimp shells. In the study of Mohammed, Williams and Tverezovskaya (2013), they produced about 25 %wt of chitosan from the dried shrimp shells powder.

As mentioned, this method was a direct derivation from the study of Mohammed, Williams and Tverezovskaya (2013) which has a lowest process time among the four methods (refer to Table 3.1). However, it is the most complicated method used among the four with the use of reflux condition and implication of high temperature. Nevertheless, it is suggested as one of the most efficient way to produce chitosan in the study.

4.1.4 Method 4 (M4)

Begin with a precursor treatment similar to deproteinisation, it was combined with demineralisation as first stage. Collectively, both give a yield of ~45 %wt from shrimp shells powder. Next, deproteinisation in second stage produces ~45 %wt of product from what was left. Then, decolourisation took out ~34 %wt of remained from deproteinisation. Lastly, N-deacetylation produces 2.83 g of product which is 182 %wt of the residue from deproteinisation.

Adding up all the time in treatment, M4 requires a total treatment time of 120 hours. 28 %wt of product was extracted from shrimp shells powder by using M4. Modification was suggested on the chemical used for decolourisation where, acetone

was chosen as being more common and simplicity (Mirzadeh et al., 2002, Mohammed, Hember, Richardson and Morris, 1998, Bolat et al., 2010) instead of potassium permanganate ($KMNO_4$) and Oxalic Acid (Teli and Sheikh, 2012).

This method was derived from a method to extracted chitosan from shrimp shells used by Teli and Sheikh (2012). Unlike other methods, this method did not include any heating process and ratio of chemical used as it was not mentioned in the reference journal. The solute to solvent ratio for residue and chemical is very important in the processes of synthesizing chitin / chitosan (Mohammed, Williams and Tverezovskaya, 2013, Islam et al., 2011, No and Lee, 1995). Thus, ratio of 1 g : 10 ml (w/v) was suggested in references to Moorjani et al. (1978).

Furthermore, the method did not include any heating process especially on deproteinisation as common practiced (Mirzadeh et al., 2002, Islam et al., 2011, Mohammed, Williams and Tverezovskaya, 2013, No and Lee, 1995, Bolat et al., 2010). Heat is a vital factor for deproteinisation process, where it deforms the structure of protein through denaturisation and enable chemical to withdraw the decomposed protein (deMan, 1999). Without heat, protein cannot be efficiently withdrawn and other stage such as N-deacetylation cannot perform effectively and conversion of shrimp shells into chitosan will be restricted.

In general yield, M4 gives about 28 %wt of product from shrimp shells powder followed by M3 giving 19 %wt, M1 of 17%, and 8% of M2. Comparing the mass of the product before and after N-deacetylation, it was observed that the mass had gone up by 182 %.

N-deacetylation is a process that partially withdraw acetyl group from 2-acetamido -2deoxy-D-glucose polymer chain of chitin (Al Sagheer, Al-Sughayer, Muslim and Elsabee, 2009). Therefore, after N-deacetylation a reduction in weight should be observed (Mohammed, Williams and Tverezovskaya, 2013). The increase in weight is suggested as a possibility of the compound being contaminated.

Among the four methods, M3 proposed the least treatment time of 60 hours while M2 and M4 required 120 hours of treatment time. Although all of the methods

were proposed to produce chitosan, however the product from each process may not be definite chitosan. Meanwhile, the effectiveness of each method in this study greatly depends on the whether the product produced is chitosan. Therefore, characterisation test like infrared spectroscopy was used to justify the effectiveness of each method.

Although a detailed characterisation testing can allow us to identify the compound, but a preliminary test can give the researcher a pre-justification on the product to decide what test should be done to examine the sample. So the solubility differences between chitin and chitosan act as a test to differ and give brief idea on the products produced from each method.

4.2 Solubility Test

In common, it is justified that main physical differences between chitin and chitosan is the ability of chitosan to be soluble in organic acid such as acetic acid. Chitosan with higher content of protonated amino group are readily to form well ordered arrangement in Van der Waals force and hydrogen bond which exceed its tendency for intramolecular chemical bonds (Zhang et al., 2012, He, Chen and Dong, 2001). This explains its solubility in acidic chemical and partial solubility in hydrogen containing solvent.

As shown in Figure 4.1, solubility was observed from M2_CHS and M3_CHS while many residues were still remains as insoluble for M1_CHS and M4_CHS after 24 hours of immersion. As chitosan contains higher contents of highly protonated free amino groups which attracts ionic compound, this allows chitosan to dissolve in certain inorganic acid such as acetic acid (Kumar, 2000, Zhang et al., 2012). Chitin with insufficient protonated amino group due to lack of degree of deacetylation (DDA) was insoluble in acidic medium (Hudson and Smith, 1998, Mohammed, Williams and Tverezovskaya, 2013, Islam et al., 2011, Kumar, 2000, Alvarenga, 2011, Zhang et al., 2012). Therefore, those that are not soluble in acidic acid first presumed as chitin with insufficient DDA.

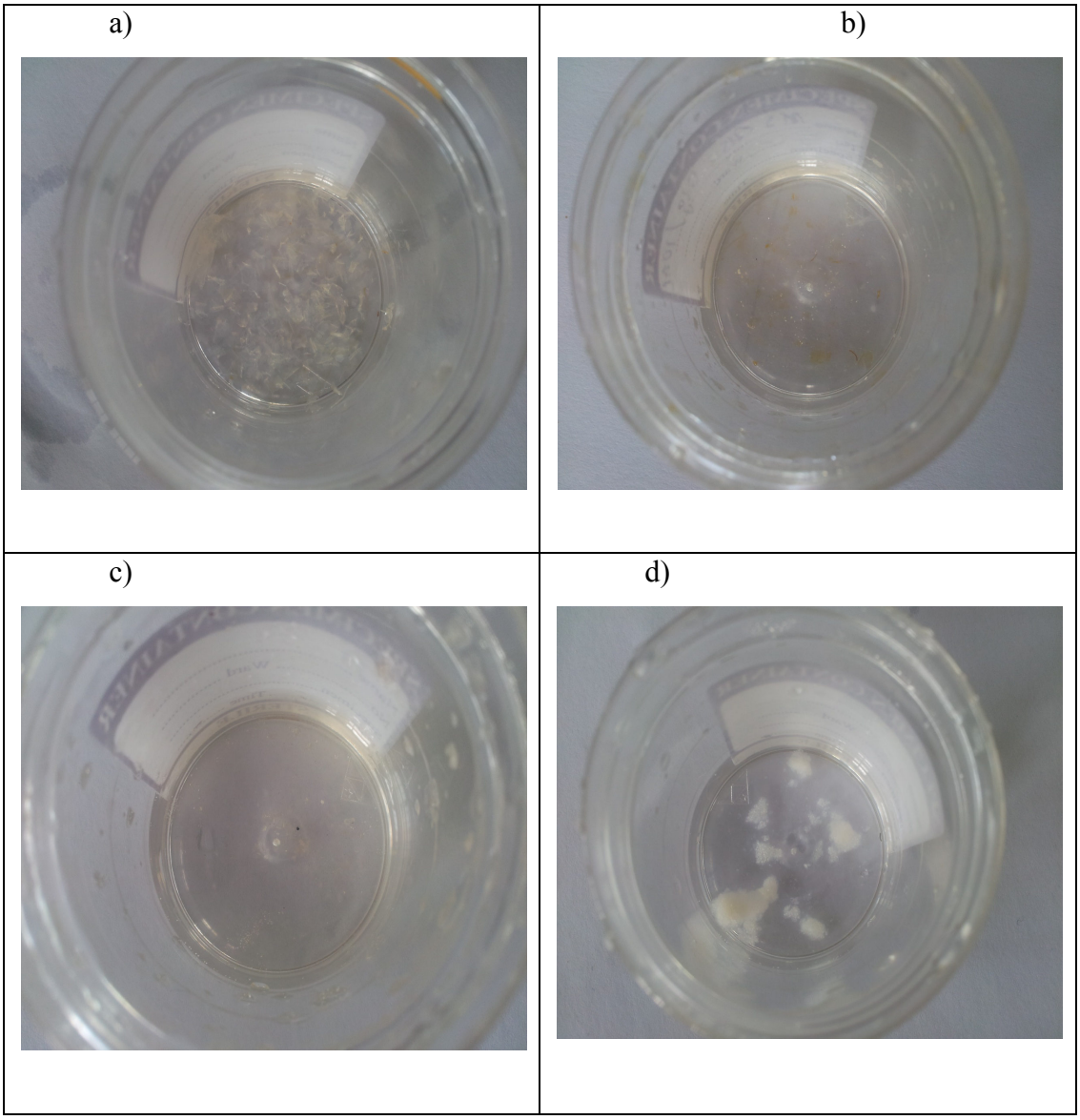

Figure 4.1 : Solubility Test on Final Product for 4 Methods in 10% Acetic Acid for 24 hours (a) M1_CHS, (b) M2_CHS, (c) M3_CHS and (d) M4_CHS

Zhang et al. (2006) stated that half deacetylated chitosan appearing as viscous and translucent in solvent where some fraction at lower molecular weight were soluble and the others may swollen. This is observed in the M1_CHS of M1 as shown in Figure 4.1(a).

M4_CHS appeared as coagulation of white powders was not influenced by the acetic acid (AA) after 24 hours immersed (Figure 4.1d). However, after 72 hours

the white coagulation had dissolved and a white solution was formed as shown in Figure 4.2. This may due to the formation of contamination layer on the surface of particle product which prevents solubility when going through the N-deaectylation process with 50% NaOH in M4 (Arbia, Arbia, Adour and Amrane, 2011).

Figure 4.2 : M4_CHS in 10% Acetic Acid after 72 hours

After the preliminary test, the potential of the product to be chitosan is understood. Next, the product of each method was brought towards to microscopy scale on the surface to understanding its morphology using SEM microscope.

4.3 Scanning Electron Microscopy (SEM)

Figure 4.3 shows the SEM micrograph of dried shrimp shells powder in 1000 × magnification. The morphology has globules of crystalline structure with smooth surface. As it was prepared as fine ground powder, the morphology shows that the specimen is in particle structures.

In a study of Zhang et al. (2012), the morphology of shrimp shells was described as microfibrillar crystalline structure with large portion of surface structure. As the authors used a magnification of 2000 ×, this observation may had focused on the smooth surface of the globule particle structure showed at 1000 × magnification of Figure 4.3.

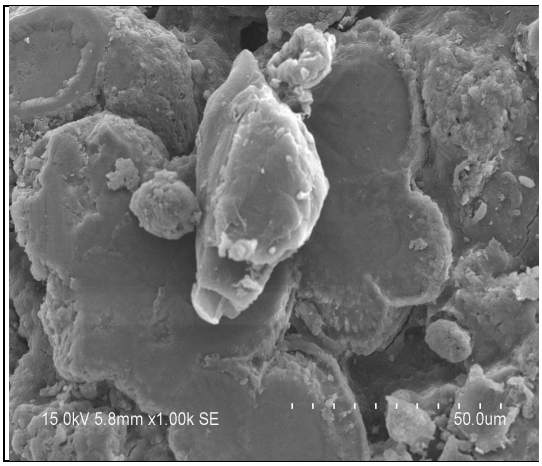

Figure 4.3 : SEM Micrograph of Shrimp Shells Powder

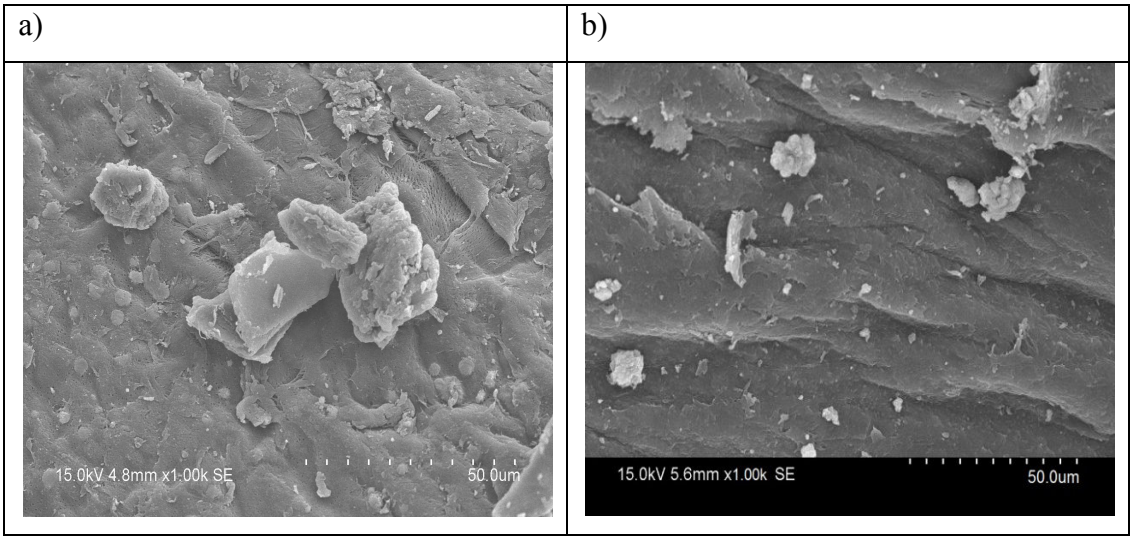

Figure 4.4 : SEM Micrographs of (a) M1_CHT and (b) M1_CHS from M1

From Figure 4.4(a), it is observed that M1_CHT shows lesser and smaller globule structures and larger surface structures compare to shrimp shells powder. Compare to Figure 4.4(a), Figure 4.4(b) shows smaller and lesser globule structures on M1_CHS with obvious lamellar surface organisation.

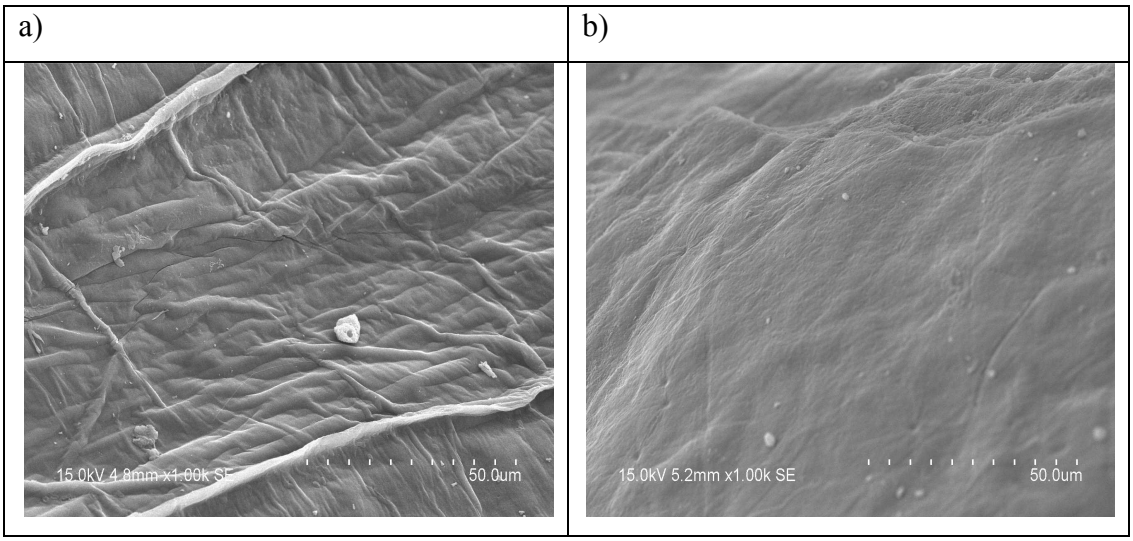

Figure 4.5 : SEM Micrographs of (a) M2_CHT and (b) M2_CHS from M2

The Figure 4.5(a) shows M2_CHT of having few crystal structures on surface with straps and shrinkage. Meanwhile, Figure 4.5(b) shows M2_CHS having a clearer and smoother surface with slight inhomogeneous and tiny particle.

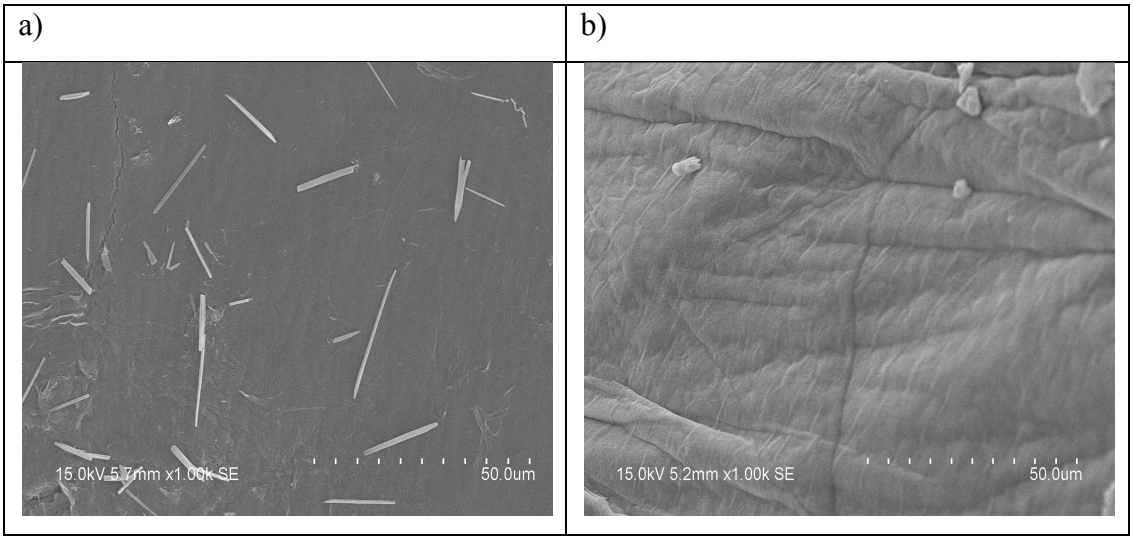

Figure 4.6 : SEM Micrographs of (a) M3_CHT and (b) M3_CHS from M3

The morphology of M3_CHT showed in Figure 4.6(a) has long and thin crystal structure on a relative smooth surface. Meanwhile, M3_CHS shows some particle structure on a lamellar surface with shrinkage and straps in Figure 4.6(b).

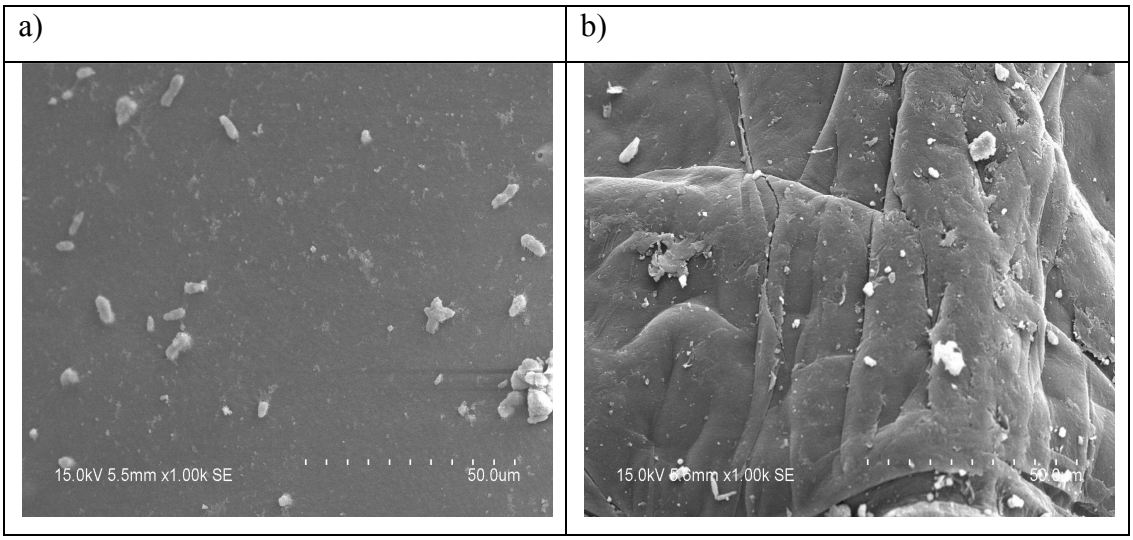

Figure 4.7 : SEM Micrographs of (a) M4_CHT and (b) M4_CHS from M4

Figure 4.7(a) displays the surface morphology of M4_CHT which shows some small particles laying on a smooth surface. The surface of M4_CHS in Figure 4.7(b) shows a lamellar organisation with dark contrast of straps and shrinkage on surface which contains much particle structures of variable size.

The morphology chitin as studied by Al Sagheer, Al-Sughayer, Muslim and Elsabee (2009) was a very uniform structure with dense lamellar organisation and some crystalline structure on surface. This description is best match to morphology of M2_CHT at Figure 4.5(a), but is also partially matching to M1_CHS at Figure 4.4(b) and M4_CHS at Figure 4.7(b) as they both show lamellar organisation on surface but having too much crystal on surface.

For M1_CHT at Figure 4.4(a) which was proposed as chitin from M1 has morphology more alike to shrimp shells powder with much globule structures. No lamellar arrangement on Figure 4.6(a) shows the morphology of M3_CHT to be different with the description of Al Sagheer, Al-Sughayer, Muslim and Elsabee (2009) but some crystal structure was observed. This is similar to M4_CHT at Figure 4.7(a) with differences in particle size and shape.

Islam et al. (2011) reported that chitosan has a non homogenous and non smooth surface with straps and shrinkage. This morphology type was also supported

by El-Hefian, Nasef, Yahaya and Khan (2010). M2_CHS at Figure 4.5(b) and M3_CHS at Figure 4.6(b) which show that the proposed chitosan of respective M2 and M3 having such trends on morphology. Meanwhile, the proposed chitosan of M1 and M4 (M1_CHS and M4_CHS) are having surface with much crystal residues which are much alike to the morphology of chitin.

Apart from morphology, EDS as an add-on function of SEM is a common spectroscopy to identify chemical elements distributed on the surface of the sample. This test provides further understanding on the substances contained on surface.

4.4 Electron Dispersive Spectroscopy (EDS)

Electron Dispersive Spectroscopy (EDS) is a test to examine the presence of elements through amplitude of wavelength for the x-ray emitted after the electron was hit by the electron beam. For the emission of x-ray, the atoms must contain minimum of K-shell and L-shell where the electron is allow to dislodge from shell to shell. Therefore, hydrogen being the only elements in the periodic table with only K-shell is not detectable with EDS (Swapp, 2012, Goldstein, 2003, Egerton, 2005).

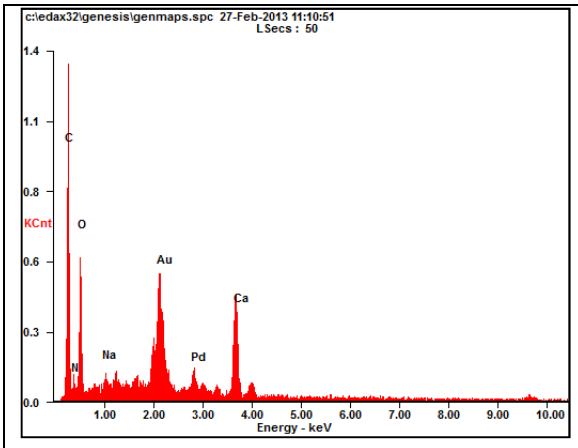

Element	Wt%	At%
CK	09.51	38.74
NK	01.16	04.05
OK	08.27	25.31
NaK	00.41	00.87
AuM	65.56	16.29
PdL	04.83	02.22
CaK	10.26	12.53
Matrix	Correction	MThin

Figure 4.8 : EDS Spectrum and Distribution of Element for Shrimp Shells Powder

As shown in Figure 4.8, shrimp shells powder shows the existence of carbon, nitrogen, oxygen, sodium, calcium, gold and palladium.

Generally, shrimp shells are composed of carbohydrate as its main component, some mineral content (Calcium Carbonate, $CaCO_3$) to act as a external protection for the shrimp, some protein content to link the shells to its flesh and pigment content to show nature colour of shrimp (Ravichandran, Rameshkumar and Prince, 2009).

Polysaccharides are commonly composed of carbon, oxygen, hydrogen and some nitrogen. During the inspection of SEM, the prepared sample was usually sputter coated to give better morphology for non–conductive material (Egerton, 2005, Goldstein, 2003). As for chitosan this practice is common (Islam et al., 2011, Zhang et al., 2012, Teli and Sheikh, 2012, Mirzadeh et al., 2002). Therefore, the content of gold and palladium indicates that the existence of the coated layer of gold and palladium composite.

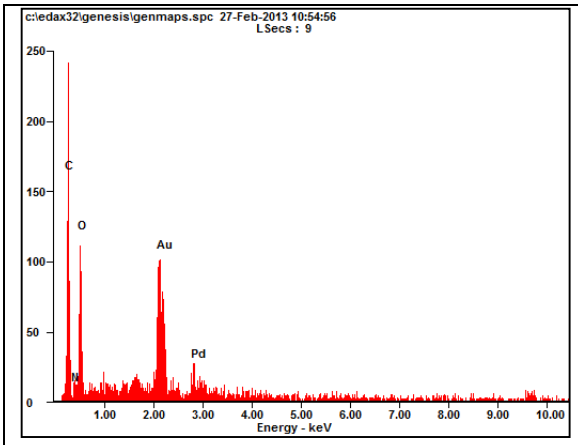

Element	Wt%	At%
CK	08.31	39.83
NK	01.27	05.24
OK	08.16	29.39
AuM	76.24	22.29
PdL	06.01	03.25
Matrix	Correction	MThin

Figure 4.9 : EDS Spectrum and Distribution of Element for M1_CHS of M1

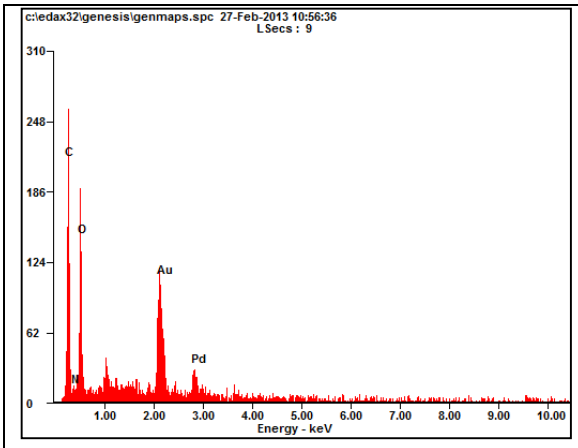

Element	Wt%	At%
CK	09.64	40.56
NK	00.82	02.98
OK	11.06	34.94
AuM	72.06	18.48
PdL	06.41	03.04
Matrix	Correction	MThin

Figure 4.10 : EDS Spectrum and Distributions of Element for M2_CHS of M2

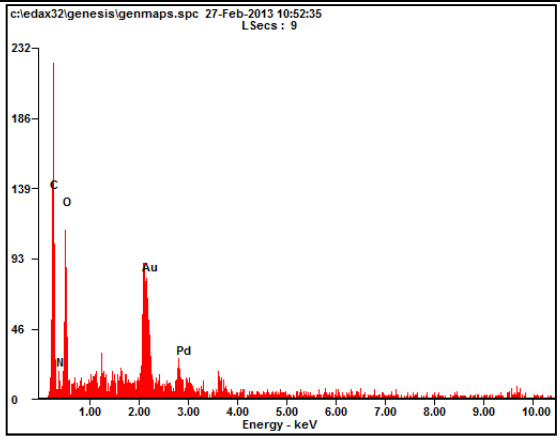

Element	Wt%	At%
CK	09.00	39.86
NK	01.33	05.05
OK	09.67	32.14
AuM	74.17	20.02
PdL	05.83	02.91
Matrix	Correction	MThin

Figure 4.11 : EDS Spectrum and Distributions of Element for M3_CHS of M3

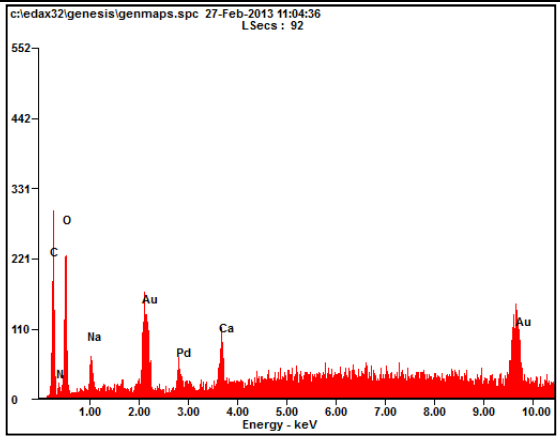

Element	Wt%	At%
CK	07.03	29.29
NK	00.97	03.48
OK	11.37	35.58
NaK	02.05	04.46
AuM	66.07	16.79
PdL	06.69	03.15
CaK	05.82	07.26
Matrix	Correction	MThin

Figure 4.12 : EDS Spectrum and Distributions of Element for M4_CHS of M4

Figure 4.9 - 4.12 show the EDS spectra of product for all four methods. M1_CHS, M2_CHS and M3_CHS show the composition of carbon, nitrogen,

oxygen, gold and palladium while M4_CHS also shows presence of calcium and sodium elements.

Chitosan is a homopolymer of β-(1-4)-linked D-glucosamine and N-acetyl-D-glucosamine where the ratio of the compound strongly depends on the degree of deacetylation (DDA). Chitin was converted from shrimp shells after deproteinisation, demineralisation and decolourisation. Then, chitin represented by chemical formula of $(C_8H_{13}O_5N)_n$ was derived to chitosan after partial withdrawal of acetyl (C_2H_3O) group. Therefore, the remaining element in chitosan should only be carbon, hydrogen, oxygen and nitrogen (Marthur and Narang, 1990, Kumar, 2000, Shahidi and Abuzaytoun, 2005, Harish Prashanth and Thanathan, 2007).

M4_CHS shows content of calcium and sodium. Different with others, it displays the possibility of the sample to be contaminated. As these extra elements existed on the shrimp shells powder, the contaminations may due to insufficient process or improper process condition. M4 did not incorporate any heat in the deproteinisation process, it is suggested the protein may not be withdrawn effectively and further influence on the withdrawal of mineral during demineralisation. However, the degree of protein withdrawal was not able to detect using EDS. This is because the elements in protein are carbon, hydrogen, nitrogen and oxygen (deMan, 1999) and are similar to chitin or chitosan (Shahidi and Abuzaytoun, 2005). Therefore, protein content in the sample is undetectable under EDS.

EDS only provides details of chemical distribution in the sample, so it is unable to provide adequate characterisation of samples. Thus, the information of chemical structure can be understood through lattice parameter by x-ray Diffractometry (XRD). In addition, the crystallinity or each substance can be investigated simultaneously.

4.5 X-ray Diffactometry Analysis (XRD)

Figure 4.13 shows the comparison of XRD diffractograms between M1_CHS and M2_CHT. M1_CHS was not able to dissolve accordingly in diluted acetic acid as compared to M2_CHS and M3_CHS. So diffractogram of M1_CHS is compared to M2_CHT which is expected as chitin that displays insolubility in acetic acid.

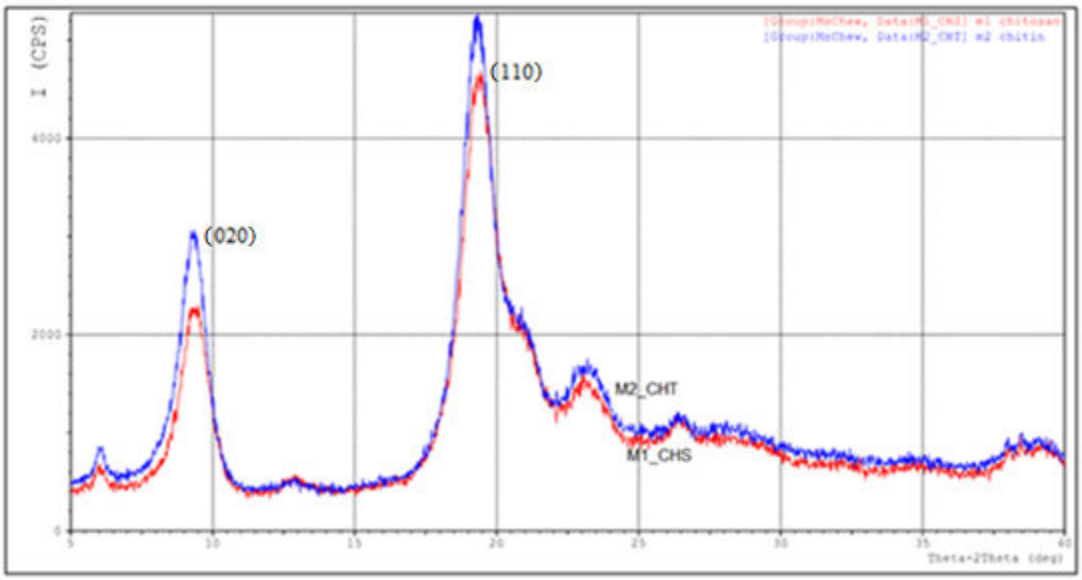

Figure 4.13 : Comparison of XRD Diffractogram between M1_CHS and M2_CHT

Reffering to Appendix A and B, the strongest three peaks of M1_CHS are 19.42° with an intensity of 1590 counts, 9.35° with intensity of 740 counts and 21.14° with intensity of 490 counts. Meanwhile, the three strongest peak in M2_CHT are 19.33° with intensity of 1790 counts, 9.29° with intensity of 1008 counts and 21.10° with intensity of 504 counts. As compared, the M1_CHS has significant peaks similar with M2_CHT. Both diffractograms display some overlapping but M1_CHS having lesser intensity than M2_CHT displaying a general trend of lesser crystallinity.

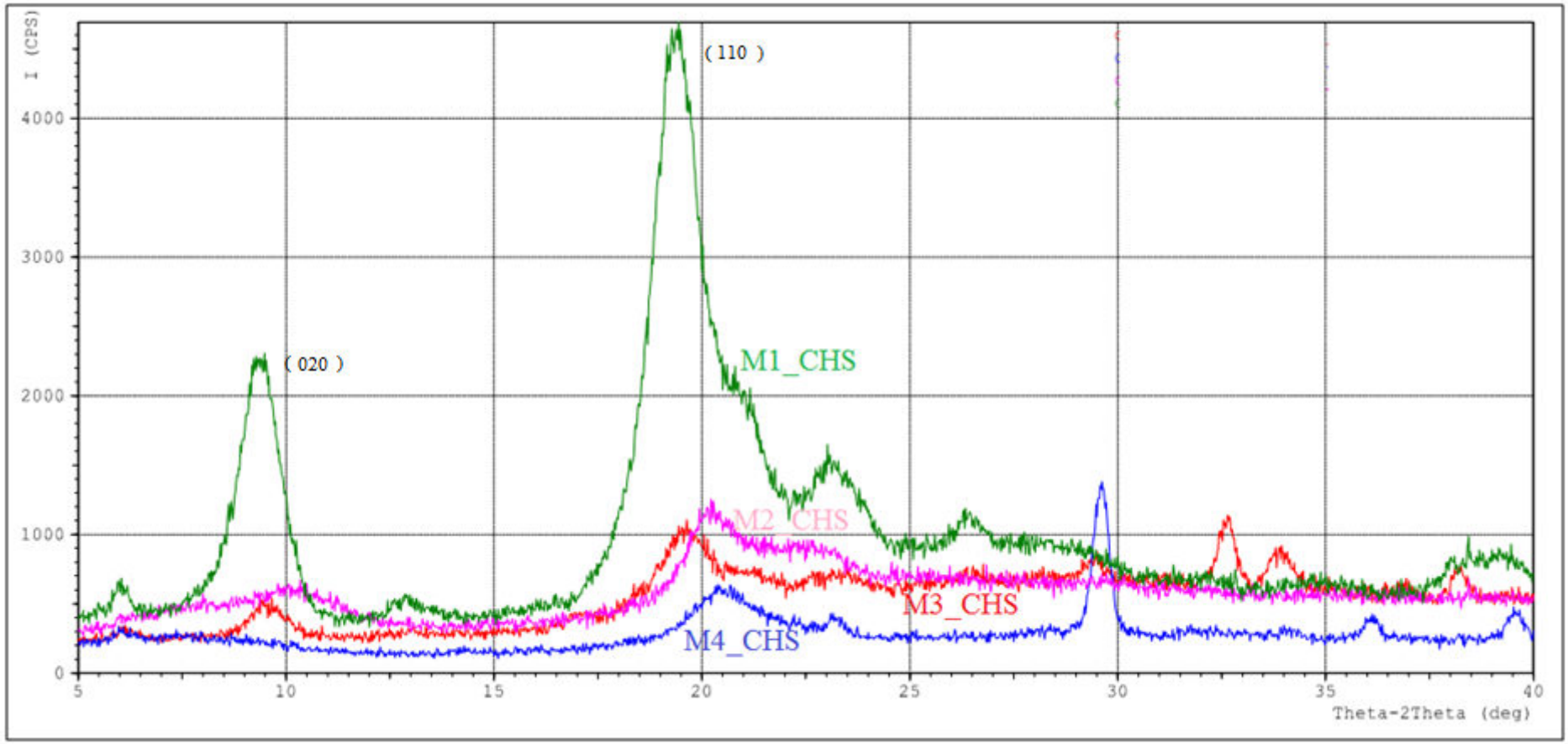

Figure 4.14 : XRD Diffractogram for M1_CHS, M2_CHS, M3_CHS and M4_CHS

Chitin described by Zhang et al. (2005) has significant peaks near 9.39° and 19.22° which were slightly differed with chitosan. Thus, M2_CHT having these characterisation peaks can be determined as chitin. Correspondingly, M1_CHS with peaks at 9.35° and 19.42° are more proximate towards the peak of chitin than chitosan (Islam et al., 2011, Bangyekan, Aht-Ong and Srikulkit, 2006, Trung et al., 2006). Therefore, M1_CHS is suggested to be chitin.

Figure 4.14 shows the comparison of XRD diffractogram among the products of the four extraction methods. In addition, data of the diffractograms are attached as APPENDIX A, B, C, D and E.

As for M2_CHS, the strongest three peaks are at 20.12° with intensity of 267 counts, 22.36° with intensity of 150 counts and 9.94° with intensity of 104 counts. Then, the strongest three peaks for M3_CHS are 19.65° with intensity of 236 counts, 32.58° with intensity of 178 counts and 33.89° with intensity of 115 counts. It also has lower but broader peak at 9.55° and displays an intensity of 93 counts. Next, the strongest three peaks for M4_CHS are 29.57° with intensity of 426 counts, 20.48° with intensity of 144 counts and 39.52° with intensity of 78 counts. It also has a lower but broader peak at 9.78° and displays an intensity of 14 counts.

M2_CHS and M3_CHS exhibit significant broad diffraction peaks on around 10° and 20°. Meanwhile, M4_CHS displays less significant peaks near 20° at 10°. M2_CHS has the two significant peaks more approximate to 10° and 20°.The broad diffraction peaks 10° and 20° are typical identification for semi-crystalline chitosan (Islam et al., 2011, Bangyekan, Aht-Ong and Srikulkit, 2006, Trung et al., 2006, Zhang et al., 2012, Zhang et al., 2006).

An intense peak shown by M4_CHS near 30° displays the possible content of contaminant. As the strongest peaks in diffractogram with intensity of 426 counts, it is shown as other crystalline substance as the peaks is not consistent to diffractograms of other samples or chitosan from other studies (Al Sagheer, Al-Sughayer, Muslim and Elsabee, 2009). The high intense peaks appeared in near 30° was also significant in the XRD diffractogram of shrimp shells powder displayed as APPENDIX F. This is suggested that the contamination on M4_CHS was pre-

accumulated in the form of shrimp shells before being processed. It is proposed that a compound with high crystallinity could fail to be withdrawn during the process. In a study, Rao, Muňoz and Stevens (2000) found that chitin was shielded with a layer of protein structure in the form of shrimp shells and easily calcified with salts forming a hard shells structure if not properly withdrawn (Arbia, Arbia, Adour and Amrane, 2011). From the result of EDS shown in Figure 4.12, it was observed that M4_CHS contains content of calcium and sodium which are the source of calcification. These evidences explained the condition of M4_CHS in solubility test of topic 4.2.

In a study by Trung et al. (2006), it is observed chitosan with lower DDA have ower and broader diffraction peaks with lower level of crystallinity index. However, this phenomenon was found to be contrast to the study of Zhang et al. (2006) where lower crystallinity is reported with higher DDA. In general, chitosan exhibits a crystallinity index at 020 reflection of less than 70%. (CrI_{020}) (Zhang et al., 2005, Zhang et al., 2006).

Zhang et al. (2005) indexed 10° as 020 reflection while 20° as 110 reflection. Zhang et al. (2005) proposed the potential for crystalline index (CrI,%), CrI_{020} and CrI_{110} to be related with DDA of chitosan where both CrI show decrease with increase of DDA. However, CrI_{020} displays a more significant relationship in DDA. The crystallinity index of 020 diffraction angle is calculated based on Equation 2.4 for the product of four methods and shown in Table 4.2.

By comparing with the result of Zhang et al. (2005), it is observed that the CrI_{020} of M1_CHS is approximated with chitin with CrI_{020} of 91.3 % and having DDA of 16.9 %. Therefore, this strengthens that M1_CHS is chitin. Meanwhile, other samples with CrI020 of less than 70% were comparable as chitosan sample with CrI_{020}.

Chitin is easily distinguished with high value of CrI_{020} shown in Table 2.4. Meanwhile, M2_CHS, M3_CHS and M4_CHS have diffractograms and CrI_{020} approximated as chitosan, should only be concluded as chitosan with matching of functional group and measurement on DDA by FT-IR analysis.

Table 4.2 : Crystallinity Calculation in refer to 020 Reflection for Products from All Four Method and Comparable CrI_{020} and Corresponding DDA by Zhang et al. (2005)

Sample	I_{020}	I_{am}	CrI_{020} (%)	Result of Zhang et al. (2005)	
				CrI_{020}	DDA (%)
M1_CHS	740 counts at 9.35°	49 counts at 16°	93.37	91.3	16.9
M2_CHS	104 counts at 9.94°	36 counts at 16°	65.38	66.1	59.4
M3_CHS	93 counts at 9.55°	35 counts at 16°	62.37	64.2	63.5
M4_CHS	36 counts at 6.02°	14 counts at 16°	61.11	61.6	58.7

4.6 Fourier Transform Infrared Spectroscopy (FT-IR)

Zhang et al. (2012) reported that chitin and chitosan contain three characteristic band which are 1577 cm^{-1} , 1654 cm^{-1} and 2932 cm^{-1} corresponding to vibration of -NH, -C-O and $–CO-CH_3$ group. Meanwhile, the content of polysaccharide is represented by bands between 890 and 1156 cm^{-1} (Liu et al., 2012). Futhermore, chitin has more intense band for 2932 and 1577 cm^{-1} than commercial chitosan, this difference is the evidence of deacetylation (Zhang et al., 2012).

Pawlak and Mucha (2003) mentioned that the FT-IR analysis of chitosan was based on the identification of bands and its vibrations. The bands wave numbers are as Table 4.3 : Wavenumbers and Chemical Group of FT-IR Absorption Bands for Chitosan [Adapted by Pawlak and Mucha (2003)].

The presence of these bands will be investigated later by using FT-IR spectra of the samples verification to be chitosan.

Table 4.3 : Wavenumbers and Chemical Group of FT-IR Absorption Bands for Chitosan [Adapted by Pawlak and Mucha (2003)]

Wave number (cm^{-1})	Chemical group
3450	OH hydroxyl group
3360	NH group-stretching vibration.
2920, 2880, 1430, 1320,	Symmetric or asymmetric CH_2 stretching vibration
1275,1245	Attributed to pyranose ring
1730	Carbonyl group vibration.
1660	C=O in amide group (amide I band)
1560	NH-bending vibration in amide group.
1590	NH_2 in amino group
1415, 1320	Vibrations of OH, CH in the ring
1380	CH_3 in amide group.
1255	C–O group.
1150–1040	–C–O–C– in glycosidic linkage
850, 838	CH_3COH group

4.6.1 Shrimp Shells Powder

The shrimp shells powder's spectrum is shown in Figure 4.15. It can be observed that some bands at 1781.01, 1544.74, 1412.35, 1419.73 and 871.92 cm^{-1} (Appendix G). According to Mohammed, Williams and Tverezovskaya (2013), 1798, 1420-1430 and 876 cm^{-1} showing the presence of mineral ($CaCO_3$) and 1540 cm^{-1} showing the presence of protein are found in the FT-IR spectrum of shrimp shells. These mineral and protein should be diminished by demineralisation and deproteinisation steps of chitosan extraction method. Therefore, these bands should not be existed in the spectrum of product of all methods.

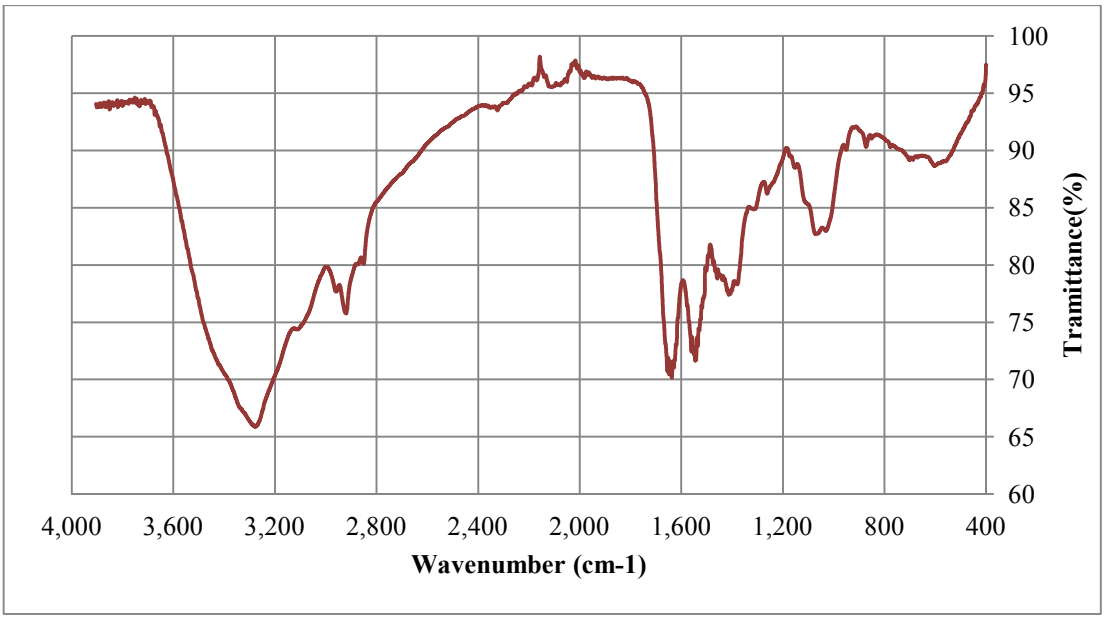

Figure 4.15 : FT-IR Spectrum of Shrimp Shells Powder at Transmittance

4.6.2 Method 1 (M1)

Figure 4.16 is the FT-IR spectrum for M1_CHS. The spectrum displays absorption bands at 3438.69, 3258.71, 3105.27, 2959.48, 2918.78, 2891.24, 1666.75, 1621.05, 1557.10, 1428.76, 1377.33, 1309.31, 1260.79 1203.47, 1154.79, 1114.53, 1072.27 1026.31, 952.77 and 896.50 cm^{-1} (Appendix H).

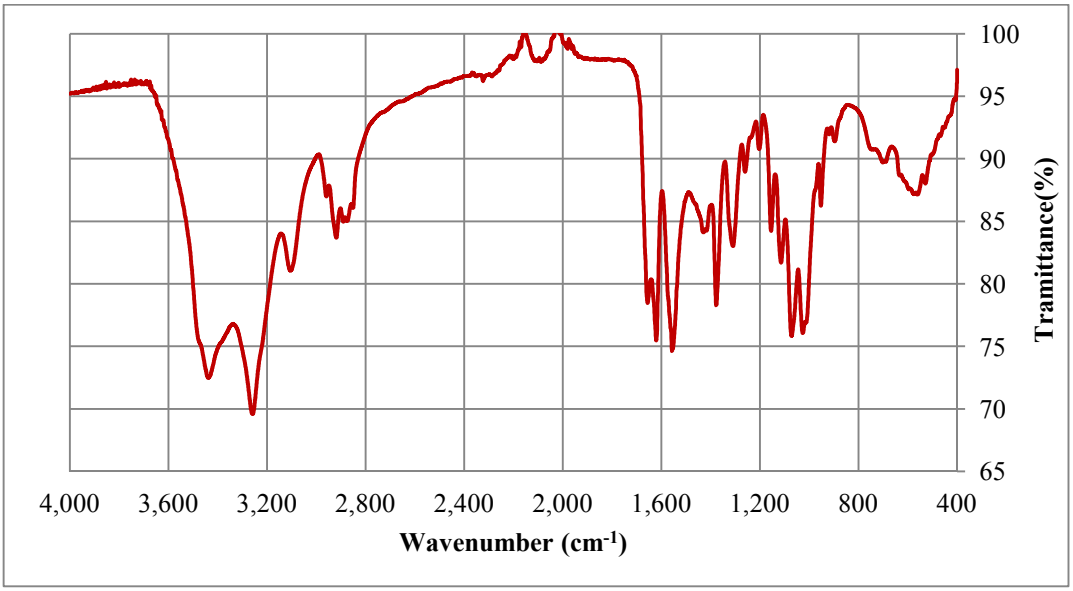

Figure 4.16 : FT-IR Spectrum of M1_CHS at Transmittance

These bands shown in M1_CHS are consistent with the result of α-chitin of Mohammed, Williams and Tverezovskaya (2013) and Acosta, Jimenez, Borau and Heras (1993). In addition, NH stretching bands are found in the spectrum of M1_CHS as 3258.71 and 3105.27 cm^{-1}. In the study of Mohammed, Williams and Tverezovskaya (2013), NH stretching band found at 3262 and 3114 cm^{-1} act as a characteristic band for α-chitin.

Furthermore, the absorption bands used to distinguish protein (1540 cm^{-1}) and mineral (1798, 1420-1430 and 876 cm^{-1}) are not observed in the spectrum of M1_CHS. This shows the effectiveness of the deproteinisation and demineralisation steps.

4.6.3 Method 2 (M2)

Figure 4.17 shows the FT-IR spectrum of M2_CHS. The spectrum displays absorption bands at 3422.43, 3359.00, 3283.00 2918.78, 2866.00, 1654.18, 1640.62, 1560.17, 1412.62, 1255.89, 1149.91, 1080.25 and 1033.03 cm^{-1} (Appendix J).

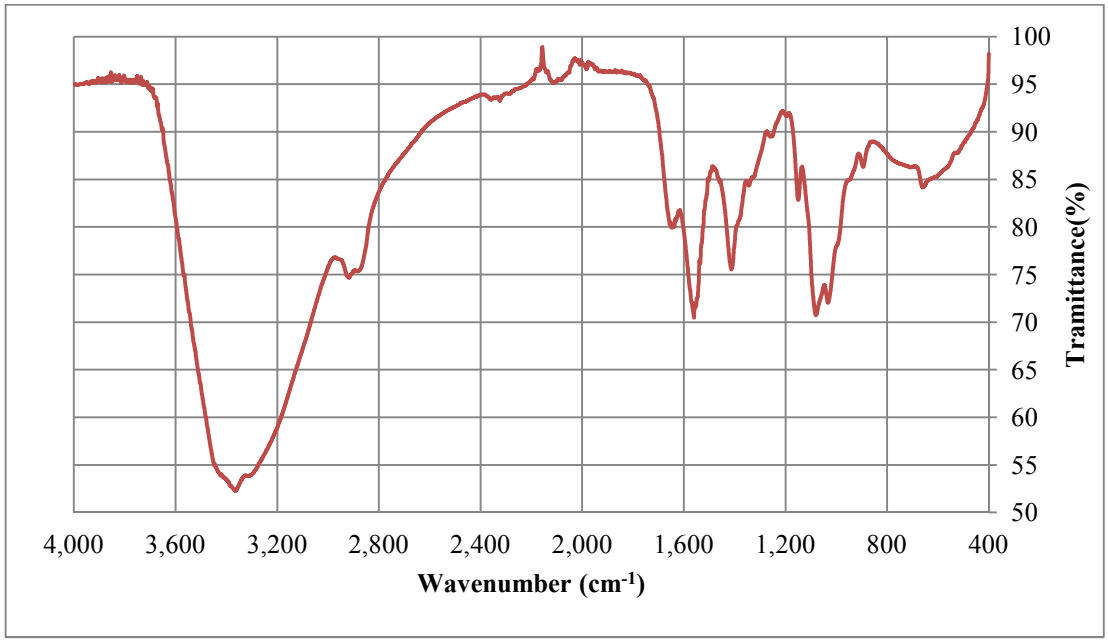

Figure 4.17 : FT-IR Spectrum of M2_CHS at Transmittance

Al Sagheer, Al-Sughayer, Muslim and Elsabee (2009) reported the FT-IR spectrum of chitosan exhibits major bands at 3444, 2919, 1659, 1420, 1080 and 1033 cm^{-1}. According to Pawlak and Mucha (2003), these band corresponded to OH group (3444 cm^{-1}), stretching CH_2 (2919 cm^{-1}), amide I band (1659 cm^{-1}), vibration of ring OH (1420 cm^{-1}) & CH (1080 cm^{-1}), and –C-O-C linkage (1033 cm^{-1}). Being the major characteristic of chitosan, these bands are observed in the spectrum of M2_CHS shown in Figure 4.17.

In addition, Mohammed, Williams and Tverezovskaya (2013) stated that a band at 1632 cm^{-1} representing $–NH_2$ deformation of primary amine are found in the spectrum of chitosan. Approximated to this band, a band at 1640.62 cm^{-1} was observed from the spectrum of M2_CHS.

Furthermore, Pawlak and Mucha (2003) reported that a band at 3360 cm^{-1} which represents the stretching $–NH_2$ in amine group. This shows the existence for free amino group which is supposed to be presented in chitosan. This is approximated to the band at 3359 cm^{-1} observed from the spectrum of M2_CHS. From the above evidence, it can be determined that M2_CHS is suggested as chitosan.

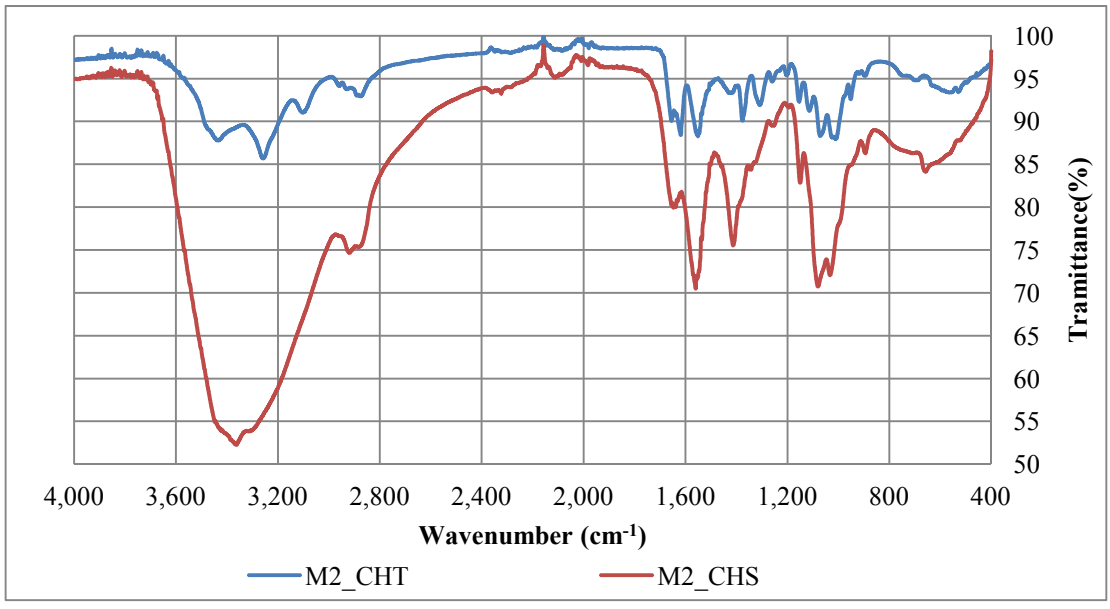

Figure 4.18 : Comparison of FT-IR Spectra for M2_CHT, M2_CHS and Shrimp Shells Powder

Comparison of FT-IR Spectra between M2_CHT and M2_CHS is shown as Figure 4.18. From the spectrum, it is observed that M2_CHT representing chitin of M2 displays higher transmittance compared to M2_CHS. Unfortunately, only Paulino, Simionato, Garcia and Nozaki (2006) supported the trend with its chitosan and chitin synthesized from silk worm chrysalides.

Nevertheless, the bands used to identify content of protein (1540 cm^{-1})and mineral (1798, 1420-1430 and 876 cm^{-1}) are not found in both M2_CHT and M2_CHS demonstrating the effectiveness of demineralisation and deproteinisation (Mohammed, Williams and Tverezovskaya, 2013).

4.6.4 Method 3 (M3)

Figure 4.19 shows the FT-IR spectrum of M3_CHS. The spectrum displays absorption bands at 3344.00, 3270.00, 2919.52, 2869.00, 1651.64, 1644.84, 1581.32, 1406.00, 1261.19, 1149.56, 1066.29 and 1028.04 cm^{-1} (Appendix L).

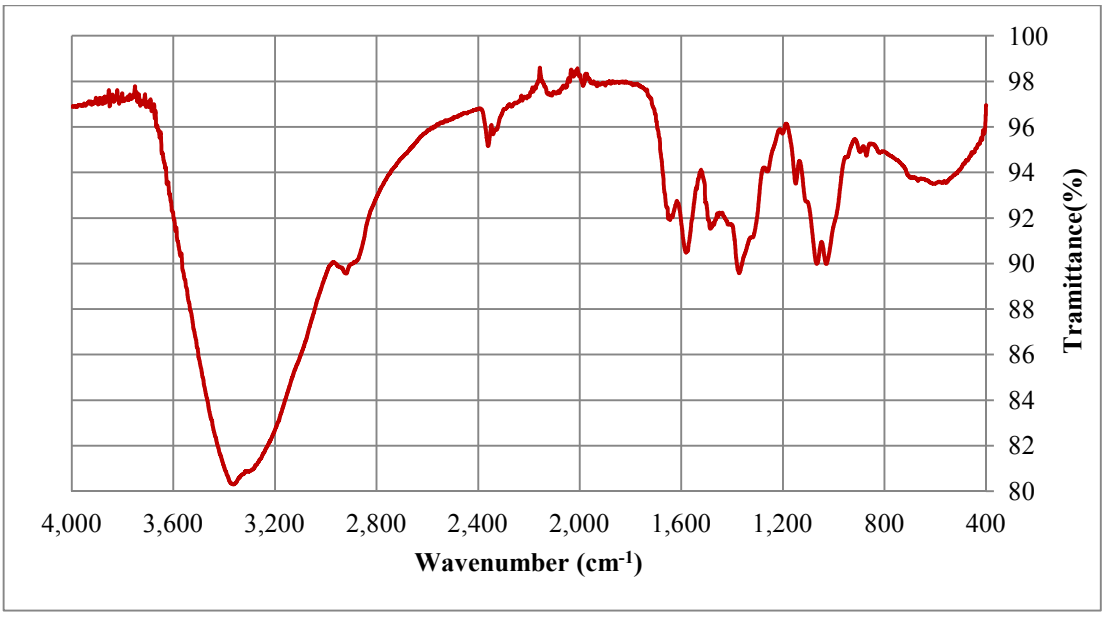

Figure 4.19: FT-IR Spectrum of M3_CHS at Transmittance

As previous discussion, bands exhibited by the FT-IR spectrum of M3_CHS are found to be similar to chitosan in M2_CHS (3422.43, 3359.00, 3283.00 2918.78, 2866.00, 1654.18, 1640.62, 1560.17, 1412.62, 1255.89, 1149.91, 1080.25 and 1033.03 cm^{-1}). Similar to M2_CHS, bands representing NH_2 (1632, 3360 cm^{-1}) of amine group in chitosan found by Mohammed, Williams and Tverezovskaya (2013) are observed in the spectrum of M3_CHS as 1644.84 and 3360 cm^{-1} in Figure 4.19.

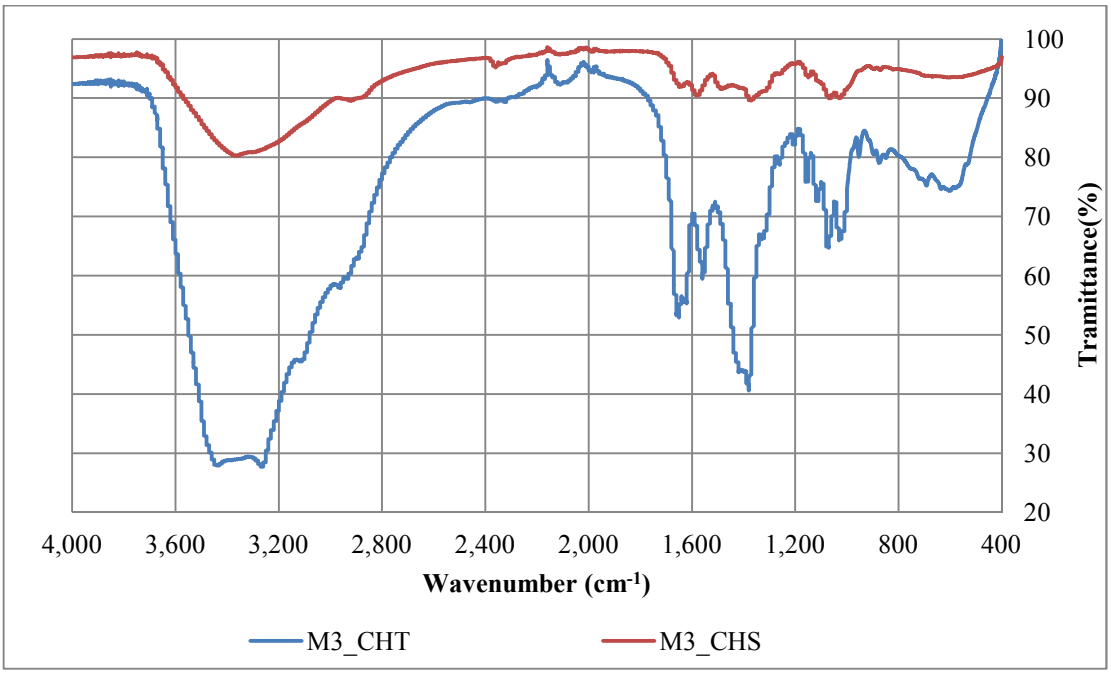

Figure 4.20 : Comparison of FT-IR Spectra for M3_CHT, M3_CHS and Shrimp Shells Powder

The comparison of FT-IR Spectra between M3_CHT and M3_CHS is shown in Figure 4.20. As observed from the spectrum, the transmittance of M3_CHT representing chitin is way lower than M3_CHS representing chitosan. Supporting the trend, common studies (Mirzadeh et al., 2002, Mohammed, Williams and Tverezovskaya, 2013, Zhang et al., 2012, Zhang et al., 2005, Zhang et al., 2006) also showed general trend of chitin having lower transmittance than chitosan in FT-IR spectrum.

Bands in M3_CHT are generally at higher intensity compared to M3_CHS. Besides, a significant reduce in amide-I band is observed between M3_CHT and

M3_CHS showing the evidence of N-deacetylation. The band near 3450 cm^{-1} representing OH stretching becomes broader with lower intensity as it has undergone N-deaectylation and are supported with the result ofZhang et al. (2006).

4.6.5 Method 4 (M4)

Figure 4.21 shows the FT-IR spectrum of M4_CHS. The spectrum displays absorption bands at 3413.00, 3258.00, 2940.00, 2869.00, 1652.09, 1563.87, 1404.00, 1255.00, 1155.20, 1072.78 and 1031.14 cm^{-1} (Appendix M).

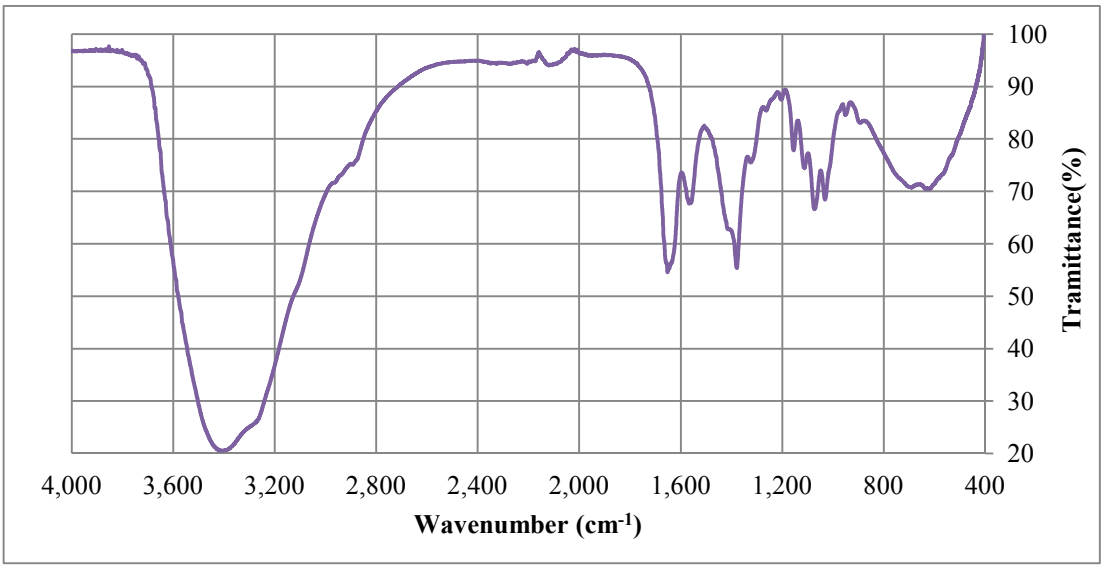

Figure 4.21 : FT-IR Spectrum of M4_CHS at Transmittance

Having similar to other chitosan found in the study (M2_CHS, M3_CHS), it also contains amine bands which proves that M4_CHS is chitosan. However, the intensity of absorption of the suspected OH hydroxyl (3450 cm^{-1}) is high which is abnormal. Furthermore, the tall OH bands give a deduction of high concentration of OH, which can be explained as of the hydroxyl group presented in water molecule (Zhang et al., 2006). It may suggested that the outer layer of calcified protein have store portion of water and NaOH within the shell, forbidding them to be withdrawn via drying process.

Other than the normal characteristic band of chitosan, the spectrum shows an slight band at 1541 cm^{-1}. This is found to be approximate to the identification band of protein at 1540 cm^{-1} which act as an evidence for possibility of an outer layer of calcified protein mentioned (Mohammed, Williams and Tverezovskaya, 2013, Rao, Muňoz and Stevens, 2000). Without heat, the protein was unable to be denaturised and withdrawn from the chitin main structure and instead are calcified with salt forming a hard shell (Rao, Muňoz and Stevens, 2000). This hard shell prevents solubility and supported the result of M4_CHS in topic 4.2.

After matching of identification bands, DDA are calculated based on Equation 2.2 for the product of all four methods. The DDA of all the four sample and its corresponding CrI_{020} is tabulated as Table 4.4.

Table 4.4 : Degree of Deacetylation Calculated from Absorption at Reference to 1655cm^{-1} and 3450cm^{-1} and Its Corresponding CrI_{020} for All Expected Chitosan of All Four Methods

Sample	A_{1655}	A_{3450}	DDA(%)	CrI_{020}(%)
M1_CHS	0.1052	0.1352	10.5153	93.37
M2_CHS	0.0956	0.2576	57.3250	65.38
M3_CHS	0.0341	0.0801	51.0870	62.37
M4_CHS	0.2499	0.6536	56.0308	61.11

In previous discussion, M1_CHS is deduced as chitin with XRD and identification band from FT-IR spectrum. The calculated DDA of M1_CHS is 10.51%. Based on the definition of Peter (1995), chitin need to have DDA of more than 50% to be chitosan if not it is still considered as chitin. With low DDA M1_CHS is again suggested as chitin. Thus, the parameters in M1 are not significant enough to produce chitosan.

It is observed that the DDA of M2_CHS, M3_CHS and M4_CHS are above 50%. This acted as a proof that strongly suggest them as chitosan. These results are

found to be consistent with the earlier suggestion done with XRD and matching bands of FT-IR spectrum.

Figure 4.22 displays the comparison of FT-IR spectra of products from four methods, it is observed that pattern of the spectrum in the region 900-1700 cm^{-1} are consistent among the products. The density of band between 900- 1700 cm^{-1} and 2900-3700 cm^{-1} are comparable where they represent the basis structure of shrimp shells, polysaccharides. Although they are having similar structure, the intensity of functional and chemical groups within them will decide what substance they are. Difference in amide-I band near 1655cm^{-1} is the one of the most significant difference between the spectra of four samples. Another significant difference is the band around 3450 cm^{-1} representing stretching OH (Mohammed, Williams and Tverezovskaya, 2013). Besides, band near 2920 cm^{-1} in chitosan does not vary much in intensity among methods. The band is found to be attributed to –CH- stretch (Ma et al., 2008).

Although M1 with lesser time and complexity is unable to produce chitosan, but M2, M3 and M4 using different parameters are able to produce chitosan. They are deduced by the similarity in FT-IR bands with commercial chitosan. Although the produced produced chitosan with various paramaters exhibit different FT-IR spectra, still it is deduced as chitosan with the presence of amine bands and some other common characterisation band of chitosan (Ok and Kim, 2004).

To further investigate on the ability in chelation and absorption of heavy metal, iron oxide nanoparticles are mixed with dissolved chitosan to form a nanocomposite material. M2_CHS is chosen because it is the first sample that exhibit complete dissolution in acetic acid. Unfortunately, due to time constraints only FT-IR test was carried out. The result will be discussed in the following topic.

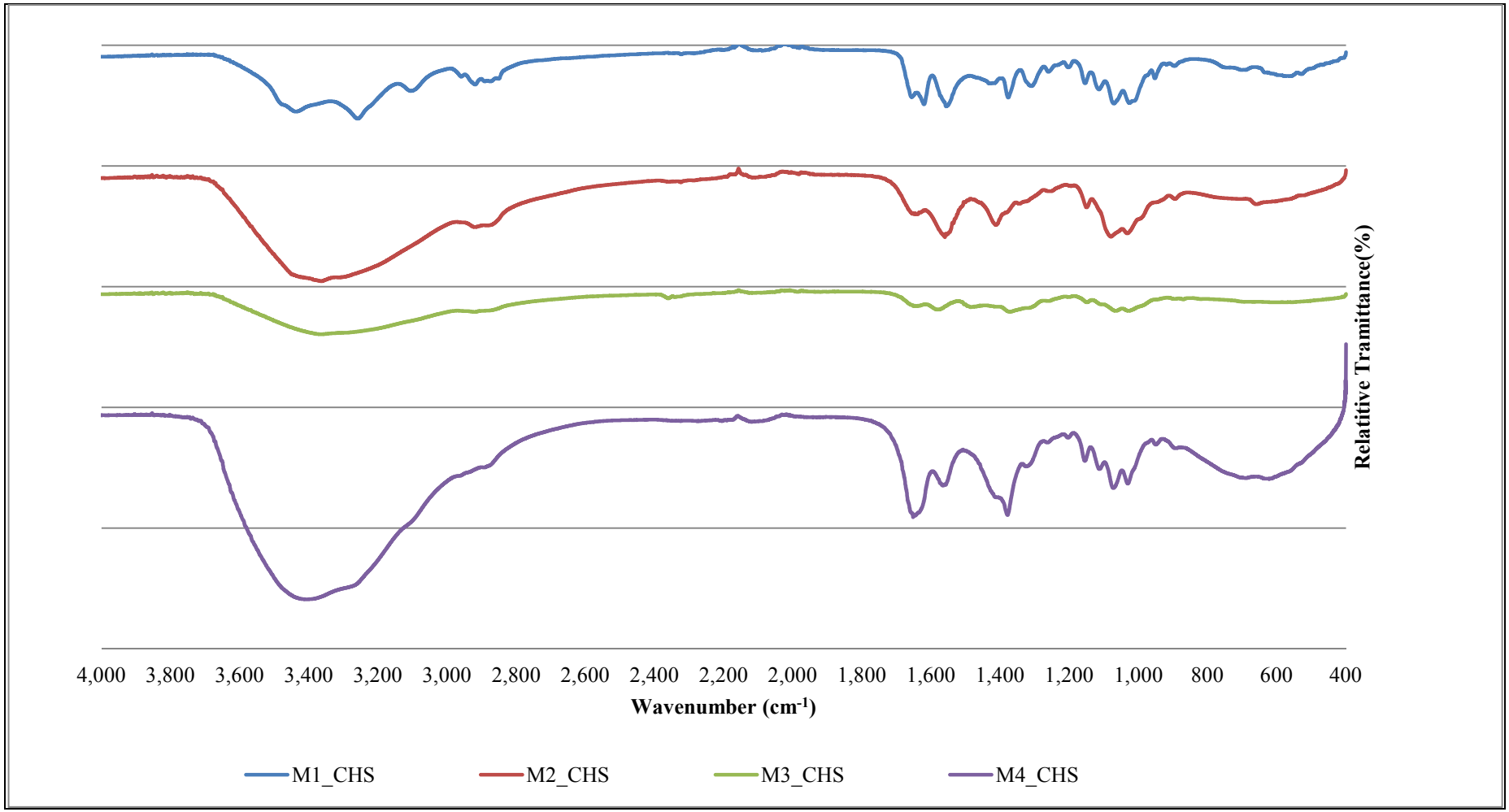

Figure 4.22 : Comparison of FT-IR Spectra for M1_CHS, M2_CHS, M3_CHS & M4_CHS at Relative Transmittance

4.7 Dissolved Chitosan and Its Mixture with Iron Oxide Nanoparticles

Figure 4.23 shows the comparison of FT-IR spectra among chitosan of M2, M2_CHS_AA which is the dissolved M2_CHS in 10% acetic acid and M2_S2_AA which is the mixture of dissolved M2_CHS with iron oxide nanoparticles produced by Ong (2013) in 10% acetic acid. Both spectra of M2_S2_AA and M2_CHS_AA are almost similar and display up to 60% of similarity to water, H_2O. Although both substance are dissolved in 10% acetic acid which compiled of 90% distilled water, the spectra still display certain difference as compared to water.

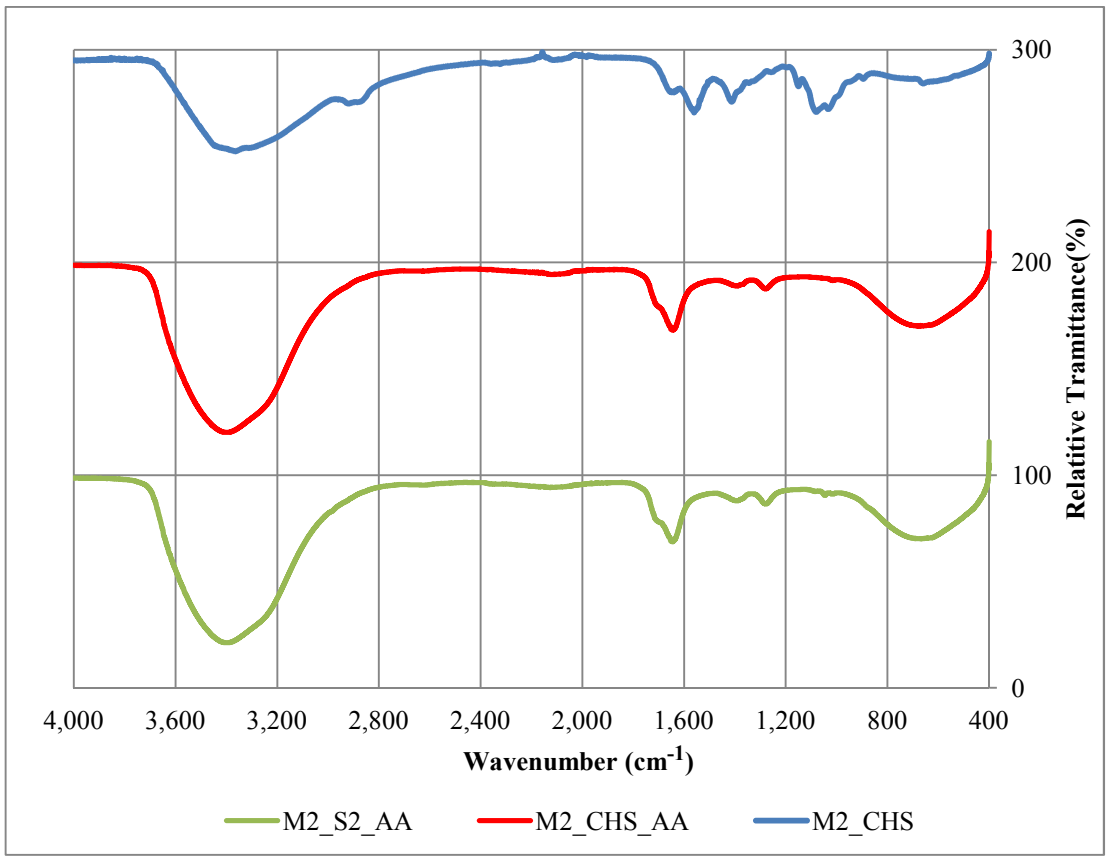

Figure 4.23 : Comparison of FT-IR Spectra between Dissolved M2_CHS and Mixture of M2_CHS with Iron Oxide Nanoparticles in 10% Acetic Acid

Both solutions as compared to the spectrum of M2_CHS have narrower and less sharp band is observed at near 3450 cm^{-1}. This similarity between them is attributed to –NH, –OH stretching vibration and inter, extra-molecular hydrogen bonding of chitosan molecule. The band near 1655 cm^{-1} representing amide-I is

observed to be consistent between the 2 solution and M2_CHS. The phenomenon shows that the content of amide group did not differ as the chitosan dissolved.

The bands between 800-1400 cm^{-1} representing the OH and CH in the hydrocarbon ring, C-O group and -C-O-C in glycosidic bridge of chitosan, are either mostly disappear or become less significant. This phenomenon is described as the dissolution of hydrocarbon ring in chitosan as polysaccharide. However, the band near 1380 cm^{-1} from FT-IR spectrum of M2_CHS remains unchanged after dissolved. This band attributes to the structure of amine group (Pawlak and Mucha, 2003, Alvarenga, 2011). Consistency in the band shows that amine group is not dissolved into the acetic acid.

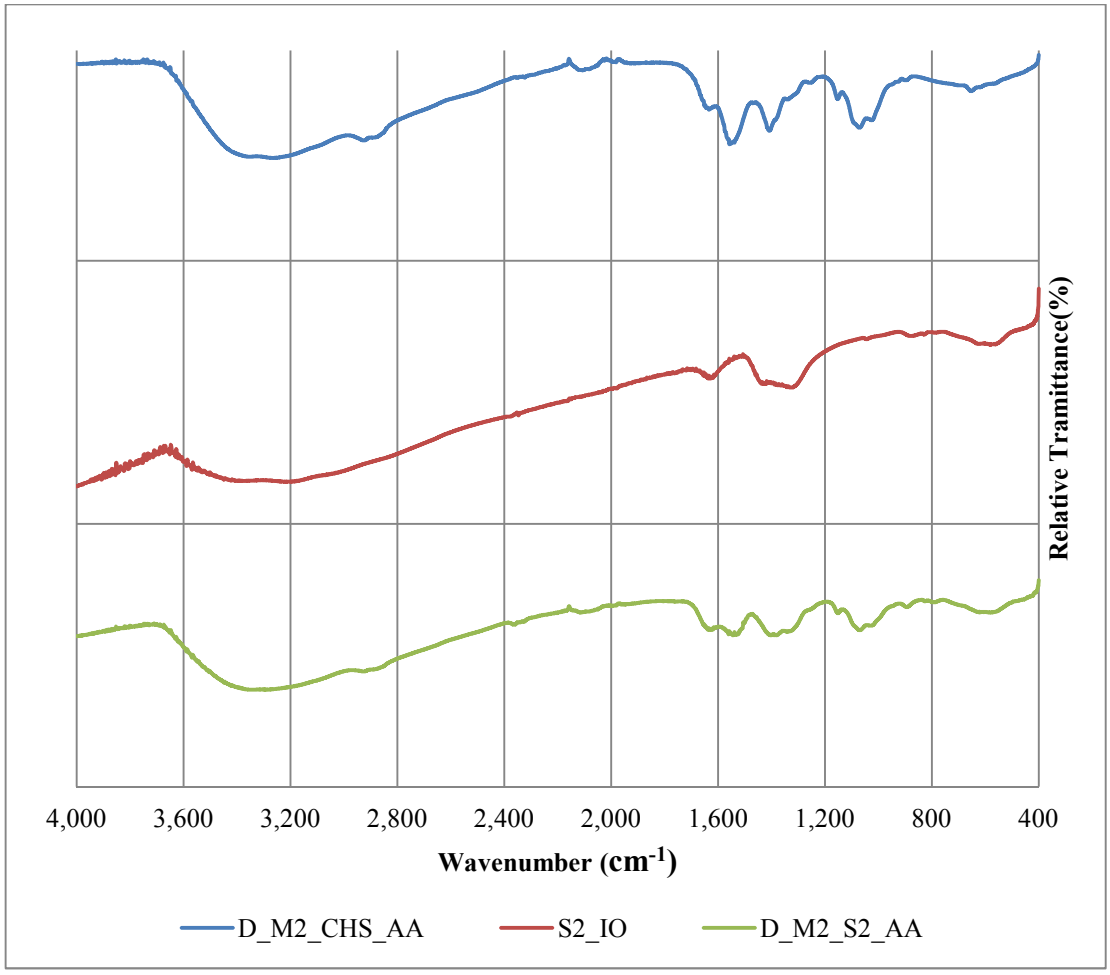

Figure 4.24 : Comparison of FT-IR Spectra between Dried Dissolved M2_CHS, Iron Oxide Nanoparticles and Mixture of M2_CHS with Iron Oxide Nanoparticles in 10% Acetic Acid

Figure 4.24 shows the relative transmittance of dried dissolved chitosan (D_M2_CHS), iron oxide nanoparticles (S2_IO) and dried mixture of dissolved chitosan and iron oxide nanoparticles (D_M2_S2_AA). The chitosan dissolved in 10% acetic acid was mixed with iron oxide nanoparticles produced by Ong (2013). After the dissolved chitosan was dried on aluminium foil, it shows absorption bands at 3362.00, 3350.00, 2925.98, 2855, 1651.53, 1633.97, 1562.85, 1408.75, 1256.83, 1070.84 and 1025.58cm^{-1} (Appendix N).

The resulting bands of D_M2_CHS shows that the main structure of chitosan did not alter as it undergo dissolution process by acetic acid. The result is found to be significantly similar to chitosan produced in this study as well as others references (Mohammed, Williams and Tverezovskaya, 2013, Islam et al., 2011, Alvarenga, 2011, Teli and Sheikh, 2012).

The iron oxide nanoparticles produced by Ong (2013) was identified as iron oxide in the form of nanorange particle. It tends to exhibit paramagnetism which can be used to magnetically attract heavy metal (Butter, 2003, Ummartyotin, Juntaro, Sain and Manuspiya, 2012). The intention to mix chitosan and iron oxide nanoparticles together is to create a composite with enhanced ability to deal with heavy metal (Huang, Shieh, Shih and Twu, 2010).

After the mixture, the solution of sample was dried on aluminium foil which named as D_M2_S2_AA and the spectrum is shown in Figure 4.24. As compared to FT-IR spectrum of dried dissolve chitosan of M2 (D_M2_CHS__AA) and iron oxide nanoparticles (S2_IO), the adaption of bands into spectrum is observed in spectrum of dried mixture of M2 chitosan and iron oxide nanoparticles (D_M2_S2_AA).

Generally, the spectrum follows the shape of S2_IO but has adapted some bands and intensity from D_M2_CHS_AA. From 4000-3700 cm^{-1}, reduce intensity to match D_M2_CHS_AA is observed. Then, 3700-1600 cm^{-1} also follows the general shape of S2_IO but has adapted several bands at 3372, 2868 and 2080 cm^{-1} from D_M2_CHS_AA. As 1600-800 cm^{-1}, the sharp band in the region exhibited in D_M2_CHS_AA was broadened by S2_IO retaining one region around 1080 cm^{-1} with sharp and narrow band.

The FT-IR spectrum D_M2_S2_AA of shows that the original compound and structure in the composite was neither altered nor diminished. It shows the characteristic of composite where the both spectra of D_M2_CHS_AA and S2_IO combined into a new spectrum with identification bands of both substances (Griffiths and de Hasseth, 2007). Thus, chitosan and iron oxide nanoparticles are suggested to have the potential to form composite materials with compositional interaction. The composite is believed to be able to have ability of both substances (Huang, Shieh, Shih and Twu, 2010). However, further investigation is needed to understand the in depth structures of this nanocomposite.

CHAPTER 5

CONCLUSION AND RECOMMENDATIONS

5.1 Findings

Chitosan is one of the most useful biopolymer which having the properties of polysaccharide such as biocompatibility, biodegradability and non-toxicity. Besides, it can be applied in waster water treatment to deal with heavy metal by chelation and absorption, antibacterial properties to inhibit the activities of microbial. This created the demands for chitosan and the needs for mass production. Therefore, understanding the effect of different variation on parameters will lead to better quality in chitosan production. The study aimed to produce chitosan from shrimp shells using several methods to observe their significant differences. As shown in CHAPTER 3, variations on parameters were finalised into four processing methods (M1, M2, M3 and M4) and their final products were named as (M1_CHS, M2_CHS, M3_CHS and M4_CHS).

Based on the result obtained, chitosan that extracted from shrimp shells using different the four processing methods shows some achievement on the main aim. However, not all processing methods were able to produce effective chitosan. The final products were successfully characterised by solubility test, SEM, EDS, XRD and FT-IR. The conclusions of each method were drawn as follows:-

Method 1 (M1) has a treatment time of 80 hours and general yield is 17 %wt from shrimp shells. The stage to chitin was done by treatment time of hours and remaining 72 hours were N-deacetylation to convert chitin to chitosan. Being insoluble in 10% acetic acid, it was preliminary eliminated as chitosan. Next, the

M1_CHS extracted from M1 was defined as chitin by matching bands of FT-IR spectrum with commercial chitin and chitin produced in other studies. It has shows high crystallinity of 93.37% at 020 phase and displaying the properties of high crystalline chitin. Then, M1_CHS has proven as chitin with low DDA of 10.51%. SEM shows that M1_CHS having surface morphology with residue and elements distribution of common polysaccharides detected by EDS.

Method 2 (M2) has the longest treatment time of 120 hours and generated 8 %wt yield of shrimp shells to chitosan. Although it has the lowest yield percentage but it is the first method which successfully produces chitosan (M2_CHS) that is completely soluble in 10% acetic acid. The chitosan produced was verified by matching bands in FT-IR spectrum of chitosan from other study. The evidence was strengthen with the calculated CrI_{020} of 65.38% and DDA of 57.325%. Surface morphology of M2_CHS shows inhomogeneous but clean surface while EDS exhibit distribution of elements of common polysaccharides.

With the best efficient with moderate degree of complexity, Method 3 (M3) achieves the whole extraction process with 60 hours and a yield of 19 %wt from shrimp shells. It is rather the most complicated method of extraction among the four, where high temperature of 100 °C and reflux condition was used. The product (M3_CHS) was verified as chitosan by its FT-IR identification bands matching with chitosan of other study while showing solubility in 10 % acetic acid. The calculated DDA and CrI_{020} were 51.08 % and 61.11 % respectively which again indicates M2_CHS as chitosan.

Being the simplest way to produce chitosan in this study, Method (M4) does not involve the implication of heat and pressure. However, it does have additional precursor processes which compiled 120 hours of processing time and have yield of 28 %wt from shrimp shells. Although having the highest yield, it was not reliable as an outer layer of calcified protein was formed preventing solubility in first 24 hours of immersion. This is supported by EDS where addition substances of sodium and calcium were found. In FT-IR and XRD verification, it displays that DDA of 56.03% and CrI_{020} of 62.37%. With matching bands in FT-IR spectrum, it is categorised as chitosan having a layer of calcified protein.

Other than M1_CHS, the chitosan produced from M2, M3 and M4 show a FT-IR spectrum similar to other studies and have DDA of more than 50%. In addition, the three sample also exhibit CrI_{020} of less than 70% by XRD analysis.

Lastly, FT-IR Spectrum shows relative relationship between chitosan and iron oxide nanoparticles.

5.2 Limitations, Recommendations and Future Improvements

In the study, the attempts for extracting chitosan were limited to certain extends such as equipment, chemical and time. Due to the limitation, the potential findings of this study were limited to allow further understandings on the effects of different parameters of the chitosan production.

In chitosan extraction, most of the time was used for drying purpose other than the treatment time. Having certain degree of water binding capacity, the synthesized chitosan was not easy to dried to a constant weight. Usually taking up to 24 hours in vacuum or under fume hood, it did consume a large portion of entire extraction process. The product was defined as constant weight as the measured weight of the specimen did not differ after 3 hours. This does not deny that the possibility of water content to be still retained in the final product.

In the study, shrimp shells were manually discarded from shrimp brought from local hypermarket. Unfortunately, the species of the shrimp was undefined and may differ from time to time. The result may be affected if different species of shrimp was used for each method. It is recommended in future studies that the shrimp species of the shrimp shells used is identified and the source of shrimp shells can be self established to limit the variation caused by difference in breed of shrimp.

In the XRD test, the samples were unable to fill the specimen dish due to particle size and lack of compressibility. During the characterisation, addition glue substance was used to attach the specimen to the specimen dish. The slight shifting

of XRD diffractorgram might due to the used of the adhesive. It is recommended that a smaller specimen dish should be used by the test.

Furthermore, some other parameters such as nitrogen purging (Mirzadeh et al., 2002), forced penetration (Zhang et al., 2006) and fermentation (Zhang et al., 2012) may be incorporated to investigate the properties from different methods.

More properties such as molecular weight, density and so on can be further investigated. The accuracy of DDA can also be verified using a few testing apparatus such as ^{1}H NMR or titration calorimetric. The thermal properties can also be investigated to understand the thermal behaviour at higher temperature.

REFERENCES

Abdou, E. S., Elkholy, S. S., Elsabee, M. Z. & Mohamed, E. 2008. Improved antimicrobial activity of polypropylene and cotton nonwoven fabrics by surface treatment and modification with chitosan. *Journal of Applied Polymer Science,* 108 (1)**,** pp. 2290-2296.

Acosta, N., Jimenez, C., Borau, V. & Heras, A. 1993. Extraction and characterization of chitin from crutaceans. *J. Biomass and Bioenergy,* 5**,** pp. 145-153.

Al Sagheer, F. A., Al-Sughayer, M. A., Muslim, S. & Elsabee, M. Z. 2009. Extration and characterization of chitin and chitosan from marine sources in Arabian Gulf. *Carbohydrate Polymers* 77 (1)**,** pp. 410-419.

Alvarenga, E. S. d. 2011. Characterization and Properties of Chitosan. *In:* Elnashar, P. M. (ed.) *Biotechnology of Biopolymers.* Rijeka, Croatia: InTech.

Arbia, W., Arbia, L., Adour, L. & Amrane, A. 2011. Chitin Extraction from Crustacean Shells by Biological Methods - A review. *Food Technol. and Biotechnol.,* 51 (1)**,** pp. 12-25.

Bangyekan, C., Aht-Ong, D. & Srikulkit, K. 2006. Preparation and properties evaluation of chitosan-coated cassava starch films. *Carbohydrate Polymers,* 63 (1)**,** pp. 61-71.

Baxter, A., Dillon, M., Anthony Taylor, K. D. & Roberts, G. A. F. 1992. Improved method for i.r. determination of the degree of N-acetylation of chitosan. *International Journal of Biological Macromolecules,* 14 (3)**,** pp. 166-169.

Bish, D. L. 1989. *Modern Powder Diffraction.* , Mineralogical Society of America.

Bolat, Y., Bilgin, e., Günlü, A., Izci, L., Koca, S. B., Çetinkaya, S. & Koca, H. U. 2010. Chitin-Chitosan Yield of Freshwater Crab (Potamon potamios,Olivier 1804) Shell. *Pakistan Veterinary Journal,* 30 (4)**,** pp. 227-231.

Butter, K. 2003. *Iron(oxide) ferrofluids: synthesis, structure and catalysis.,* Tekst, Proefschrift Universiteit Utrecht.

Crini, G. & Badot, P.-M. 2008. Application of chitosan, a natural aminopolysaccharide, for dye removal from aqueous solutions by adsorption processes using batch studies: A review of recent literature. *Progress in Polymer Science,* 33 (4)**,** pp. 399-447.

Cullity, B. 1978. *Elements of X-ray diffraction,* Reading, Mass, Addison-Wesley.

deMan, J. M. 1999. *Principles of Food Chemistry,* Maryland, USA, Aspen

Dutrow, B. L. & Clark, C. M. 2012. X-ray Powder Diffraction (XRD). Available: http://serc.carleton.edu/research_education/geochemsheets/techniques/XRD.html [Accessed 28/3/2013].

Egerton, R. F. 2005. Physical principles of electron microscopy : an introduction to TEM, SEM, and AEM. Berlin, Germany: Springer.

El-Hefian, E. A., Nasef, M. M., Yahaya, A. H. & Khan, R. A. 2010. Preparation and Characterization of Chitosan/Agar Blends:Rheological and Thermal Studies *J. Chil. Chem. Soc,* 55 (1)**,** pp. 1212-1219.

Focher, B., Beltrame, P. L., Naggi, A. & Torri, G. 1990. Alkaline N-deacetylation of chitin enhanced by flash treatments. Reaction kinetics and structure modifications. *Carbohydrate Polymers,* 12**,** pp. 405-418.

Gardner, K. H. & Blackwell, J. 1975. Refinement of the structure of Beta- Chitin *Biopolymers,* 14**,** pp. 1581-1595.

Goldstein, J. 2003. Scanning electron microscopy and x-ray microanalysis. Kluwer Adacemic: Plenum Pulbishers.

Griffiths, P. & de Hasseth, J. A. 2007. *Fourier transform Infrared Spectrometry,* Blackwell, Wiley.

Harish Prashanth, K. V. & Thanathan, R. N. 2007. Chitin/chitosan: modifications and their unlimited application potential - an overview. *Trends Food Science Technology,* 18**,** pp. 117-131.

He, M. J., Chen, W. X. & Dong, X. X. 2001. *Macromolecular physics,* Shanghai, China, University Press.

Huang, H.-Y., Shieh, Y.-T., Shih, C.-M. & Twu, Y.-K. 2010. Magnetic chitosan/iron (II, III) oxide nanoparticles prepared by spray-drying. *Carbohydrate Polymers,* 81 (4)**,** pp. 906-910.

Hudson, S. M. & Smith, C. 1998. Polysaccharide: chitin and chitosan: chemistry and technology of their use as structural material. *Biopolymers from renewable resource.* New York: Springer-Verlag.

Ibrahim, H. M., Salama, M. F. & El-Banna, H. A. 1991. Shrimp's waste: Chemical composition nutritional value and utilization. *Nahrung,* 43**,** pp. 418-423.

Islam, M. M., Masum, S. M., Molla, M. A. I., Rahman, M. M., Shaikh, A. A. & Roy, S. K. 2011. Preparation of Chitosan from Shrimp Shell and Investigation of Its Properties. *Intenational Journal of Basic & Applied Sciences* 11 (1)**,** pp. 116-130.

Kaplan, D. L. 1998. Introduction to biopolymers from renewable resource. *Biopolymers from Renewable Resources.* MA, USA: Springer-Verlag Berlin Heiderberg New York.

Kasaai, M. R. 2008. A Review of several reported procedures to determine the degree of N-acetylation for chitin and chitosan using infrared spectroscopy. *Carbohydrate Polymers,* 71**,** pp. 497-508.

Kasapis, S., Norton, I. T. & Ubbink, J. B. 2009. *Modern biopolymer science: bridging the divine between fundamental treatise and industrial application,* London, UK, Elsiver.

Klug, H. P. & Alexander, L. E. 1974. *X-ray diffraction procedures: For polycrystalline and armophous materials (2nd version),* New York, John Wiley & Sons Inc.

Kumar, M. N. V. R. 2000. A review of chitin and chitosan applications. *Reactve and Functional Polymer,* 46 (1)**,** pp. 1-27.

Lapasin, R. & Pricl, S. 1999. *Rheology of industrial polysaccharides: theory and application,* New York, USA, Aspen Publication.

Liu, S., Sun, J., Yu, L., Zhang, C., Bi, J., Zhu, F., Qu, M., Jiang, C. & Yang, Q. 2012. Extraction and Characterization of Chitin from the Beetle Holotrichia parallela Motschulsky. *Molecules,* 17 (4)**,** pp. 4604-4611.

Ma, G., Yang, D., Zhou, Y., Xiao, M., Kennedy, J. F. & Nie, J. 2008. Preparation and characterization of water-soluble N-alkylated chitosan. *Carbohydrate Polymers,* 74 (1)**,** pp. 121-126.

Marthur, N. & Narang, C. 1990. Chitin and Chitosan, Versatile Polysaccharides From Marine Animals. *Journal of Chemical Education,* 67**,** pp. 938-42.

McNaught, A. D. & Wilkinson, A. 2006. *Compendium of Chemical Terminology,* Blackwell Scientific Publications, Oxford, IUPAC.

Minke, R. & Blackwell, J. 1978. The Structural of Alpha-Chitin *Journal of Molecular Biology,* 120**,** pp. 167-181.

Mirzadeh, H., Yaghobi, N., Amanpour, S., Ahmadi, H., Mohagheghi, M. A. & Hormozi, F. 2002. Preparation of chitosan derrived from shrimp's shell persian gulf as Blood Hemostasis Agent. *Iranian Polymer Journal,* 11 (1)**,** pp. 63-68.

Mohammed, M. H., Williams, P. A. & Tverezovskaya, O. 2013. Extraction of chitin from prawn shells and conversion to low molecular mass chitosan. *Food Hydroculloids,* 31**,** pp. 166-171.

Mohammed, Z. H., Hember, H. W. N., Richardson, R. K. & Morris, E. R. 1998. Application of polymer blending lawas to composite gels of agarose and crosslinked waxy maize starch. *Carbohydrate Polymers,* 36**,** pp. 27-36.

Mohanty, A. K., Misra, M. & Drzal, L. T. 2005. *Natural Fibers, Biopolymers, and Biocomposites*, Taylor & Francis.

Moorjani, M. N., Khasim, D. I., Rajalakshmi, S., Puttarajappa, P. & Amla, B. L. Chitosan of high viscosity and protein as a valuable by-product from squilla. First International Conference on Chitin/Chitosan, 1978 Cambridge, MA. . MIT Sea Grant Program, pp.187-189. .

Ng, C. H., Hein, C. S. & Stevens, W. F. 2006. The Mechanical and Biological Properties of Chitosan Scaffolds for Tissue Regeneration Templates Are Significantly Enhanced by Chitosan from Gongronella butleri. *Journal Biomedic Material Research,* 76B (1)**,** pp. 155-160.

Nishikida, K., Nishio, E. & Hannah, R. W. 1995. *Selected Applications of Modern Ft-Ir Techniques*, Gordon and Breach.

No, H. K. & Lee, M. Y. 1995. Isolation of chitin from crab shell waste. *Journal of the Korean Soiety of Food Science and Nutrition,* 24 (1)**,** pp. 105-113.

No, H. K., Park, N. Y., Lee, S. H. & Meyers, S. P. 2002. Antibacterial activity of Chitosans and chitosan oligomers with different molecular weights. *International Journal of Food Microbiology,* 74.**,** pp.65-72.

Nunn, S. & Nishikida, K. Advanced ATR Correction Algorithm. *In:* Scientific, T. F. (ed.). Madison, WI, USA.

Ok, S. & Kim, F. 2004. *Physicochemical And Functional Properties Of Crawfish Chitosan As Affected By Different Processing Protocols.* Master of Science Louisiana State University.

Ong, K. W. 2013. *Effect of Concentration of Iron (II) Chloride on the of Maghemite Nanoparticles and its Nanocomposite.* Material and Manufacturing Engineering, University Tunku Abdul Rahman.

Paulino, A. T., Simionato, J. I., Garcia, J. C. & Nozaki, J. 2006. Characterization of chitosan and chitin produced from silkworm crysalides. *Carbohydrate Polymers,* 64 (1)**,** pp. 98-103.

Pawlak, A. & Mucha, M. 2003. Thermogravimetric and FTIR studies of chitosan blends. *Thermochimica Acta,* 396 (1–2)**,** 153-166.

Peter, M. 1995. Applications and environmental aspects of chitin and chitosan. *Journal of Macromolecular Science, Part A:Pure Applied Chemistry,* A32 (4)**,** pp. 629-40.

Pradip, K. D., Joydeep, D. & Tripathi, V. S. 2004. Chitin and chitosan : Chemistry, properties and applications. *Journal of Science and Industrial Research,* 63**,** pp. 20-31.

Rao, M. S., Muňoz, J. & Stevens, W. F. 2000. Critical factors in chitin production by fermentation of shrimp biowaste. *Appl. Microbiol. Biotechnol,* 54 (1)**,** pp. 808-813.

Ravichandran, S., Rameshkumar, G. & Prince, A. R. 2009. Biochemical Composition of Shell and Flesh of the Indian White Shrimp Penaeus indicus

(H.milne Edwards 1837). *American-Eurasian Journal of Scientific Research,* 4 (3)**,** pp. 191-194.

Robert, G. A. F. 1992. *Chitin Chemistry (1st ed),* London, Macmillan.

Rout, S. K. 2001. Physicochemical, Functional, and Spectroscopic analysis of crawfish chitin and chitosan as affected by process modification. *Dissertation*.

Shahidi, F. & Abuzaytoun, R. 2005. Chitin, Chitosan, and Co-products: Chemistry, Production, Applications, and Health Effects. *Advance Food Nutrition Research,* 49**,** pp. 93-135.

Swapp, S. 2012. Scanning Electron Microscopy (SEM). Available: http://serc.carleton.edu/research_education/geochemsheets/techniques/SEM.html.

Tan, S. C., Khor, E., Tan, T. K. & Wong, S. M. 1996. The degree of deacetylation of chitosan: advocating the first derrivative UV spectrophotometry method of determination. *Talanta,* 45 (1)**,** pp. 713-719.

Teli, M. D. & Sheikh, J. 2012. Extraction of chitosan from shrimp shells waste and application in antibacterial finishing of bamboo rayon. *International Journal of Biological Macromolecules,* 50**,** pp. 1195-1200.

Tharanathan, R. N. & Kittur, F. S. 2003. Chitin-The Undisputed Biomolecule of Great Potential. *Critical Review on Food Science and Nutrition,* 43**,** pp. 61-87.

ThermoNicolet 2001. Introduction to Fourier Transform Infrared Spectrometry. *In:* Electron, T. (ed.). Madison,USA.

Trung, T. S., Thein-Han, W. W., Qui, N. T., Ng, C.-H. & Stevens, W. F. 2006. Functional characteristics of shrimp chitosan and its membranes as affected by the degree of deacetylation. *Bioresource Technology,* 97 (4)**,** pp. 659-663.

Ummartyotin, S., Juntaro, J., Sain, M. & Manuspiya, H. 2012. The role of ferrofluid on surface smoothness of bacterial cellulose nanocomposite flexible display. *Chemical Engineering Journal,* 193-194**,** pp. 16-20.

US Congress 1993. *Biopolymers: making materials the nature's way- Background paper,* Washington, USA, DIANE Publishing.

Wang, S.-L., Lin, T.-Y., Yen, Y.-H., Liao, H.-F. & Chen, Y.-C. 2006. Bioconversion of Shellfish Chitin Wastes for The Production of Bacillus Subtilis W-118 chitinase. *Carbohydrate Research***,** 341(15),2507-15.

Yaghobi, N. & Hormozi, F. 2010. Multistage deacetylation of chitin: Kinetics study. *Carbohydrate Polymers,* 81 (4)**,** pp. 892-896.

Yen, M.-T., Yang, J.-H. & Mau, J.-L. 2009. Physicochemical characterization of chitin and chitosan from crab shells. *Carbohydrate Polymers,* 75**,** pp. 15-21.

Zhang, H., Jin, Y., Deng, Y., Wang, D. & Zhao, Y. 2012. Production of chitin from shrimp shell powders using Serratia marcescens B742 and Lactobacillus plantarum ATCC 8014 successive two-step fermentation. *Carbohydrate Research,* 362 (1)**,** pp. 13-20.

Zhang, Y., Xue, C., Li, Z., Zhang, Y. & Fu, X. 2006. Preparation of half-deacetylated chitosan by forced penetration and its properties. *Carbohydrate Polymers,* 65 (3)**,** pp. 229-234.

Zhang, Y., Xue, C., Xue, Y., Gao, R. & Zhang, X. 2005. Determination of the degree of deacetylation of chitin and chitosan by X-ray powder diffraction. *Carbohydrate Research,* 340 (11)**,** pp. 1914-1917.

APPENDICES

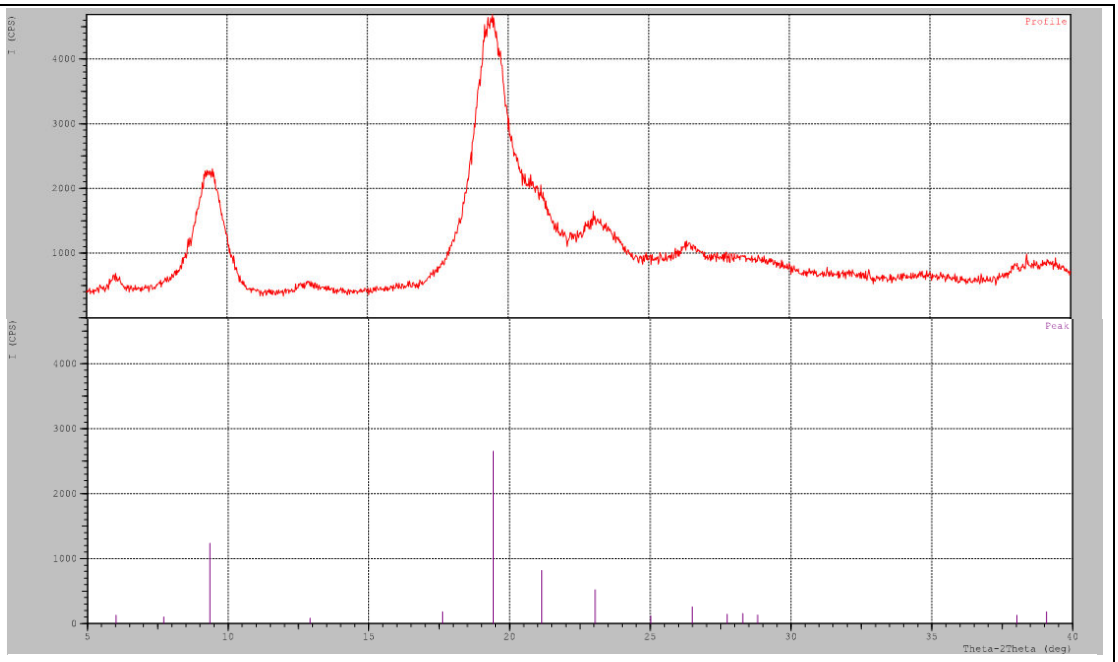

Strongest 3 peaks

no.	peak no.	2Theta (deg)	d (A)	I/I1	FWHM (deg)	Intensity (Counts)	Integrated Int (Counts)
1	6	19.4241	4.56618	100	1.47930	1590	111712
2	3	9.3563	9.44476	47	1.18640	740	46680
3	7	21.1400	4.19927	31	1.37140	490	36963

Peak Data List

peak no.	2Theta (deg)	d (A)	I/I1	FWHM (deg)	Intensity (Counts)	Integrated Int (Counts)
1	6.0275	14.65128	5	0.66500	75	3018
2	7.7200	11.44258	4	0.66660	57	3814
3	9.3563	9.44476	47	1.18640	740	46680
4	12.9150	6.84917	3	0.87000	49	2304
5	17.6200	5.02944	7	0.64000	107	7193
6	19.4241	4.56618	100	1.47930	1590	111712
7	21.1400	4.19927	31	1.37140	490	36963
8	23.0400	3.85709	19	1.96000	309	30292
9	25.0200	3.55616	4	0.00000	68	0
10	26.4900	3.36206	10	1.54000	152	13194
11	27.7400	3.21334	5	0.00000	85	0
12	28.2800	3.15319	6	0.00000	91	0
13	28.8200	3.09533	5	2.08000	77	7568
14	38.0200	2.36482	5	0.77000	76	3088
15	39.0800	2.30308	7	1.72000	107	7383

APPENDIX A : Peaks Data on XRD DIffractogram for M1_CHS

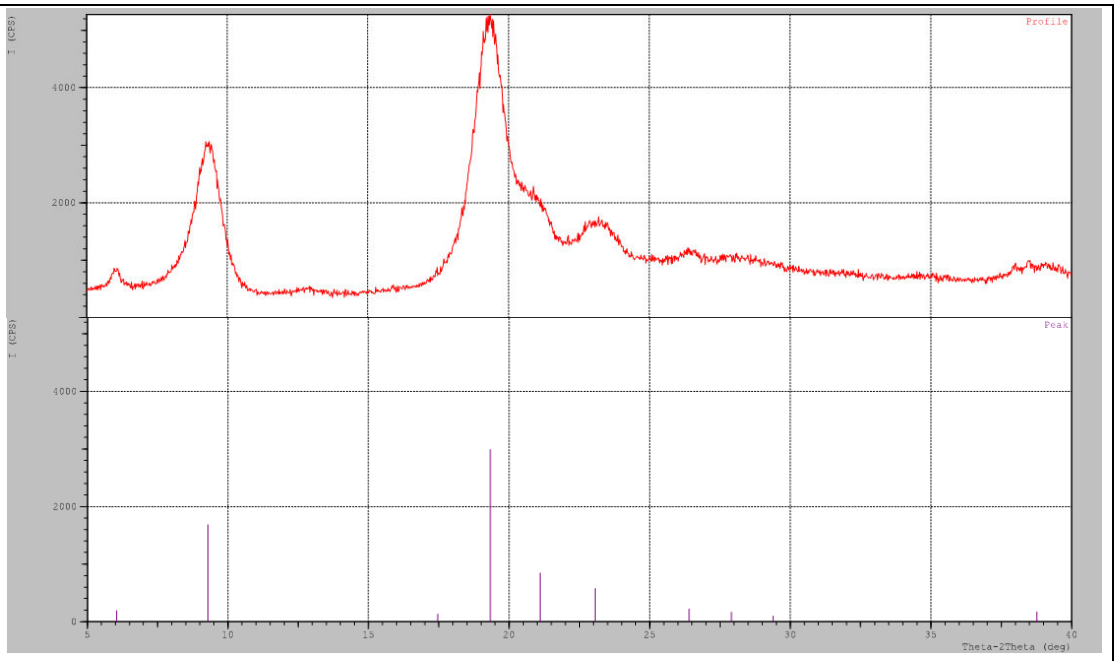

Strongest 3 peaks

no.	peak no.	2Theta (deg)	d (A)	I/I1	FWHM (deg)	Intensity (Counts)	Integrated Int (Counts)
1	4	19.3317	4.58780	100	1.36230	1790	123225
2	2	9.2958	9.50610	56	1.12840	1008	66982
3	5	21.1000	4.20714	28	1.23420	504	38409

Peak Data List

peak no.	2Theta (deg)	d (A)	I/I1	FWHM (deg)	Intensity (Counts)	Integrated Int (Counts)
1	6.0471	14.60384	6	0.68290	113	5503
2	9.2958	9.50610	56	1.12840	1008	66982
3	17.4600	5.07516	4	0.47000	77	4061
4	19.3317	4.58780	100	1.36230	1790	123225
5	21.1000	4.20714	28	1.23420	504	38409
6	23.0600	3.85379	19	1.86400	345	40329
7	26.4000	3.37332	7	0.00000	131	0
8	27.9000	3.19527	6	0.00000	99	0
9	29.3800	3.03759	3	1.37340	58	8996
10	38.7641	2.32112	6	2.10170	101	11292

APPENDIX B: Peaks Data on XRD Diffractogram for M2_CHT

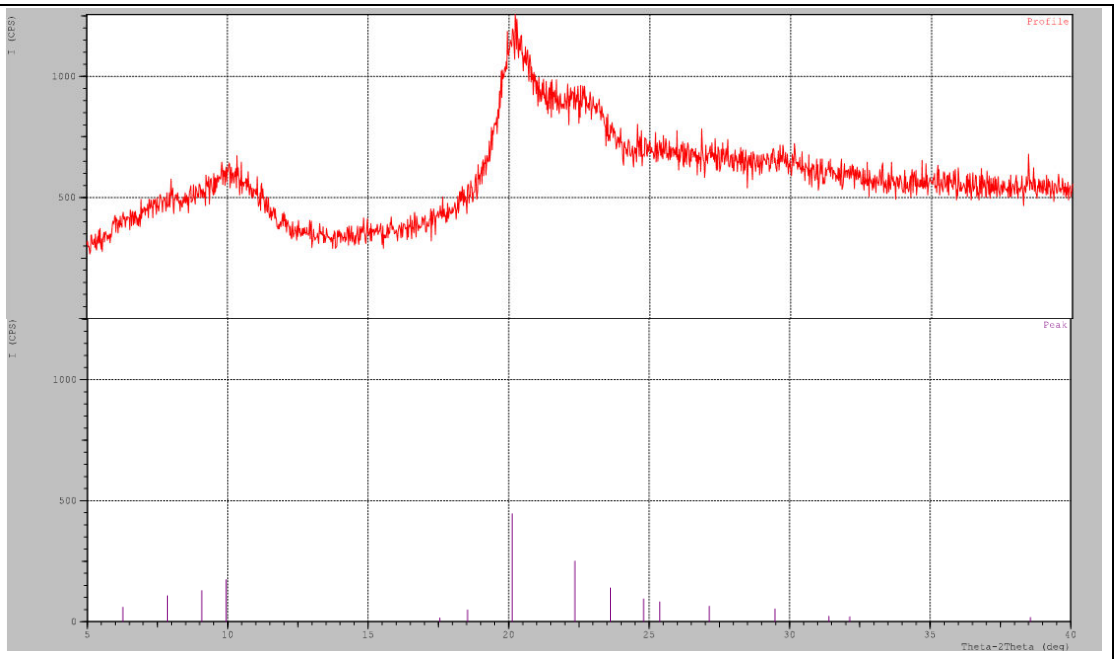

Strongest 3 peaks

no.	peak no.	2Theta (deg)	d (A)	I/I1	FWHM (deg)	Intensity (Counts)	Integrated Int (Counts)
1	7	20.1200	4.40979	100	1.24000	267	29052
2	8	22.3600	3.97283	56	0.00000	150	0
3	4	9.9400	8.89142	39	2.88000	104	11259

Peak Data List

peak no.	2Theta (deg)	d (A)	I/I1	FWHM (deg)	Intensity (Counts)	Integrated Int (Counts)
1	6.2800	14.06275	13	0.84000	35	4458
2	7.8600	11.23908	24	0.00000	64	0
3	9.0800	9.73153	28	0.00000	76	0
4	9.9400	8.89142	39	2.88000	104	11259
5	17.5500	5.04934	3	0.26000	9	168
6	18.5400	4.78189	11	0.77340	29	1955
7	20.1200	4.40979	100	1.24000	267	29052
8	22.3600	3.97283	56	0.00000	150	0
9	23.6200	3.76368	31	0.00000	83	0
10	24.8000	3.58721	21	0.00000	56	0
11	25.3800	3.50653	18	0.00000	49	0
12	27.1400	3.28300	14	0.00000	37	0
13	29.4800	3.02751	12	1.94000	31	4589
14	31.3933	2.84722	5	0.62670	13	372
15	32.1350	2.78318	4	0.47000	12	308
16	38.5666	2.33255	4	0.41330	10	277

APPENDIX C : Peaks Data on XRD Diffractogram for M2_CHS

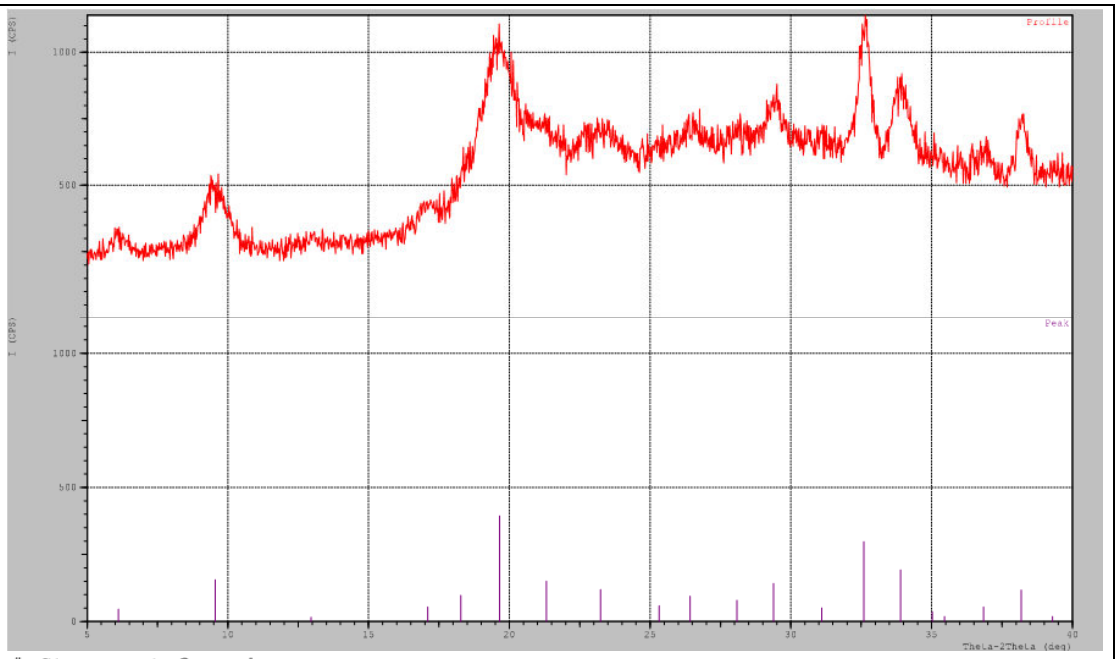

Strongest 3 peaks

no.	peak no.	2Theta (deg)	d (A)	I/I1	FWHM (deg)	Intensity (Counts)	Integrated Int (Counts)
1	6	19.6516	4.51383	100	1.59670	236	20207
2	14	32.5850	2.74577	75	0.67000	178	7416
3	15	33.8946	2.64261	49	0.80270	115	4629

Peak Data List

peak no.	2Theta (deg)	d (A)	I/I1	FWHM (deg)	Intensity (Counts)	Integrated Int (Counts)
1	6.1150	14.44183	11	0.67000	27	1015
2	9.5508	9.25285	39	1.04830	93	5556
3	12.9566	6.82727	4	0.59330	9	322
4	17.1000	5.18119	14	0.76000	32	1289
5	18.2800	4.84931	25	0.64000	58	2363
6	19.6516	4.51383	100	1.59670	236	20207
7	21.3200	4.16422	38	0.00000	90	0
8	23.2400	3.82435	30	1.78000	71	10346
9	25.3200	3.51470	15	0.00000	35	0
10	26.4200	3.37081	24	1.76000	56	5346
11	28.0800	3.17520	20	0.00000	47	0
12	29.3850	3.03709	36	1.03000	85	6890
13	31.1000	2.87340	13	0.00000	30	0
14	32.5850	2.74577	75	0.67000	178	7416
15	33.8946	2.64261	49	0.80270	115	4629
16	35.0200	2.56022	9	0.82000	21	847
17	35.4600	2.52946	4	0.92000	10	492
18	36.8400	2.43781	14	0.64000	32	1063
19	38.1816	2.35518	30	0.60330	70	2141
20	39.2900	2.29125	4	0.50000	10	326

APPENDIX D : Peaks Data on XRD Diffractogram for M3_CHS

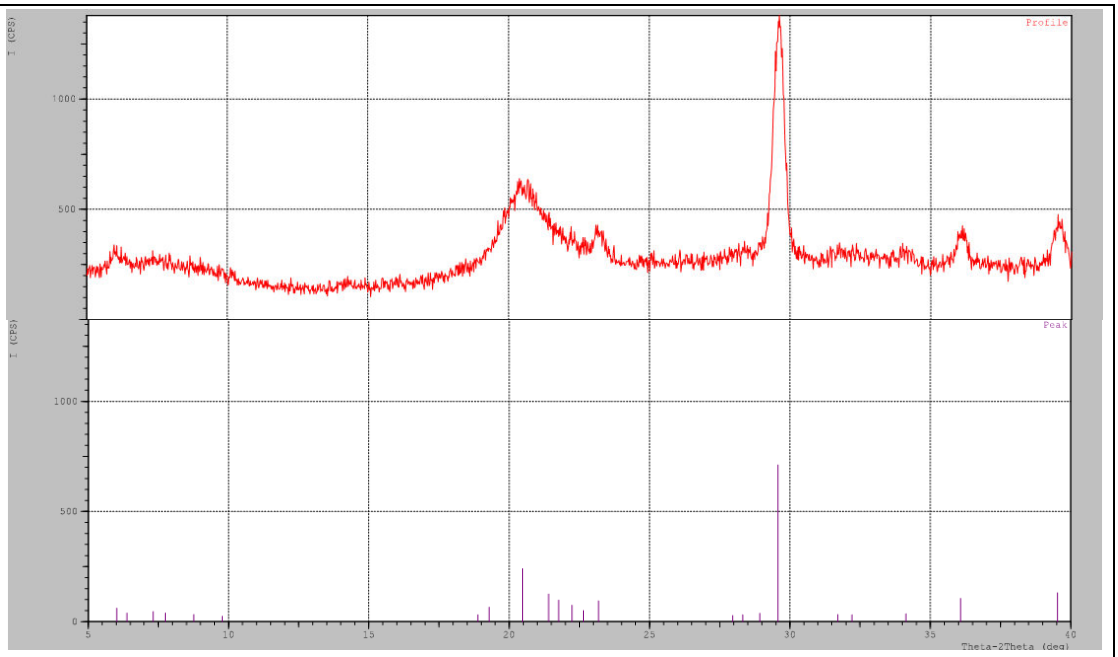

Strongest 3 peaks

no.	peak no.	2Theta (deg)	d (A)	I/I1	FWHM (deg)	Intensity (Counts)	Integrated Int (Counts)
1	18	29.5746	3.01805	100	0.46920	426	10674
2	9	20.4800	4.33308	34	1.58000	144	9973
3	23	39.5262	2.27811	18	0.47250	78	2091

Peak Data List

peak no.	2Theta (deg)	d (A)	I/I1	FWHM (deg)	Intensity (Counts)	Integrated Int (Counts)
1	6.0200	14.66952	8	0.46000	36	1099
2	6.3800	13.84255	5	0.00000	23	0
3	7.3200	12.06693	6	1.16000	27	1113
4	7.7600	11.38368	5	1.48000	23	751
5	8.7600	10.08629	4	1.40000	19	995
6	9.7800	9.03652	3	0.28000	14	309
7	18.8800	4.69653	4	0.44000	18	658
8	19.2800	4.59999	9	0.54660	39	997
9	20.4800	4.33308	34	1.58000	144	9973
10	21.4000	4.14883	17	0.00000	74	0
11	21.7600	4.08100	14	0.00000	58	0
12	22.2400	3.99400	10	0.00000	44	0
13	22.6400	3.92433	7	0.00000	29	0
14	23.1770	3.83460	13	0.53400	56	1796
15	27.9600	3.18855	4	0.24000	16	223
16	28.3300	3.14774	4	0.42000	18	360
17	28.9200	3.08485	5	0.28000	22	584
18	29.5746	3.01805	100	0.46920	426	10674
19	31.7166	2.81894	4	0.51330	19	471
20	32.2066	2.77716	4	0.45330	18	592
21	34.1300	2.62492	5	0.46000	21	681
22	36.0783	2.48751	15	0.42330	62	1632
23	39.5262	2.27811	18	0.47250	78	2091

APPENDIX E : Peaks Data on XRD Diffractogram for M4_CHS

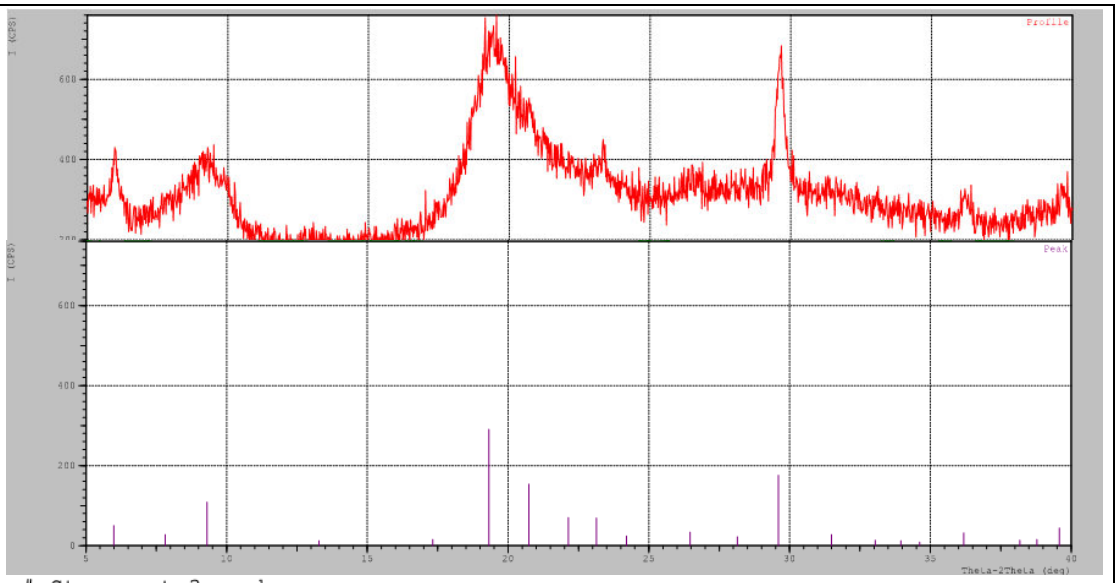

Strongest 3 peaks

no.	peak no.	2Theta (deg)	d (A)	I/I1	FWHM (deg)	Intensity (Counts)	Integrated Int (Counts)
1	6	19.3200	4.59055	100	1.56000	174	12337
2	13	29.5964	3.01587	60	0.65290	105	3363
3	7	20.7400	4.27935	53	2.08000	92	8579

Peak Data List

peak no.	2Theta (deg)	d (A)	I/I1	FWHM (deg)	Intensity (Counts)	Integrated Int (Counts)
1	5.9900	14.74292	17	0.54000	30	845
2	7.8200	11.29647	9	0.54660	16	563
3	9.3050	9.49672	37	1.65000	65	5160
4	13.2800	6.66173	4	0.20000	7	162
5	17.3200	5.11587	5	0.00000	9	0
6	19.3200	4.59055	100	1.56000	174	12337
7	20.7400	4.27935	53	2.08000	92	8579
8	22.1400	4.01181	24	0.00000	42	0
9	23.1400	3.84065	24	1.04000	41	2864
10	24.2000	3.67477	8	0.32000	14	313
11	26.4600	3.36580	11	0.76000	20	816
12	28.1400	3.16856	7	1.72000	13	1247
13	29.5964	3.01587	60	0.65290	105	3363
14	31.5000	2.83782	9	1.24000	16	1245
15	33.0400	2.70899	5	0.28000	8	156
16	33.9600	2.63767	4	0.08000	7	80
17	34.6150	2.58925	3	0.11000	5	97
18	36.1800	2.48075	11	0.52000	19	588
19	38.1800	2.35528	5	0.24000	8	127
20	38.7800	2.32021	5	0.56000	9	347
21	39.5800	2.27513	15	0.60000	26	845

APPENDIX F : Peaks Data on XRD Diffractogram for M4_CHS

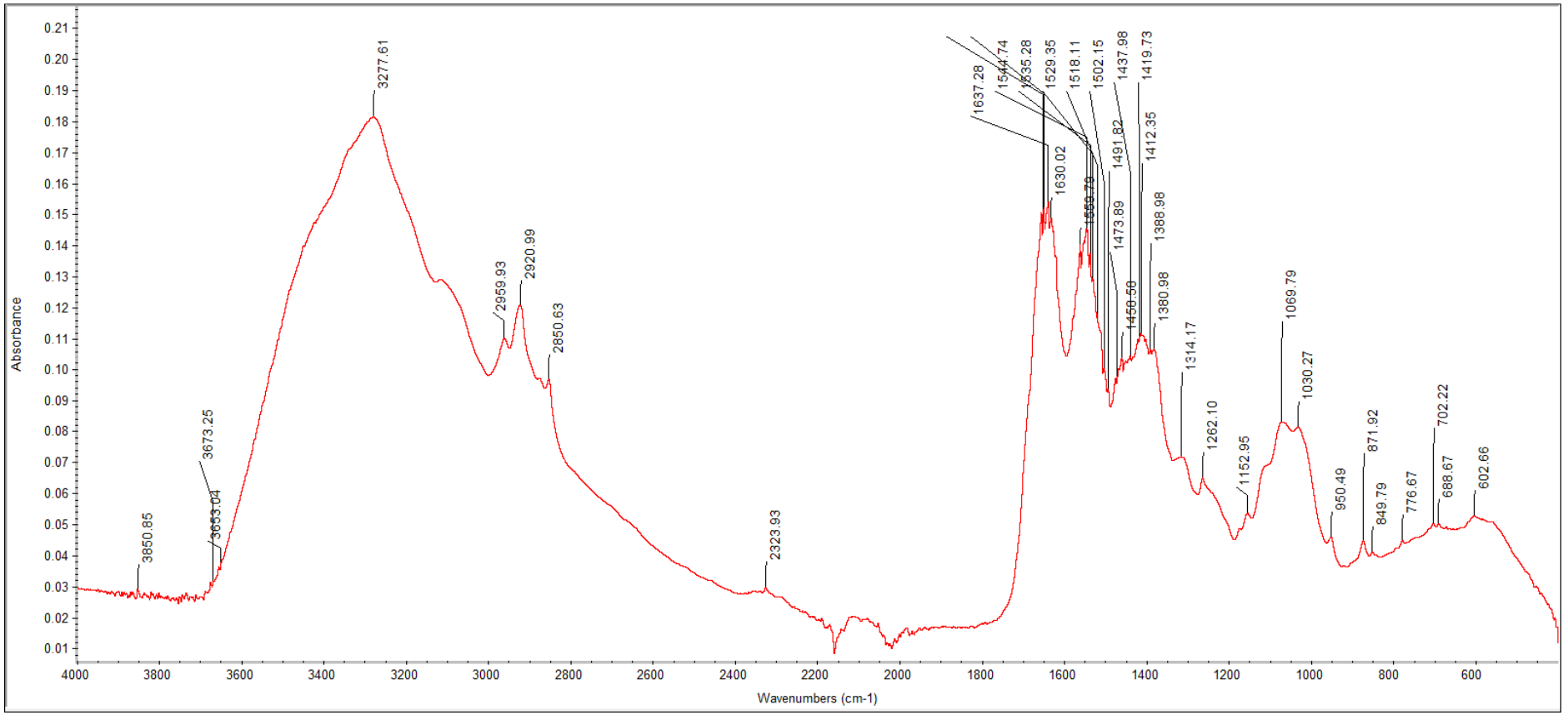

APPENDIX G : Bands Data of FT-IR Spectrum for Shrimp Shell Powder

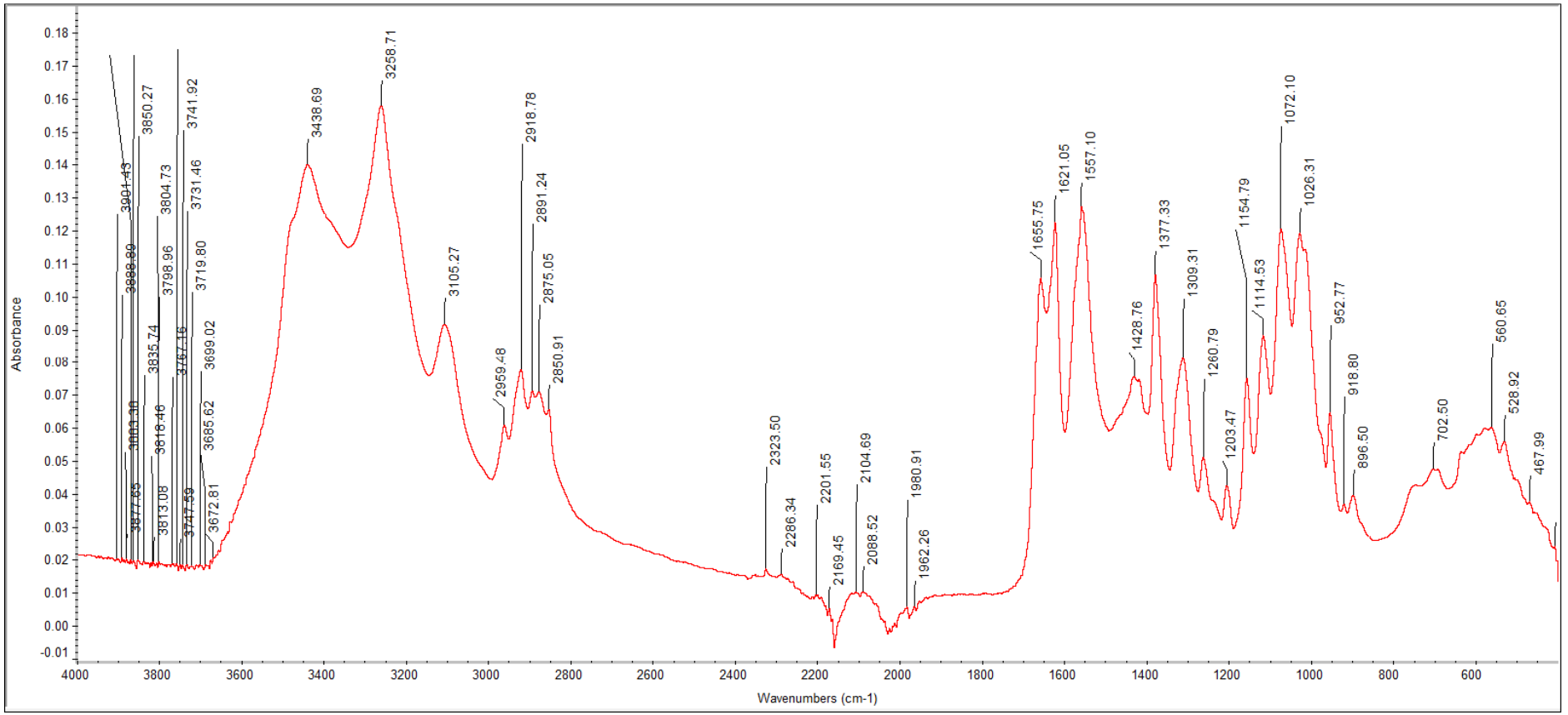

APPENDIX H : Bands Data of FT-IR Spectrum M1_CHS

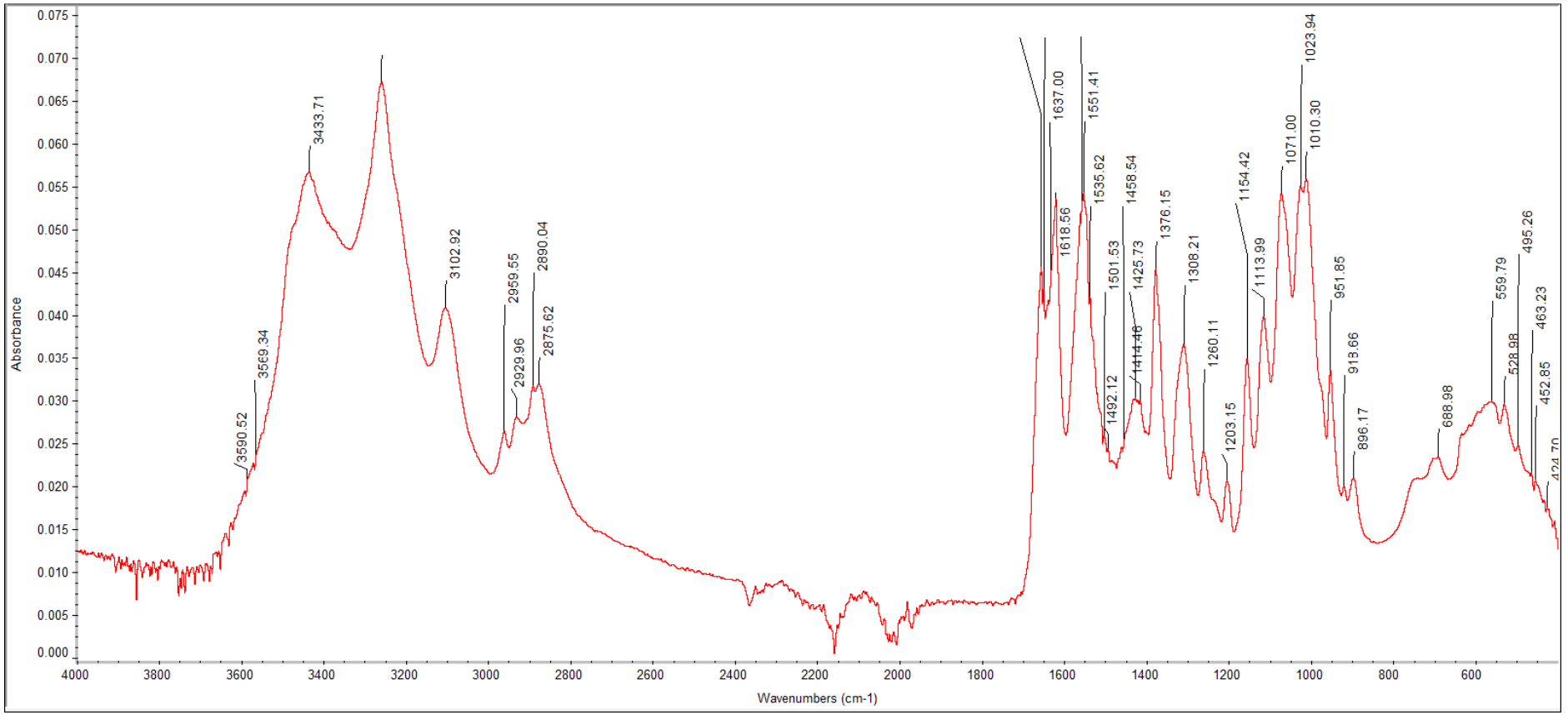

APPENDIX I : Bands Data of FT-IR Spectrum M2_CHT

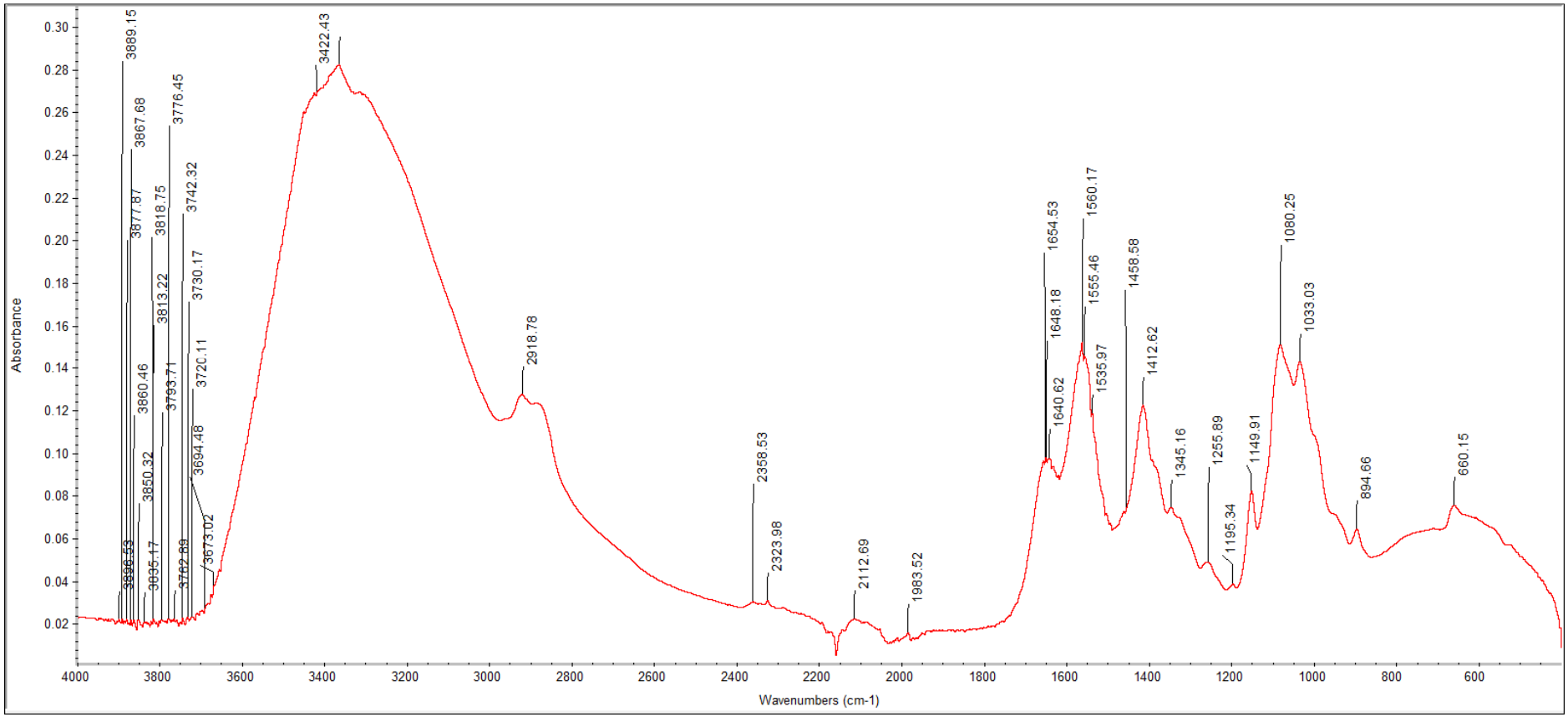

APPENDIX J : Bands Data of FT-IR Spectrum M2_CHS

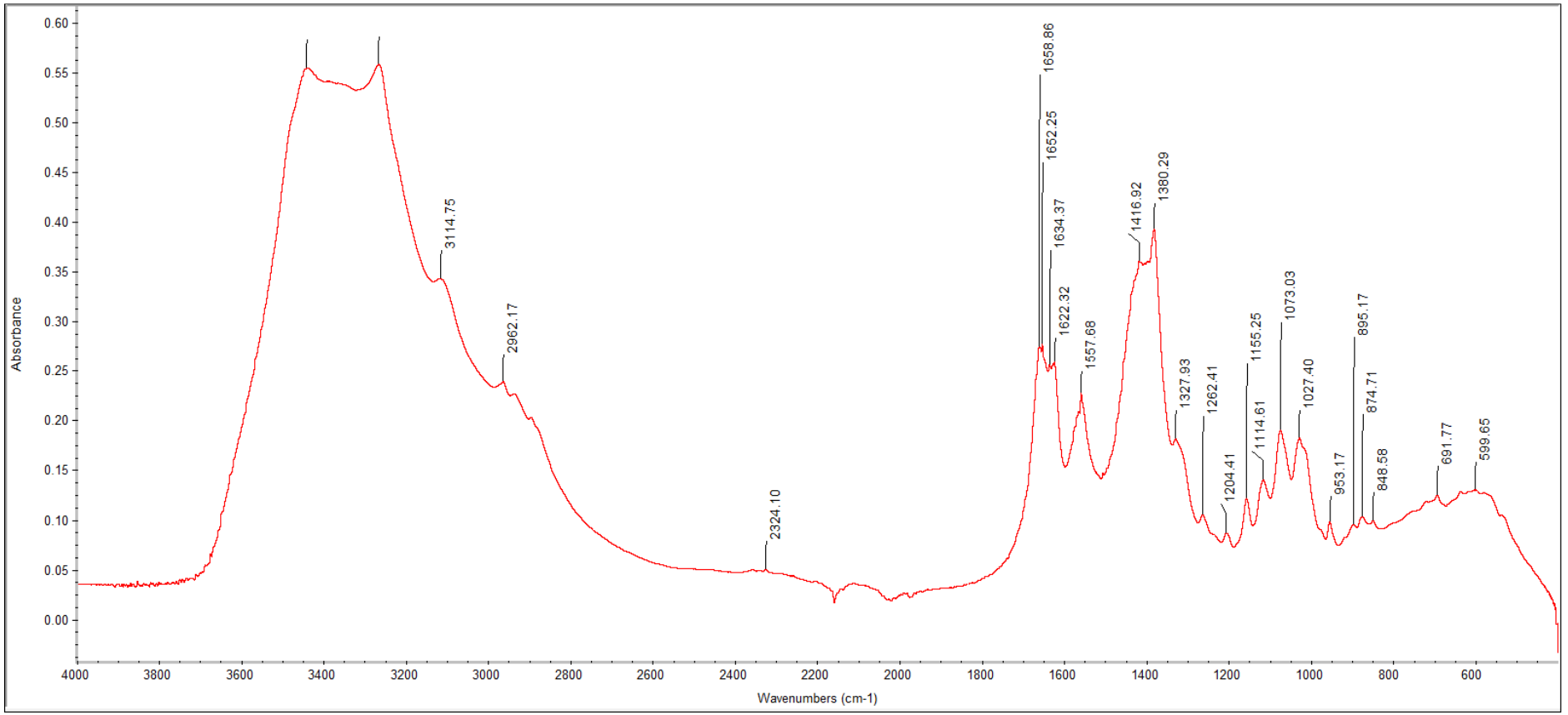

APPENDIX K : Bands Data of FT-IR Spectrum M3_CHT

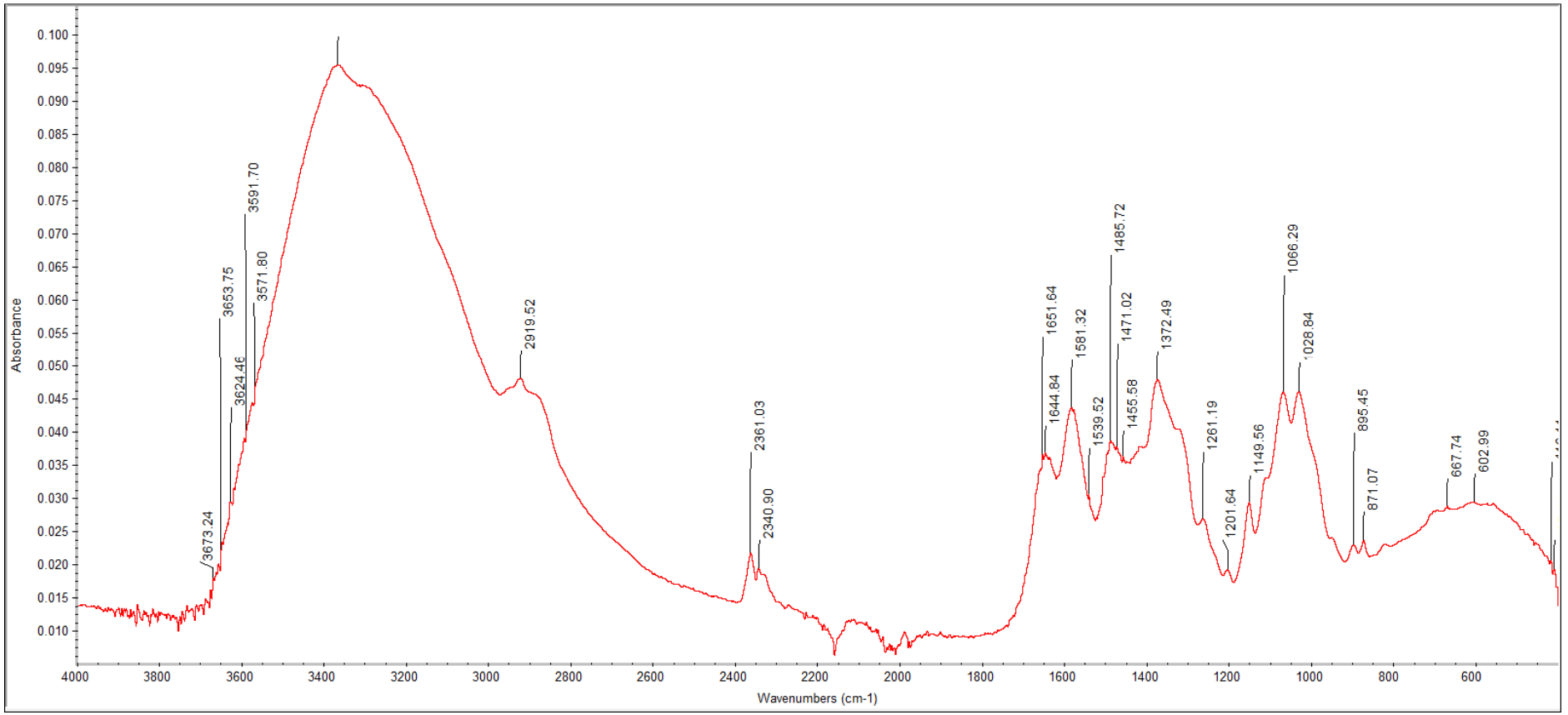

APPENDIX L : Bands Data of FT-IR Spectrum M3_CHS

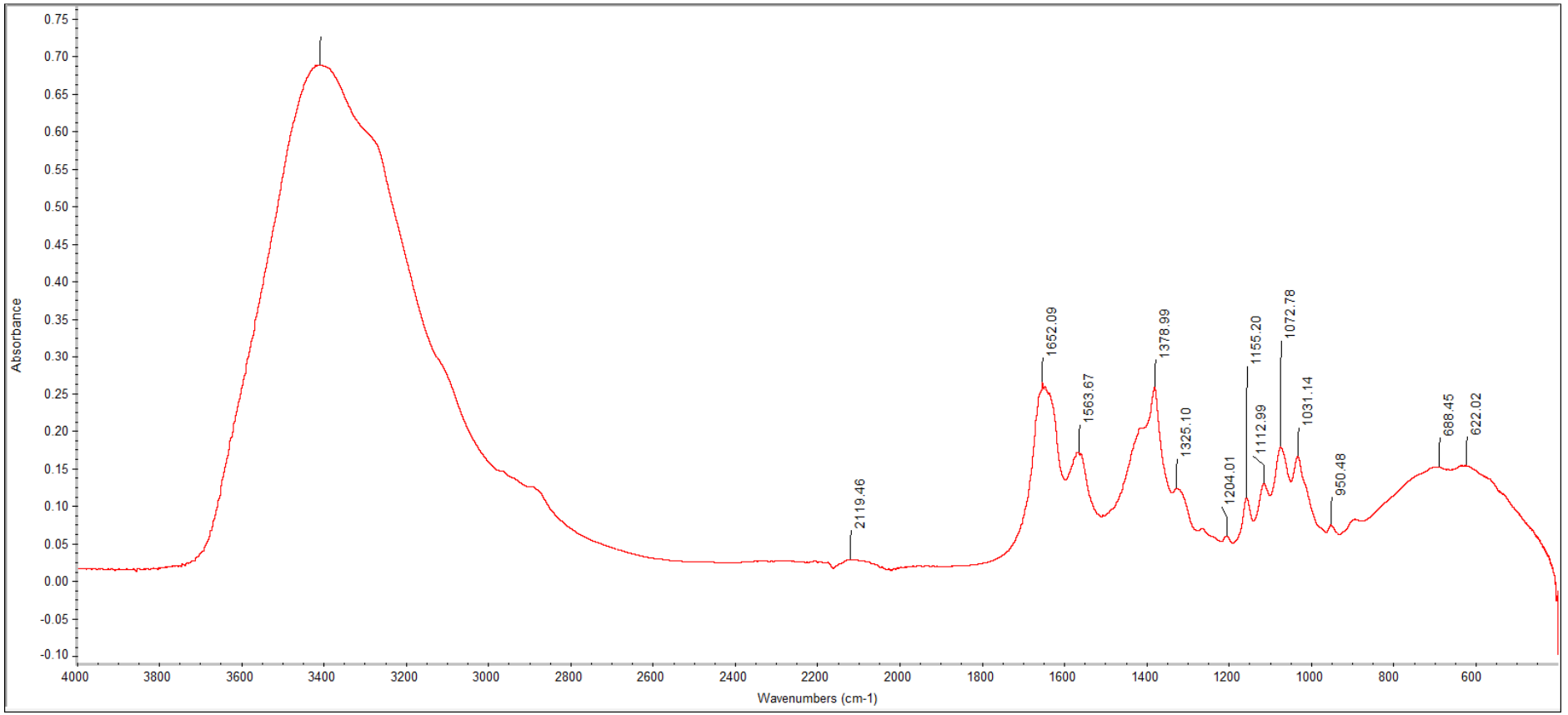

APPENDIX M : Bands Data of FT-IR Spectrum M4_CHS

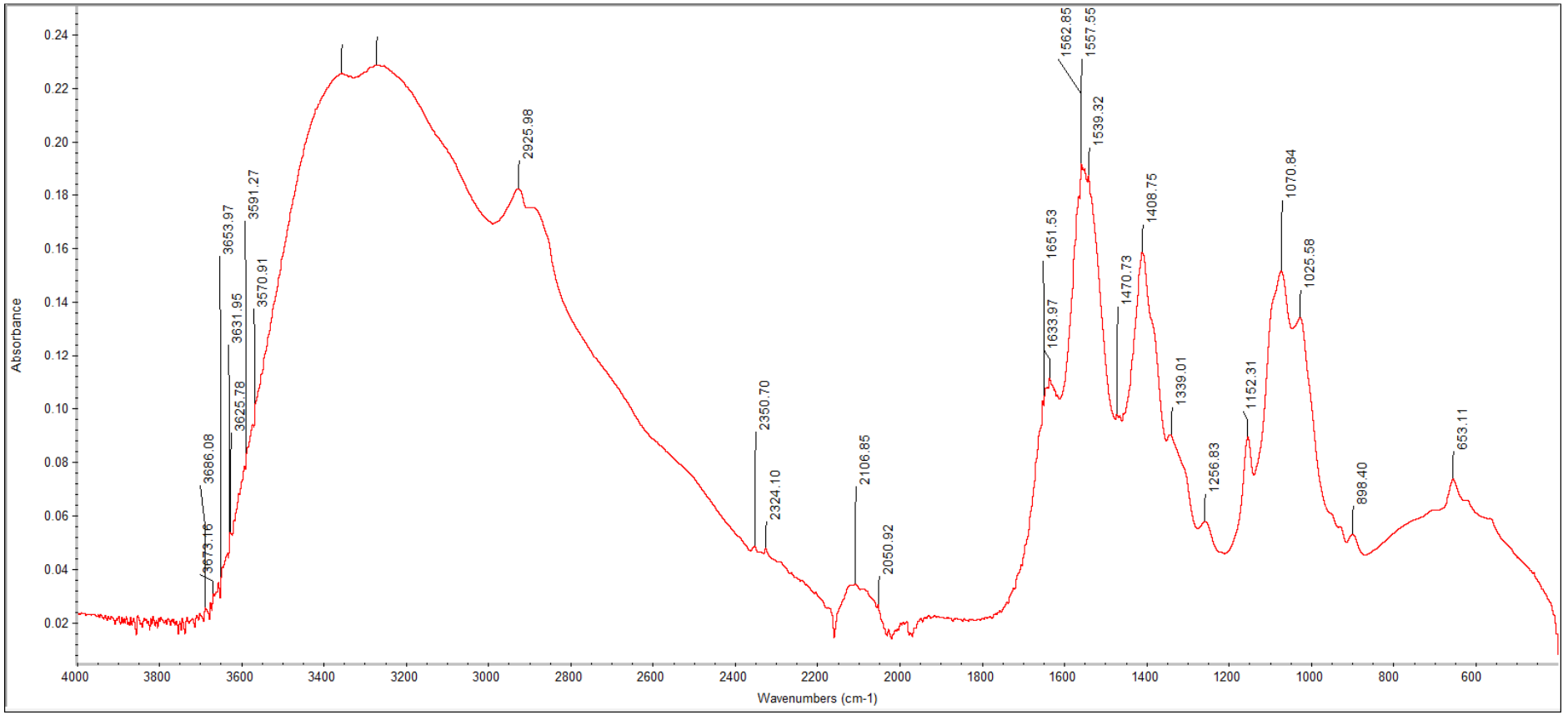

APPENDIX N : Bands Data of FT-IR Spectrum for Dried M2 Chitosan After Dissolved by Acetic Acid (D_M2_CHS_AA)

APPENDIX O : Bands Data of FT-IR Spectrum for Iron Oxide Nanoparticles Produced by Ong (2013) (S2_IO)

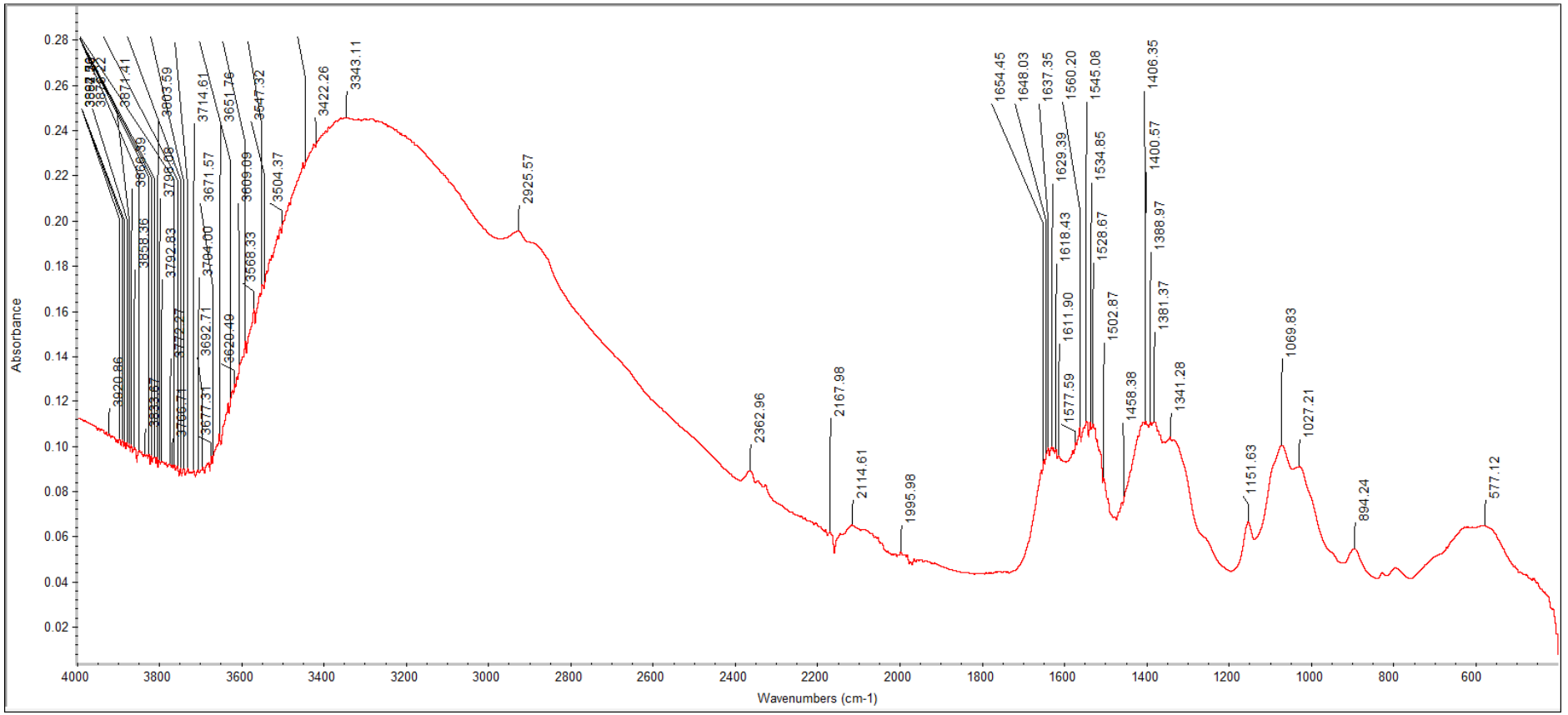

APPENDIX P : Bands Data of FT-IR Spectrum for Dried Mixture of M2 Chitosan and Iron Oxide Nanoparticles (D_M2_S2_AA)

	Activities	FYP 1														FYP2													
		Wk1	Wk2	Wk3	Wk4	Wk5	Wk6	Wk7	Wk8	Wk9	Wk10	Wk11	Wk12	Wk13	Wk14	Wk1	Wk2	Wk3	Wk4	Wk5	Wk6	Wk7	Wk8	Wk9	Wk10	Wk11	Wk12	Wk13	Wk14
1	Literature Survey																												
2	Literature Review																												
3	Analyze the Project (uncertainties, Risk, resource available, etc)																												
4	Project Planning																												
5	Estimate Budget																												
6	Define & sequence work's activities																												
7	Estimate work's activities duration & resources																												
8	Reservation & Preparation of Lab																												
9	Acquire Necessary Tool & Equipment																												
10	Developing parameters to synthesize chitosan																												
11	first set synthesizing parameters																												
12	Second set of synthesizing parameters																												
13	Reservation and Characterisation of Product (SEM, XRD)																												
14	Progress Report																												
15	Preparation for Proposal Presentation																												
16	Develop procedure to investigate effect of DDA on chitosan																												
17	Synthesize chitosan with different DDA																												
18	Reservation of Equipment and Characterisation for chitosan with varying DDA(SEM,XRD, FTIR, TGA, etc)																												

19	Synthesizing Chitosan/Iron(III) Oxide Composite																													
20	Reservation of Equipment and Characterisation for Chitosan/Iron(III) Oxide Composite																													
21	Collection and Tabulation of Data																													
22	Data Analysis																													
23	Final Report Preparation																													
24	Preparation Final Report Presentation																													
25	Amendments on Final Report																													
26	Completion of Project																													
		FYP 1														FYP2														
Mile Stone		Wk1	Wk2	Wk3	Wk4	Wk5	Wk6	Wk7	Wk8	Wk9	Wk10	Wk11	Wk12	Wk13	Wk14	Wk1	Wk2	Wk3	Wk4	Wk5	Wk6	Wk7	Wk8	Wk9	Wk10	Wk11	Wk12	Wk13	Wk14
9	Acquire Necessary Tool & Equipment																													
12	Second set of synthesizing parameters																													
15	Progress Report																													
17	Synthesize chitosan with different DDA																													
18	Synthesizing Chitosan/Iron(III) Oxide Composite																													
21	Collection and Tabulation of Data																													
22	Final Report Preparation																													
28	Completion of Project																													

APPENDIX Q : Gantt Chart Planning for the Study

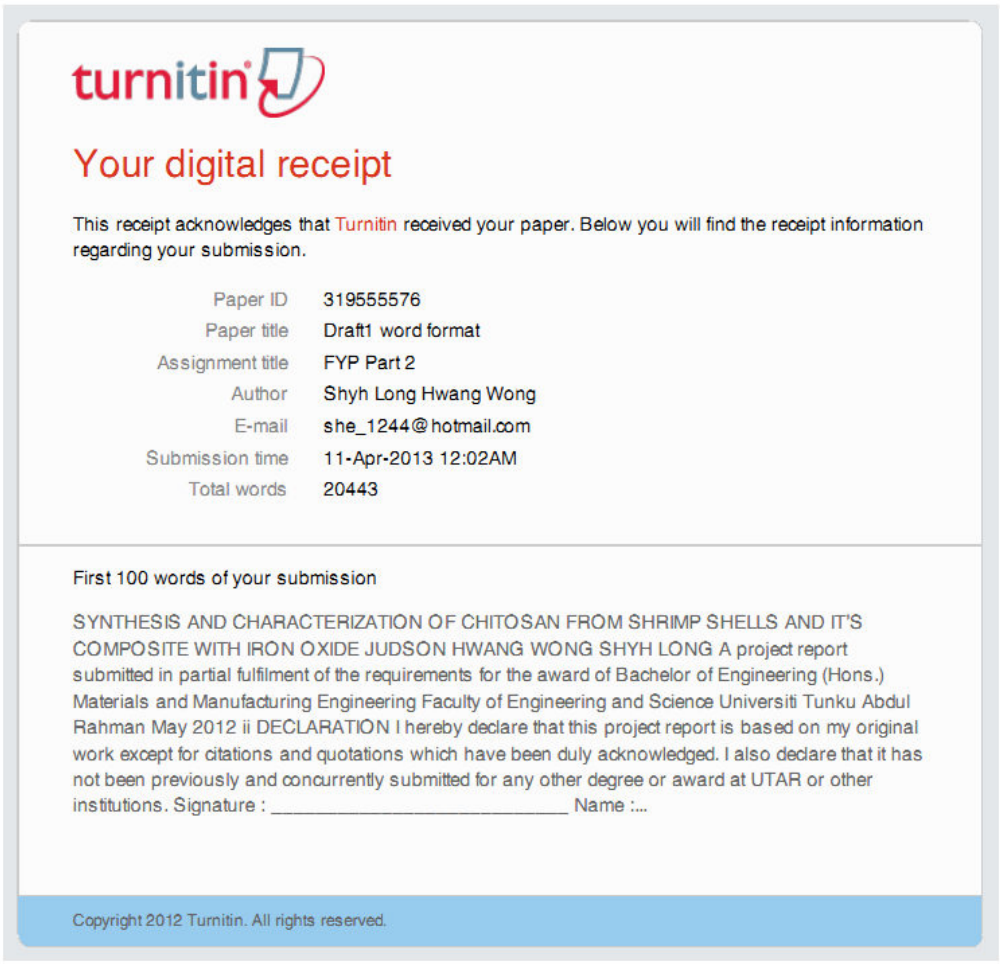

turnitin

Your digital receipt

This receipt acknowledges that Turnitin received your paper. Below you will find the receipt information regarding your submission.

Paper ID	319555576
Paper title	Draft1 word format
Assignment title	FYP Part 2
Author	Shyh Long Hwang Wong
E-mail	she_1244@hotmail.com
Submission time	11-Apr-2013 12:02AM
Total words	20443

First 100 words of your submission

SYNTHESIS AND CHARACTERIZATION OF CHITOSAN FROM SHRIMP SHELLS AND IT'S COMPOSITE WITH IRON OXIDE JUDSON HWANG WONG SHYH LONG A project report submitted in partial fulfilment of the requirements for the award of Bachelor of Engineering (Hons.) Materials and Manufacturing Engineering Faculty of Engineering and Science Universiti Tunku Abdul Rahman May 2012 ii DECLARATION I hereby declare that this project report is based on my original work except for citations and quotations which have been duly acknowledged. I also declare that it has not been previously and concurrently submitted for any other degree or award at UTAR or other institutions. Signature : _____ Name :...

APPENDIX R : Turnitin Receipt

Turnitin Originality Report

Draft1 word format by Shyh Long Hwang Wong

From FYP Part 2 (FYP May 2012)

- Processed on 18-Apr-2013 00:30 MYT
- ID: 319555576
- Word Count: 20443

Similarity Index
4%
Similarity by Source

Internet Sources:
2%
Publications:
3%
Student Papers:
2%

sources:

1 1% match (publications)
Sagheer, F.A.A.. "Extraction and characterization of chitin and chitosan from marine sources in Arabian Gulf", Carbohydrate Polymers, 20090610

2 1% match (Internet from 20-Feb-2012)
http://ijens.org/Vol%2011%20I%2001/110201-8484%20IJBAS-IJENS.pdf

3 1% match (publications)
Mohammed, Musarrat H., Peter A. Williams, and Olga Tverezovskaya. "Extraction of chitin from prawn shells and conversion to low molecular mass chitosan", Food Hydrocolloids, 2013.

4 1% match (Internet from 01-Nov-2012)
http://ethesis.nitrkl.ac.in/3259/1/projectfinaal.pdf

5 1% match (publications)
Kasaai, M.R.. "A review of several reported procedures to determine the degree of N-acetylation for chitin and chitosan using infrared spectroscopy", Carbohydrate Polymers, 20080307

paper text:

SYNTHESIS AND CHARACTERIZATION OF CHITOSAN FROM SHRIMP SHELLS AND IT'S COMPOSITE WITH IRON OXIDE JUDSON HWANG WONG SHYH LONG A project report submitted in partial fulfilment of the requirements for the award of Bachelor of Engineering (Hons.) Materials and Manufacturing Engineering Faculty of Engineering and Science Universiti Tunku Abdul Rahman May 2012 ii DECLARATION I hereby declare that this project report is based on my original work except for citations and quotations which have been duly acknowledged. I also declare that it has not been previously and concurrently submitted for any other degree or award at UTAR or other institutions. Signature : _____ Name :

APPENDIX S : First Page of Originality Report